

## The Pluto Energetic Particle Spectrometer Science Investigation (PEPSSI) on the New Horizons Mission

Ralph L. McNutt Jr. · Stefano A. Livi · Reid S. Gurnee · Matthew E. Hill · Kim A. Cooper · G. Bruce Andrews · Edwin P. Keath · Stamatiios M. Krimigis · Donald G. Mitchell · Barry Tossman · Fran Bagenal · John D. Boldt · Walter Bradley · William S. Devereux · George C. Ho · Stephen E. Jaskulek · Thomas W. LeFevre · Horace Malcom · Geoffrey A. Marcus · John R. Hayes · G. Ty Moore · Mark E. Perry · Bruce D. Williams · Paul Wilson IV · Lawrence E. Brown · Martha B. Kusterer · Jon D. Vandegriff

Received: 28 August 2007 / Accepted: 3 September 2008 / Published online: 25 October 2008  
© Springer Science+Business Media B.V. 2008

**Abstract** The Pluto Energetic Particle Spectrometer Science Investigation (PEPSSI) comprises the hardware and accompanying science investigation on the New Horizons spacecraft to measure pick-up ions from Pluto's outgassing atmosphere. To the extent that Pluto retains its characteristics similar to those of a "heavy comet" as detected in stellar occultations since the early 1980s, these measurements will characterize the neutral atmosphere of Pluto while providing a consistency check on the atmospheric escape rate at the encounter epoch with that deduced from the atmospheric structure at lower altitudes by the ALICE, REX, and SWAP experiments on New Horizons. In addition, PEPSSI will characterize any extended ionosphere and solar wind interaction while also characterizing the energetic particle environment of Pluto, Charon, and their associated system. First proposed for development for the Pluto Express mission in September 1993, what became the PEPSSI instrument went through a number of development stages to meet the requirements of such an instrument for a mission to Pluto while minimizing the required spacecraft resources. The PEPSSI instrument provides for measurements of ions (with compositional information) and electrons from 10 s of keV to  $\sim 1$  MeV in a  $160^\circ \times 12^\circ$  fan-shaped beam in six sectors for 1.5 kg and  $\sim 2.5$  W.

---

E.P. Keath, B. Tossman, W. Bradley, and P. Wilson IV are retired.

R.L. McNutt Jr. (✉) · R.S. Gurnee · M.E. Hill · K.A. Cooper · G.B. Andrews · E.P. Keath · S.M. Krimigis · D.G. Mitchell · B. Tossman · J.D. Boldt · W. Bradley · W.S. Devereux · G.C. Ho · S.E. Jaskulek · T.W. LeFevre · H. Malcom · G.A. Marcus · J.R. Hayes · G.T. Moore · M.E. Perry · B.D. Williams · P. Wilson IV · L.E. Brown · M.B. Kusterer · J.D. Vandegriff  
Applied Physics Laboratory, The John Hopkins University, 11100 John Hopkins Road, Laurel, MD 20723, USA  
e-mail: [Ralph.mcnutt@jhuapl.edu](mailto:Ralph.mcnutt@jhuapl.edu)

S.A. Livi  
Southwest Research Institute, 6220 Culebra Road, San Antonio, TX 78228, USA

S.M. Krimigis  
Academy of Athens, 28 Panapistimiou, 10679 Athens, Greece

F. Bagenal  
The University of Colorado, Boulder, CO 80309, USA

**Keywords** New Horizons · PEPSSI · Pluto · Energetic particle instrument

### Abbreviations

1PPS	One Pulse Per Second
ADC	Analog-to-digital converter
APL	Applied Physics Laboratory
ASIC	Application specific integrated circuit
C&DH	Command and Data Handling
CCSDS	Consultative Committee for Space Data Systems
CFD	Constant Fraction Discriminator
CSA	Charge Sensitive Amplifier
eV	Electron Volt
FITS	Flexible Image Transport System
FOV	Field of View
FWHM	Full Width Half Maximum
GSE	Ground support equipment
GSFC	Goddard Space Flight Center
HDU	Header Data Unit
HV	High Voltage Section of HVPS
HVPS	High Voltage Power Supply (HV and Bias Supply Sections)
IEM	Integrated Electronics Module
IGSE	Instrument Ground Support Equipment
ICD	Interface Control Document
ITF	Instrument Transfer Frame
LED	Leading Edge Discriminator
MCP	Micro-channel plate
MIDL	Mission Independent Data Layer
MDM	Master Data Manager
MET	Mission Elapsed Time
MOI	Moment of inertia
NA	Not applicable
NASA	National Aeronautics and Space Administration
NH	New Horizons
ns	nanosecond = $10^{-9}$ s
PDS	Planetary Data System
PEPSSI	Pluto Energetic Particle Spectrometer Science Investigation
PFF	Pluto Fast Flyby
PHA	Pulse height analysis
PIDDP	Planetary Instrument Definition and Development Program
ps	picosecond = $10^{-12}$ s
psi	Pounds per square inch
RTG	Radioisotope Thermoelectric Generator
SQL	Structured Query Language
SSD	Solid-state detector
SSR	Solid-state recorder
STP	Supplemented Telemetry Packet
SwRI	Southwest Research Institute
TDC	Time-to-digital chip
TOF	Time of flight

TRIO	Temperature remote input/output
T-V	Thermal-vacuum
UART	Universal asynchronous receive and transmit

## 1 Introduction

The Pluto Energetic Particle Spectrometer Science Investigation (PEPSSI) is one of seven scientific instruments/experiments (Weaver et al. 2008) on board the New Horizons spacecraft (Fountain et al. 2008), now on its way to Pluto (Stern 2008). While it is doubtful that Pluto has an intrinsic magnetic field and magnetosphere that accelerates charged particles to high energies, Pluto does have (or has had in the very recent past) a substantial atmosphere (Elliot et al. 1989, 2003, 2007; Brosch 1995; Sicardy et al. 2003; Fink et al. 1980) that is escaping into the solar wind in a comet-like interaction (Bagenal and McNutt 1989; McNutt 1989; Keckskemety and Cravens 1993; Bagenal et al. 1997; Trafton et al. 1997; Krasnopolsky 1999; Delamere and Bagenal 2004; Tian and Toon 2005). Measured interactions at comets show that the outgassing cometary neutral atoms and molecules charge-exchange with the solar wind and are accelerated in the process (Galeev et al. 1985; Mendis et al. 1986; Galeev 1987; Neugebauer 1990; Coates et al. 1993a, 1993b; Huddleston et al. 1993; Motschmann and Glassmeier 1993). By measuring the in situ energetic particle population, identifying those ions from the emitting body, and noting their variation with distance to the emitting body, the outgassing source strength may be deduced (Gloeckler et al. 1986). It is also important to note that energization beyond what one would naively expect from pick-up alone is also observed at comets (McKenna-Lawlor et al. 1986; Richardson et al. 1986; Sanderson et al. 1986; Somogyi et al. 1986). For example, shock acceleration of particles at Venus can elevate some of the particles to substantial ( $\sim 100$  keV) energies (Williams et al. 1991). Making these measurements to determine the “outer boundary” of the influence of Pluto’s atmosphere is the primary objective of the PEPSSI instrument. The extent of the interaction with the solar wind will be determined by comparing the PEPSSI measurements with those obtained of the solar wind by the SWAP instrument (McComas et al. 2008). A deduced atmospheric profile from the surface to the edge of Pluto’s atmosphere will be assembled from combining PEPSSI, the New Horizons ultraviolet imaging spectrometer Alice (Stern et al. 2008) and the New Horizons radio experiment (REX) (Tyler et al. 2008) measurements.

PEPSSI combines energy and time-of-flight measurements in a low-mass ( $< 1.5$  kg), low-power ( $< 2.5$  W) unit. At the same time, the instrument has a relatively large total geometric factor of  $\sim 0.1$  cm<sup>2</sup> sr and enables directional information of the particle distribution across a  $\sim 12^\circ \times 160^\circ$  swath in six  $\sim 25^\circ$ -wide angular bins. The instrument also discriminates between electrons and ions without the use of (relatively) heavy permanent magnets (or power-hungry electromagnets). While the use of silicon solid state detectors (SSDs) for measuring energetic particles date back to the near-beginning of the space program, the additional species discrimination made possible by including time-of-flight measurements (thus independently, but simultaneously, measuring both an ion energy and speed) is a relatively newer development (McEntire et al. 1985; Lanzerotti et al. 1992; Williams et al. 1992; Krimigis et al. 2004). Further, packaging of this capability into such a compact instrument provided a variety of engineering and programmatic challenges.

### 1.1 Previous Similar Instrumentation

PEPSSI combines time-of-flight (TOF) and total-energy measurements in six angular sectors packaged into a compact arrangement (Fig. 1). Unlike plasma instruments incorporating

**Fig. 1** PEPSSI mounted on the New Horizons spacecraft via its complex-angle bracket in the clean room at APL prior to being covered with its thermal blanket



a TOF system at lower energies (Gloeckler et al. 1985), no pre-acceleration, high-voltages ( $\geq 10$  s of kilovolts, kV) are used in this device.

PEPSSI is a direct outgrowth of a variety of internal research and development activities within the Johns Hopkins University Applied Physics Laboratory (APL) going as far back as 1980 (De Amicis 1988) as well as NASA's Planetary Instrument Definition and Development Program (PIDDP). The original goal of "a total instrument mass and power of less than 0.5 kg and 0.5 W" resulted in a design known colloquially as "the hockey puck" due to the cylindrical aperture/detector/time-of-flight (TOF) section that has about the same proportions and size as a regulation ice hockey puck. Little from a second PIDDP effort was available for incorporation into the MESSENGER flight hardware given the timing of MESSENGER's selection for flight (McNutt et al. 2006). Some improvements were possible for PEPSSI due to work under this second grant prior to the selection of New Horizons for flight (McNutt et al. 1996; Andrews et al. 1998). As had been predicted in 1992, the most difficult aspect was the development of a scientifically useful energetic particle instrument with the small mass and power limits that had to be met to allow for inclusion on a Pluto mission (Neugebauer et al. 1993; Lunine et al. 1995).

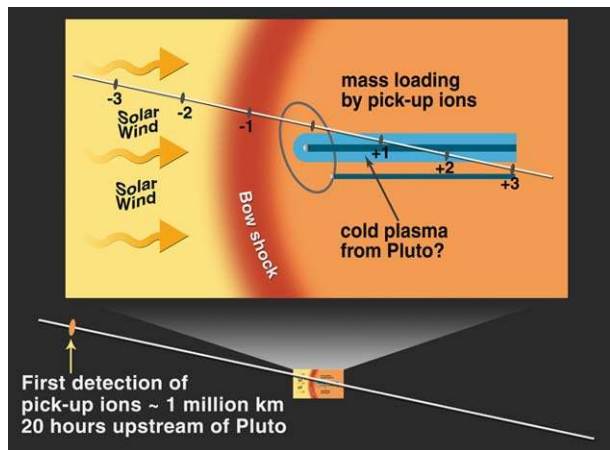
## 2 Scientific Background and Objectives

### 2.1 The Interaction of Pluto with the Solar Wind

The interaction of the various planets of the solar system with the solar wind goes back to the initial forays outside of the Earth's magnetosphere in the early 1960s. As part of the studies that eventually led to the Voyager program (Dryer et al. 1973) made an initial scoping study of what a solar wind interaction with Pluto might look like. They noted that for the anticipated scale lengths a kinetic approach was more proper for Pluto as for Mercury and that for a vanishingly small ionospheric scale height at Pluto, a long, induced magnetotail is, nonetheless, expected. With plans for a Pluto mission using grand-tour-like trajectories eventually canceled, the then-future Voyager encounter with Neptune and its large moon Triton (Morrison et al. 1982) would potentially provide the best insight into Pluto's interaction with the solar wind (McNutt 1982).

Interest in Pluto's interaction with the solar wind was reignited by the stellar occultation of 1988 (Elliot et al. 1989) and its interpretation of showing significant atmospheric escape (Bagenal and McNutt 1989; McNutt 1989). Current thinking is that the interaction of Pluto

**Fig. 2** Schematic of expected interaction of Pluto with the solar wind for the strong-interaction limit. Based upon scaling from cometary interactions, the first detection of pickup ions from Pluto are expected as early as  $\sim 20$  hours before closest approach



with the solar wind is something between that of an un-magnetized planet, such as Venus and that of a comet, depending upon the strength of the atmospheric outflow. If Pluto were to have even a weak intrinsic magnetization, then the interaction would be more akin to that of the magnetized planets due to the weak solar wind ram pressure at  $\sim 30$  AU and beyond. Estimates of the overall outgassing rate of the atmosphere  $Q_0$  are between  $\sim 10^{27}$  and  $10^{28}$  molecules  $s^{-1}$ . Such rates have effects ranging from just shielding the surface from the solar wind to producing a well-formed magnetosphere encompassing the orbit of Charon (Fig. 2). Detailed discussions of past and current thinking about the interaction is given by (Bagenal et al. 1997) and (McComas et al. 2008), respectively, and more detailed simulations have been carried out as well (Delamere and Bagenal 2004; Harnett et al. 2005).

## 2.2 PEPSSI Science Objectives

### 2.2.1 PEPSSI Objectives at Pluto

The PEPSSI sensor is designed to perform *in situ* measurements of the mass, energy spectra, and distributions of moderately energetic particles in the near-Pluto environment and in the Pluto-interaction region. The instrument measures particle velocity and energy, and derives particle mass. It discriminates between electrons, protons, alphas, and carbon-nitrogen-oxygen (CNO—taken as a closely-spaced group in atomic weight), and heavier ions. The direction of particles is also determined within one of six sectors. PEPSSI objectives, within the context of New Horizons science-mission-group objectives include:

**Group 1 Objective.** A group 1 objective is characterization of the neutral atmosphere of Pluto and its escape rate. To support this objective, PEPSSI will detect heavy ions and measure associated energy spectra and spatial variation along the trajectory. By analogy with cometary measurements, these measurements will be used to determine the neutral particle escape rate, which along with UV spectral measurements made in the upper atmosphere (Stern et al. 2008), will be used to put together a fully self-consistent model of Pluto's upper atmosphere to satisfy this group 1 objective.

**Group 2 Objectives.** A group 2 science objective is characterization of Pluto's ionosphere and interaction with the solar wind. This characterization will be aided by PEPSSI measurements of the spatial extent and composition of pickup ions; these measurements are complementary to those that will be made by SWAP (McComas et al. 2008).

*Group 3 Objectives.* A group 3 science objective is characterization of the energetic particle environment of Pluto and Charon. This will require measurement of the spatial extent and velocity-space distributions of energetic ions (e.g.,  $H^+$ ,  $N^+$ , and  $N_2^+$ ). The PEPSSI instrument will make the required energetic ion measurements.

### 2.2.2 Science at Jupiter and During Cruise

Initial scientific results from PEPSSI obtained during the New Horizons flyby of Jupiter show evidence for periodic bursts of energetic, Iogenic particles down the magnetotail of the planet (McNutt et al. 2007). In addition, this magnetospheric passage provided an opportunity for significant in-flight calibration activities that have been used to inform ongoing rehearsal activities for the Pluto flyby.

There is no official “cruise science” on the New Horizons mission. This is by design to help save the instruments for the Pluto flyby as well as minimize operational costs by putting the spacecraft in hibernation for the majority of the cruise from Jupiter to Pluto. Data on the interplanetary medium will be collected as activity during the annual check-outs allows. The general trajectory of New Horizons into the direction toward the incoming interstellar wind will allow for important comparisons of energetic particles and transients in the interplanetary medium as they propagate toward and into the inner heliosheath, now being explored by Voyagers 1 and 2.

## 2.3 Measurement Requirements

### 2.3.1 Measurement Ranges

Energy thresholds and energy ranges depend upon the energy measurement mode, i.e., TOF-only, energy (SSD) only, or coincidence measurements through the entire system (Table 1).

### 2.3.2 Derived Instrument Specifications

**2.3.2.1 Mass Resolution (Mass Uncertainty)** Particle mass is derived from energy and TOF measurements. The uncertainty in the derived mass, i.e., the mass resolution, is determined by (a) energy measurement resolution, (b) TOF measurement resolution, (c) particle mass, and (d) calibration accuracy. For Energy-plus-TOF measurements, the mass resolution for three species of particles (spanning light, medium, and heavy mass) is specified as  $< 2$

**Table 1** Energy measurement ranges for PEPSSI

Species	Energy measurement range		
	Energy + TOF measure	Energy-only measure	TOF-only measure
Energetic electrons	Not applicable	25 keV to 500 keV	Not applicable
Protons	25 keV to 1 MeV	Not applicable	~ 1 keV to 1 MeV
Atomic ions, e.g., CNO group, $Mg^+$ , $Si^+$ , $Ne^+$	60 keV to 1 MeV	Not applicable	15 keV to ~1 MeV/nucleon
Molecular ions e.g., $N_2^+$ , $O_2^+$	100 keV to 1 MeV	Not applicable	30 keV to ~1 MeV/nucleon

atomic mass units (AMU) for  $H^+$  (25 keV to 1 MeV),  $<5$  AMU for  $C^+/N^+/O^+$  (60 keV to 1 MeV), and  $<15$  AMU for  $Fe^+$  (60 keV to 1 MeV).

For TOF-Only measurements, the means to ascertain particle mass is less precise, and this requirement, with respect to mass resolution, is to distinguish between  $H^+$  and CNO group particles. To support derivation of species mass, for particle energies in the  $\sim 1$  keV to 1 MeV range, PEPSSI was specified to be capable of measuring particle TOF over a range of 1 to 320 ns. As TOF measurements respond to the energy-per-mass of an incident particle, these measurements can, in principle, respond to heavy ions up to  $\sim 30$  MeV total energy ( $\sim 1$  MeV/nucleon). However, such extremely high energies are not expected in the Pluto environment and the current capability of the instrument is only to deal with events with up to  $\sim 1$  MeV total energy.

**2.3.2.2 Species Mass Range** The PEPSSI instrument is constrained in downlink capability from Pluto as well as in the mass and power available for the instrument. Hence, prudent choices had to be made to meet all of the constraints while still enabling the collection of appropriate data from the vicinity of Pluto and its transmission to Earth following the flyby. Species resolution for the various energy spectra is limited by the counting statistics and the physical size of the detector that limits the TOF drift space. To enable the discrimination of solar wind particles (primarily protons and alpha particles, i.e. doubly-ionized helium nuclei) from pickup particles from Pluto, including atomic “debris” as well as ionized molecules of nitrogen, methane, and carbon monoxide, and allow for discovery science within the confines of the requirements, energy spectra are output for proton events, electron events, CNO events, and heavy particle events ( $>24$  AMU, typified by Fe).

**2.3.2.3 Sensitivity and Geometric Factor Requirements** With PEPSSI mounted on the spacecraft, including installation of the RTG power source, and with the PEPSSI covers closed, the background ion particle count rate was specified not to exceed one particle per second. Expected fluxes at Pluto are relatively low ( $\sim 100$  events per second), so to stay within low power limits of operation, the PEPSSI instrument was specified to be capable of processing at least  $10^3$  particle events per second, where this event rate is applicable to the total of all classes of measurements, i.e., Energy-plus-TOF, Ebris-Only, and TOF-Only. The PEPSSI instrument has the potential to measure particle events at a much higher rate; this rate should be established once the analysis of data from the Jupiter flyby is fully analyzed.

**2.3.2.4 Geometric Factor** Expected count rates at Pluto are unknown but expected to be low. Hence, the geometric factor was required to be as large as possible, consistent with the targeted low mass of the instrument of  $\sim 1.5$  kg.

On the basis of these trades, the PEPSSI geometric factors, for electron and ion detection, were specified to meet or exceed the values given in Table 2. The geometric factors for electron and ion detection are different because of the difference in numbers of ion and electron detectors. The values that follow apply to the entire aperture acceptance angle of  $160^\circ$  by  $12^\circ$ , i.e. the geometric factor per “pixel” is less.

**2.3.2.5 Integration Interval** Nominally, energy-plus-TOF measurements, used to determine particle species and associated energy spectra, are integrated over as low as a 1-second interval (based upon consideration of spacecraft speed, and hence spatial resolution, telemetry rates and data volume playback during the Pluto encounter). TOF measurements, used to determine particle velocity distribution, are integrated over the identical time interval. By command, the integration interval may be adjusted from 1 to 65,535 seconds.

**Table 2** PEPSSI sensor specifications

Ion detection geometric factor	$\geq 0.1 \text{ cm}^2 \text{ steradian}$
Electron detection geometric factor	$\geq 0.033 \text{ cm}^2 \text{ steradian}$
Acceptance angle	$160^\circ$ by $12^\circ$ , 6 sectors of $25^\circ$ by $12^\circ$ each, $2^\circ$ gaps between sectors
Aperture area	$0.6 \text{ cm} \times 1.2 \text{ cm}$ per sector
TOF length	6 cm nominal between entry, exit foils
Number of Detectors Per Sector	2
Detector Area	$>0.4 \text{ cm}^2$ , ion and electron detectors
Number of Ion Detectors	9
Number of Electron Detectors	3 (located in sectors 0,2,5)

### 2.3.3 Measurement Resolution Requirements

These specifications flow, in turn, to the next level of implementation requirements that drove the system design and implementation.

**2.3.3.1 Energy Resolution** As a goal, instrument energy measurement resolution, which includes the effects of all noise sources including analog-to digital converter (ADC) quantization noise, was 5 keV full-width at half maximum (FWHM) or less. As a requirement, instrument energy measurement resolution for ions was  $\sim 7$  keV or better, for electrons 8 keV or better; ADC quantization is equivalent to 1 keV. The Energy resolution is determined to a large degree by the performance of the energy-peak detector chips for the given SSD detector capacitance and leakage currents. The energy resolution of the energy-peak detector chips is a trade-off between power dissipation, mainly in the charge sensitive amplifier, and integration time of the shaper. Both parameters are fixed on the energy board with two resistors (common for all 12 channels) as described in more detail in the electronics section.

The overall energy resolution is also determined by the digital noise (mainly the ADC noise) on the energy board. The clock frequency of the temperature remote input/output (TRIO) application specific integrated circuit (ASIC) chip for the ADC can be set comparatively low, to 150 kHz, and, given the very low digital power dissipation of the chip (1 mW digital power), the system noise is within the specification levels.

**2.3.3.2 TOF Resolution** Time measurement resolution, which includes the effects of time jitter, time walk, path dispersion, and time quantization, are specified as 1 ns FWHM or less.

The time resolution is dependent on the time walk and time jitter of the constant fraction discriminator (CFD) ASIC chip and the time jitter of the time-to-digital converter (TDC) ASIC chip. The CFD time walk is  $\sim 200$ – $300$  ps for a 1:100 input energy dynamic range; the time jitter is in the range 50–100 ps depending on the power dissipation. The time jitter of the TDC chip is  $\sim 50$  ps. Thus the overall electronics time resolution is  $<500$  ps. The optimum is achieved with proper delay line selection and optimization of the power dissipation within the power budget limits.

### 2.3.4 Platform Requirements

For proper interpretation of the PEPSSI data, the instrument alignment with respect to the spacecraft and the knowledge of the spacecraft attitude are both required to  $1.5^\circ$ . For deciphering the measurements to be made at Pluto during the Pluto flyby, knowledge of spacecraft distance to Pluto is required to an accuracy of 225 km. This knowledge of position



figure is equal to roughly 1/10 the diameter of Pluto, and is achieved with the spacecraft timing system and navigation of the spacecraft at the system level.

### 2.3.5 Time Resolution Requirement

**2.3.5.1 Timetagging Requirements** For proper interpretation and processing of science data, knowledge of the data intervals over which PEPSSI science data is collected must be known to within to  $\pm 1$  second of spacecraft mission elapsed time (MET). To this end, data packets sent from PEPSSI to the command and data handling (C&DH) system are time tagged with MET time to 1-second resolution (Fountain et al. 2008). Based on spacecraft time-keeping requirements, knowledge of MET time relative to UTC time to  $\sim 10$  ms accuracy is known after the fact.

**2.3.5.2 Science Data Synchronization** PEPSSI science data (species energy spectra, velocity, and pulse-height analysis (PHA)) are collected over fixed time intervals. These data intervals are synchronized by, and time aligned with, one pulse-per-second (1PPS) timing epochs input from the spacecraft that are coincident with the MET one-second time increments.

### 2.3.6 Calibration Requirements

**2.3.6.1 Required Ground Calibration** Calibration of the PEPSSI instrument is required in order to meet instrument performance specifications. Ground calibration tests were planned using both linear accelerator facilities at APL and Van De Graff facilities located at GSFC. These facilities provide a calibrated source of electrons and a variety of ions (e.g., protons, helium, CNO, iron) at a variety of energies. Time and availability issues reduced the calibration plan to using the APL facility only. Calibration was performed with the PEPSSI instrument in vacuum at a temperature of 25°C for each sector. Calibration was performed prior to installation on the spacecraft. A calibrated alpha-particle source is installed in the collimator assembly and described below. This source was used during thermal vacuum tests to verify instrument performance has not changed.

**2.3.6.2 In-flight Calibration Characterization** Following launch, the PEPSSI instrument calibration had to be characterized during initial instrument test and prior to all major data collecting operations. To characterize the instrument, background particle data was collected and downlinked to the PEPSSI payload operations center. Archived energy and TOF measurement data in the PHA data packet, as well as particle species data, have been processed to evaluate instrument calibration. To correct for some drift in measurements, new 'look-up' tables have been configured and uplinked. Further characterization occurred during the close approach to Jupiter, using that planet's magnetospheric plasma as a calibration source. The characterization will be monitored during the yearly checkouts during the cruise to Pluto. The installed alpha-particle calibration source will also be monitored to look for any changes in instrument performance prior to arrival in Pluto-space in 2015.

**2.3.6.3 Energy Board Temperature Monitor** Energy measurements vary slightly as a function of energy board component temperature. A temperature sensor is installed on the energy board, and this temperature data is telemetered in instrument housekeeping telemetry. Energy board temperature information allows the instrument ground processing software to account for any slight errors in energy measurement due to energy-board temperature variation.

### 3 Technical Description

#### 3.1 Instrument Overview

Given the requirements, as well as ongoing lessons from the near-concurrent development of the EPS detector for the MESSENGER mission (Andrews et al. 2007), the required functionality was achieved within the prescribed constraints. These properties are given in Tables 3 and 4. Some of the numbers are still being refined based upon the final analysis of instrument performance during the New Horizons flyby of Jupiter (28 Feb 2007).

PEPSSI consists of a collimator and sensor assembly, referred to as the sensor module, which is mounted atop an electronic board stack (Figs. 3 and 4). The electronic stack consists of six metal-framed electronic boards. The stack is a cube measuring approximately 10 cm on a side. The sensor module is approximately 2 cm high and protrudes out from the stack an additional 6 cm. A simplified block diagram of the PEPSSI instrument is shown in Fig. 5. The corresponding simplified schematic for operation is shown in Fig. 6.

**Table 3** PEPSSI performance parameters

Geometric Factor (Start Foil)	0.15 cm <sup>2</sup> sr	
Geometric Factor (each Electron Pixel)	0.011 cm <sup>2</sup> sr	
Geometric Factor (each Ion Pixel)	0.013 cm <sup>2</sup> sr	
Electron Efficiency vs. Energy	Est. roughly at 100% at mid energies	
Low Energy Ion Efficiency vs. $En \times M$	>4% details in Sects. 4.3.3.6 and 4.4.2	
High Energy Ion Efficiency vs. $En \times M$	>4% details in Sects. 4.3.3.6 and 4.4.2	
Energy Coverage	See Table 4	
$\Delta E/E$ capability at 50 keV	14%	
$\Delta E/E$ capability at >100 keV	10%	
Energy/TOF Channel resolution	250 eV/167 ps Granularity	
TOF dispersive spread	2.5 to 3.5 ns (expected)	
Mass Species Separation	See Table 4	
Angular Coverage (total)	160° × 12°	
Angular Coverage (Electrons)	147° × 12°	
Angular Coverage (Low Energy Ions)	160° × 12°	
Angular Coverage (High Energy Ions)	147° × 12°	
Angular Coverage (Diagnostic Ions)	147° × 12°	
Angular Pixels (Electrons)	12° × 27° (13° with 13.6° gap)	
Angular Pixels (Low Energy Ions)	12° × 30° (full ~27° coverage)	
Angular Pixels (High Energy Ions)	12° × 27° (13° with 13.6° gap)	
Angular Pixels (Diagnostic Ions)	12° × 27° (13° with 13.6° gap)	
Electron Scattering Angle Contrast	Several percent	
Energy Coverage:	Technique	
Electrons	25 keV–500 keV	Singles/Foil Technique
Low Energy Ions	1 keV–1 MeV	TOF Only
Low Energy CNO	15 keV–1 MeV	PH-based mass discrimination
High Energy Protons	40 keV–1 MeV	TOF vs. Energy
High Energy CNO	100 keV–1.2 MeV	TOF vs. Energy

**Table 4** Final PEPSSI flight parameters and assessment against requirements

Parameter	Requirement	Measured or derived from measurements	Comments
<b>Engineering Parameters</b>			
Mass	<1.5 kg	1.475 kg	Measured at delivery
Power Average	2.55 W	2.49 W	Not including heater power
Power Peak	same	2.51 W	Additional power needed one time to deploy cover
Data Volume	<135 bps	91 bps	With FAST Compression
Size	<1200 cm <sup>3</sup>	352 cm <sup>3</sup>	Includes sunshade and mounting tabs/structures
<b>Performance Parameters</b>			
Geometric Factor	>0.1 cm <sup>2</sup> sr	0.15 cm <sup>2</sup> sr	Calculated: PDR
Ion Energy Range	15 keV/ <i>n</i> to 1 MeV/ <i>n</i>	~1 keV/ <i>n</i> to 1 MeV/ <i>n</i>	Lowest energies with TOF-only, as expected
Electron Energies	25 to 500 keV	25 to 500 keV	Not verified in calibration
Energy Resolution	10 keV	<5 keV	
Species	H, He, CNO, e <sup>-</sup>	H, He, CNO, Fe, e <sup>-</sup>	
Field-of-View	160° × 12°	160° × 12°	
Angular Resolution	25° × 12°	25° × 12°	
TOF Range	1–320 ns	1–320 ns	Verified electronically
TOF Resolution	<5 ns	<4 ns (FWHM)	
Integration period	10 s adjustable	10 s default	Programmable from 1 to 65,535 s

As shown in the block diagram, the sensor module includes a time-of-flight (TOF) section 6 cm long feeding a solid-state Si detector (SSD) array. The SSD array is connected to the energy board and measures particle energy. Secondary electrons, generated by ions passing through the entry and exit foils, are detected to measure ion TOF. Event energy and TOF measurements are combined to derive mass and to identify particle species.

While PEPSSI uses the same type of energy and time-of-flight measurement scheme as the previous such instruments mentioned above, it also employs multiple (six) angular apertures in a swath in order to provide angular information without relying upon either a mechanical scanning mechanism or the rotation of the spacecraft. The PEPSSI acceptance angle is fan-like and measures 160° by 12° with six 25° segments. Each segment is separated by a 2° gap. Its total ion geometric factor is greater than 0.1 cm<sup>2</sup> sr. Particle direction is determined by the particular 25° sector in which it is detected. The angular resolution of the instrument was required to determine the incoming direction to better than 40° for the ions in each of the six sectors, i.e., within a 25° by 12° window. Electron particle direction is limited to sector 0, sector 2, and sector 5.

N.B. The expected (atmospheric) species to dominate at Pluto are N<sub>2</sub><sup>+</sup>, CH<sub>4</sub><sup>+</sup>, and associated breakup products, e.g. N<sup>+</sup>. Accelerated protons from the solar wind (H<sup>+</sup>) are also likely to be seen. Fe<sup>+</sup> (at 56 AMU) is not expected from Pluto, but indicates the potential mass coverage of the instrument. Ar<sup>+</sup> (40 AMU) may be present, albeit at low concentrations, but is within the mass coverage; see discussion of Sect. 2.3.2.2.

The entrance apertures for the axially symmetric TOF section are 6 mm wide. A 50 Å aluminum/350 Å polyimide/50 Å aluminum composite foil covers each aperture. These

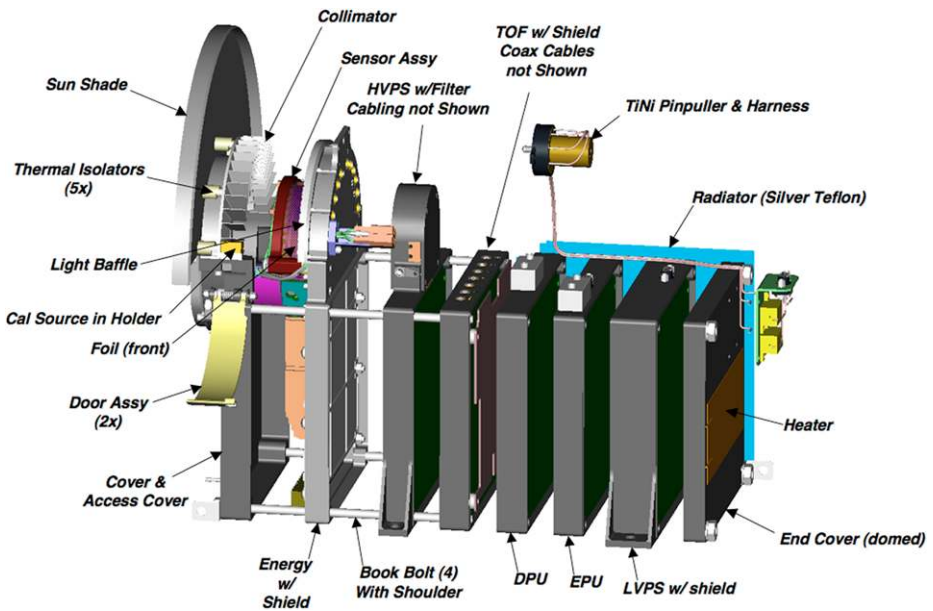


**Fig. 3** Expanded view of the PEPSSI instrument showing, *left to right*: sunshade, collimator assembly (with acoustic doors open—flight configuration), sensor assembly, and electronics boards stack

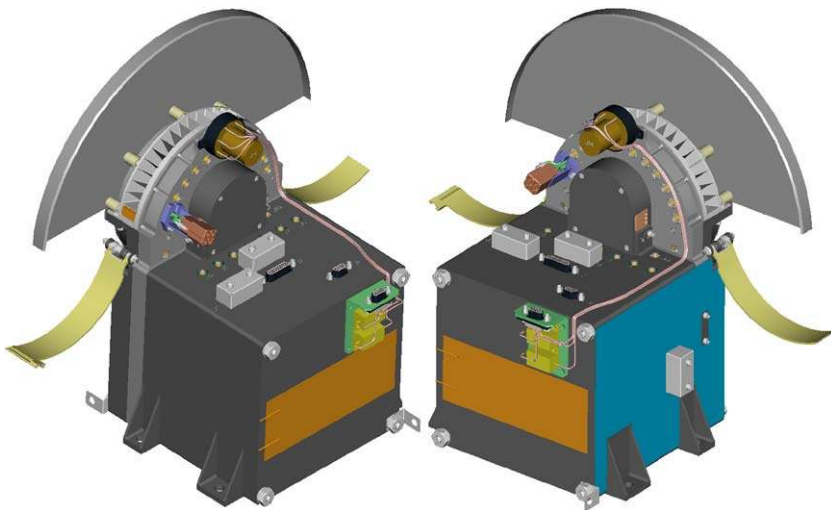


**Fig. 4** Assembled view of the sensor, again in flight configuration

foils reduce the TOF UV Lyman-alpha photon background. A 50 Å palladium/500 Å polyimide/50 Å palladium foil covers the exit apertures. Both entrance and exit aperture foils are mounted on a high-transmittance stainless steel grid supported on a stainless steel frame.

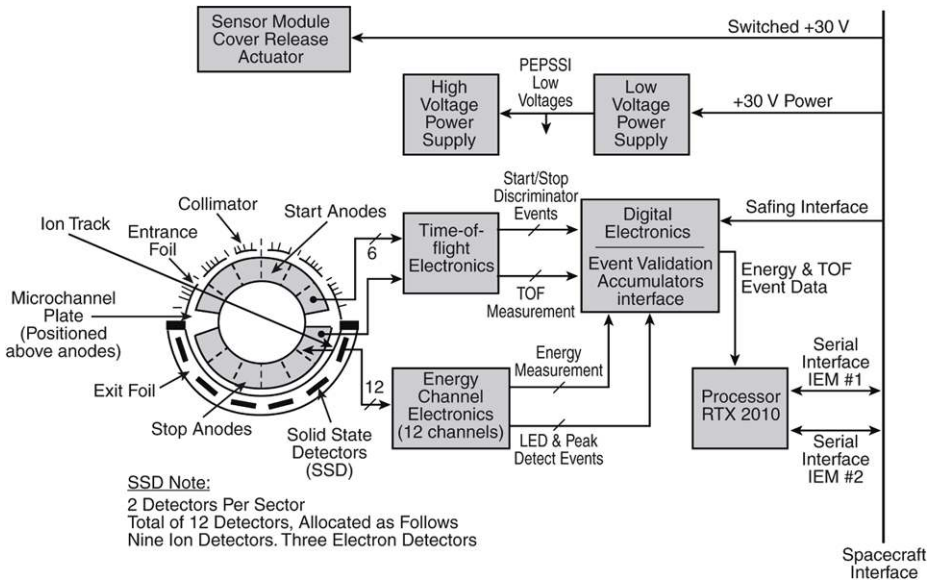


**Fig. 5** Simplified block diagram of the PEPSSI instrument. Flow of information from the sensor to the spacecraft interface is shown

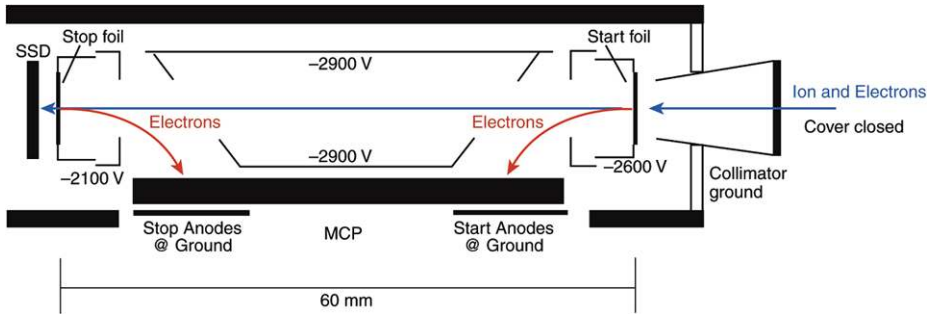


**Fig. 6** Simplified operation of the PEPSSI sensor (1 of 6 shown). Incoming ions and electrons pass through the collimator assembly hitting the “start” foil and ejecting secondary electrons. The start electrons hit the start anode flagging the time-of-flight start. The incoming particles cross the 6-cm drift space and then hit the stop foil, again ejecting secondary electrons that hit the stop anode. The incoming particle then hits the SSD where its total energy is recorded. The electronics detect and classify both nominal events and valid “triples” (that have valid start, stop, and energy signals within appropriate electronic windows such that the incoming particle can be fully categorized)

### 3.1.1 Differences from EPS on MESSENGER

The MESSENGER EPS unit was the first flight unit of this miniaturized “hockey-puck” design. PEPSSI presented different requirements with respect to available power and maximum count rates. While larger rates were anticipated for the encounter with Jupiter and could be used to good advantage for some calibration activities, PEPSSI requirements have always been focused at the conditions near Pluto. In addition, the launch of New Horizons

over two years after that of MESSENGER allowed for some upgrades to be included in the PEPSSI unit.

The combination of lower expected counting rates and the need to save power led to the implementation of (1) lower-current MCPs, (2) a new high-efficiency, low-voltage power supply (LVPS) with a complete custom converter design to save power, (3) a new energy board using new application-specific-integrated-circuit (ASIC) chips to save power, and (4) a redesigned TOF board with different amplifiers and delay lines to achieve higher gain.

With the need for long-term reliability during the cruise to Pluto, PEPSSI enabled a high-voltage (HV) safing system, which is usually active (such a system is also on EPS but causes significant cross-talk with the SSDs if active; the safing system on PEPSSI has not tripped to the date). This system samples the HV current 1000 times per second, and shuts down the supply if the HV current exceeds a threshold; it is inactive only during HV ramp up and ramp down, and then only momentarily for each step. A different HVPS driver is used on PEPSSI that provides improved performance (not incorporated on EPS due to the MESSENGER launch schedule). The PEPSSI unit also incorporates a buffer amplifier and a filter, neither of which are present in the EPS unit.

The EPS instrument has 24 detectors: six large detectors for ions, six large detectors for electrons, and corresponding small detectors as well. There are six processing chains for the ions and six for the electrons, with small or large detector usage dictated by ground command. The particle flux in the outer heliosphere in general, and near Pluto in particular is expected to be much lower than near Mercury and less variable. To ensure detection of the lowest fluxes PEPSSI uses only 12 detectors (small and large pixels as laid out on EPS and electrically tied together) and uses only three electron detectors to increase the geometric factor for the ions.

The front-end collimator is more open on PEPSSI than on EPS to increase the geometric factor, and PEPSSI also has an added sunshade to be able to look back near the solar direction (EPS is mounted well away from the Sun-looking direction on the MESSENGER spacecraft due to the high solar luminosity at Mercury's perihelion).

EPS is thermally isolated from the MESSENGER spacecraft with a separate thermal radiator to reject internal heat to space, while PEPSSI is quasi-thermally coupled to the spacecraft-mounting bracket (conductively isolated but radiatively coupled). Furthermore, the EPS thermal design uses heaters and mechanical thermostats to keep the instrument from getting too cold, while PEPSSI relies on the spacecraft to keep it sufficiently warm (a "hibernation" operational heater was installed as a precaution).

### 3.2 Mechanical Design

Top-level mechanical design requirements and design factors of safety are in accord with those used throughout the New Horizons project. In particular, the PEPSSI instrument was designed to withstand a quasi-static load limit of 30 g along three orthogonal axes (applicable to the primary structure design and as multiplied by the appropriate factor of safety). In addition, first mode structural frequencies were specified to be above 70 Hz in the spacecraft thrust direction and above 50 Hz in the lateral directions and the instrument was designed to withstand a maximum pressure rate change of 1.0 psi/s. All of these specifications were verified during environmental tests.

#### 3.2.1 Dimensions and Mounting

The PEPSSI envelope is 19.7 cm × 14.7 cm × 21.6 cm as installed and 25.1 cm × 14.7 cm × 21.6 cm following the one-time opening of the acoustic doors. The instrument itself is

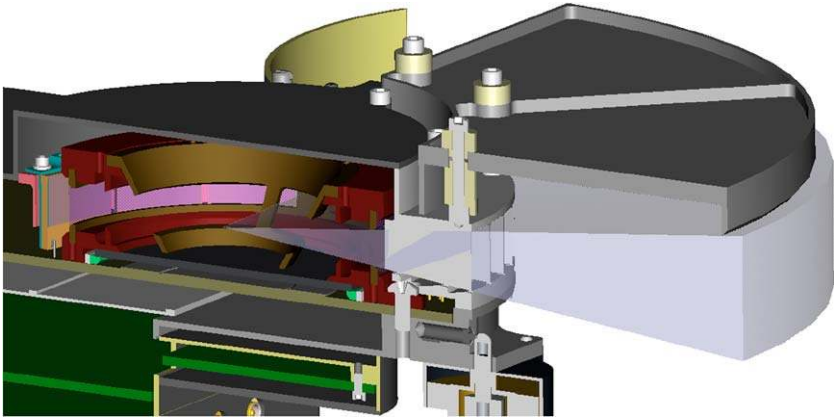
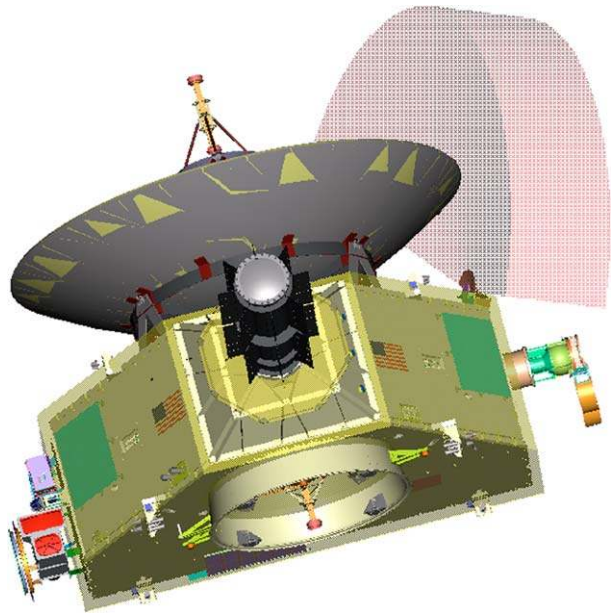


**Fig. 7** Cutaway view of the PEPSSI sensor showing the FOV defined by the internal sensor structure, collimator assembly, and Sun-shade (*top*)

**Fig. 8** Location of PEPSSI on the New Horizons spacecraft. The *lightly shaded area* denotes the PEPSSI Field-of-View (FOV)



mounted on a bracket that provides for a complex angular offset of the field of view (FOV) of the viewing fan from any of the spacecraft decks (Figs. 1, 7, and 10).

The complex angular offset was employed to optimize the viewing of freshly ionized pick-up ions in the vicinity of Pluto due to charge exchange with neutrals from Pluto's atmosphere. This allows for the instrument to be mounted to the spacecraft deck while looking past the high gain antenna (HGA) but not being obscured by it (Fig. 8).

Alignment for PEPSSI's FOV on the observatory's top deck was determined by the design and location of its mounting bracket. Alignment control was to be kept within  $1.5^\circ$  of the Euler angle rotations defining the bracket's mounting surface. Knowledge of PEPSSI's FOV was specified to be within  $1.5^\circ$  of the observatory's coordinate system, as referenced

**Fig. 9** The PEPSSI FOV in angular coordinates referenced to the main deck of the spacecraft. The shaded area above the FOV traces indicates the HGA and the shaded area to the right indicates the body of the spacecraft. The red line indicates the Sun shield, the red dot the location of the Sun and the P and C (near the center) the locations of Pluto and Charon in August 2006

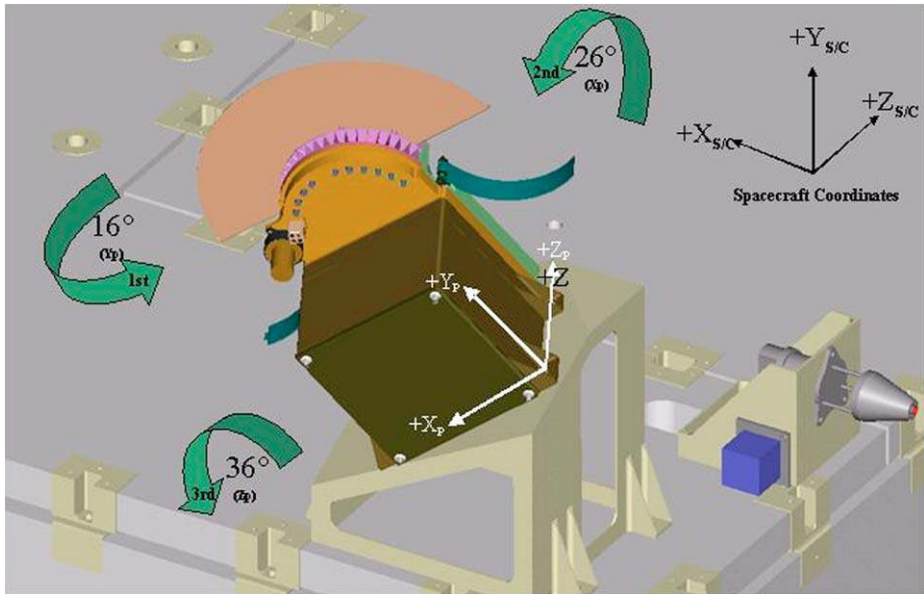
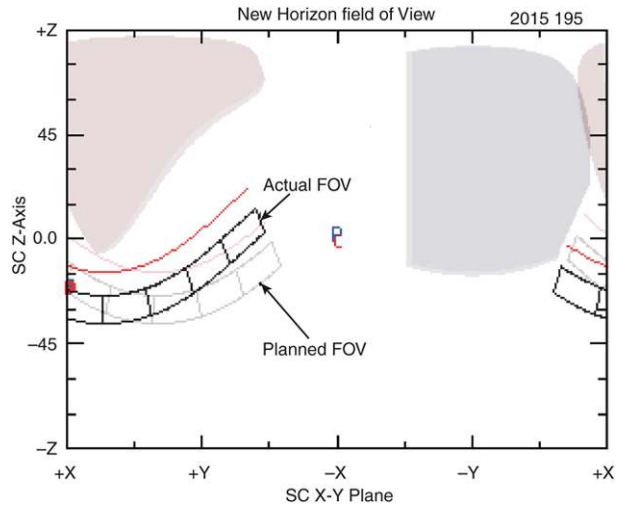


**Fig. 10** PEPSSI mounting orientation with respect to the New Horizons deck

to the orthogonal plane surfaces of the PEPSSI instrument. An error in interpretation of the one of the interface control documents (ICDs) led to a misalignment in the bracket surface as manufactured. Figure 9 shows the planned and actual fields of view in the coordinate system of the observatory, i.e., the New Horizons spacecraft.

With this FOV PEPSSI points at an off-angle to the Sun during spacecraft downlink operations and most of Pluto flyby operations. (The HGA points towards the Earth, along the +Y axis, during downlink operations). This allows PEPSSI to detect pickup ions, coming from the general direction of the Sun, while keeping the Sun out of the FOV.



There are no rigid requirements to keep the Sun out of the instrument FOV; however, for normal operation the Sun should be  $\sim 10^\circ$  from the instrument boresight. In the event the Sun is in the instrument FOV, no damage to the instrument will occur. However, the flood of energetic photons may cause a degradation of both energy and TOF measurements. An initial approach for mitigating these effects, in the event the Sun was in the FOV, was to disable individual start and stop that would be affected. This approach was abandoned during development due to reliability concerns with the switches required for its implementation. Enhanced count rates due to the presence of the Sun in the FOV was what led to the mapping of the actual FOV. For heliocentric distances beyond  $\sim 10$  AU, the low solar intensity is no longer an instrument health and safety concern.

PEPSSI is mounted to the spacecraft's top panel with four (4) #8-32 stainless-steel screws into threaded inserts on a dedicated spacecraft-designed mounting bracket. The instrument is thermally isolated from the bracket by thermal washers between the bracket and PEPSSI's mounting tabs. PEPSSI's alignment and repeatability of mounting with respect to the observatory's coordinate system was satisfied by dimensional tolerancing and position of the mounting holes in the bracket and on the spacecraft.

### 3.2.2 *Mass Properties*

The mass budget for the PEPSSI instrument was 1500 grams, including 120 grams of margin. This mass included all sensor pieces as well as the mounting bolts and was worked to on a board-by-board basis (including the metal framing for the boards). The measured sensor mass at delivery to the spacecraft was 1475 g.

### 3.2.3 *Deployable Cover*

The PEPSSI design includes two cover doors installed over the instrument aperture. One purpose of the instrument covers is to prevent acoustic (air pressure) damage to the thin entry/exit foils within the sensor module during launch. Another is to keep out air-borne dust and contaminants during instrument ground test. During all ground operations and storage, except functional test of cover release, the aperture covers were maintained in place to prevent damage to the entry/exit foils and to prevent contamination of the MCP.

The covers are crescent shaped and each covers one-half of the  $160^\circ$  aperture angle. Each cover is mounted at one end on a hinge bracket assembly that includes a Mandrel with torsion spring. In the closed position an actuator pin holds the covers in place. To open the covers, the actuator is fired to retract the retaining pin, allowing the covers to spring open. A spacecraft command must be sent to fire the actuator. Once open, the covers are maintained in the open position by torsion-spring action. To allow for ground tests (e.g., EMI tests) with the covers open, the actuator used to pin the doors closed was capable of at least 100 cycles of operation.

Cover opening was tested for correct actuator function in a vacuum chamber prior to flight. The covers were opened in flight on 3 May 2006.

### 3.2.4 *Instrument Purge*

The PEPSSI instrument interface included a purge manifold. Once PEPSSI was assembled with the MCP, it required constant purge with at least MIL-P-27401D Grade C (99.995% pure) nitrogen, at a flow rate of 0.1 liters/minute.

The purge system was capable of being disabled for a short period of time (up to 30 minutes) while in a class 10,000 or better clean room. Records were maintained of all periods when purge had either been removed or failed.

### 3.2.5 Handling Requirements

The PEPSSI instrument was kept under purge at all times, except during test in vacuum chambers. The PEPSSI door remained closed to protect the entry and exit foils. When open, all airflow toward the foils, including breath, was prevented. As long as the cover is closed and the unit is being purged, it could be in any normal room environment.

Proper procedures and equipment to eliminate the risk of electrostatic discharge were followed and used. The collimator was not cleaned or handled in any manner, and the cleaning of the outside cover was minimized.

A high-voltage power supply (HVPS) safing plug was included and removed prior to launch. In addition, a cover-release arming-plug was installed before launch to enable cover release commands in space.

### 3.2.6 Transportation and Storage

The PEPSSI instrument required a shipping container to provide protection during transportation and storage. The instrument was constrained and padded within the container, which is airtight and was purged with dry nitrogen and sealed, to minimize vibration and shock during transport.

### 3.2.7 Vacuum and Outgassing Requirement

The PEPSSI HVPS was required to be turned on to full voltage only in a vacuum environment  $<3 \times 10^{-6}$  Torr. As a consequence, the HVPS could not be activated until sufficient time in vacuum had elapsed for spacecraft and instrument outgassing. A high concentration of outgassing products and particles could contaminate the MCP under high-voltage conditions, so outgas products must be at a sufficiently low level for safe turn-on of the HVPS.

Before launch, during both instrument-level and spacecraft-level thermal-vacuum tests, appropriate detectors were placed inside the test chamber to monitor outgas products. During spacecraft-level testing, 24 hours of time in vacuum (at  $<3 \times 10^{-6}$  Torr) was required before the HVPS could be safely turned on. During instrument-level test, the test conductor determined when it was safe to turn on the HVPS. Prior to HVPS activation, the PEPSSI instrument could be (and was) powered on for low-level engineering level checkout. At full atmosphere, during instrument and spacecraft level testing, the HVPS voltage (applied to the MCP) was kept less than 700 volts. After the New Horizons launch, the requirement was for at least two weeks to pass prior to first activation of the HVPS. The PEPSSI instrument was powered earlier (with HVPS off) to allow for initial checkout (20–22 Feb 2006) and engineering-level checks (1–2 Mar, 27 Apr, and 2 May 2006).

## 3.3 Detectors and Electronics

Power as initially allocated to the instrument took into account the limited resources on the spacecraft. Referenced to the +30 V input the peak power specifications were  $<2000$  mW in science mode and  $<1750$  mW for the high voltage power supply (HVPS) disabled. During development, these numbers were found not to be realizable without extensive additional development. To remain within financial resources a request was granted to raise the allowable power required by 550 mW.

### 3.3.1 Energy Measure

Each SSD sector in the sensor module has 2 detectors. In sectors 0, 2, 5, one detects ions, the other electrons. The electron detectors are covered with a 1- $\mu\text{m}$  Al layer, to block low-energy protons and heavier ions. The detector pairs in sectors 1, 3, 4 are just ion detectors. A key to the electronics and functional layout is given in Fig. 11. The electron detectors measure energetic electrons from 25 keV to 500 keV. The Al layer blocks protons and ion particles with energies less than 100 keV, and particle energy levels above 100 keV are expected to be rare in the near-Pluto environment. For those rare events, where ion energy levels exceed 100 keV, coincident TOF measurements will be used to discriminate between ions and energetic electrons.

Ion energy measurements using the ion detectors are combined with coincident TOF measurements to derive particle mass and identify particle species. Particle energy for protons greater than 25 keV and heavy ions (such as the CNO group) greater than 60 keV are measured, up to a maximum of 1 MeV. Lower-energy ion fluxes are measured using TOF-Only measurements; detection of micro-channel plate (MCP) pulse height provides a coarse indication of low-energy particle mass.

### 3.3.2 Time-of-Flight Measure

Before an ion passes through the TOF head, it is first accelerated by a 2.6-kV potential. Secondary electrons from the foils are electrostatically separated on the MCP, providing start and stop signals for TOF measurements. The segmented MCP anode, with one start

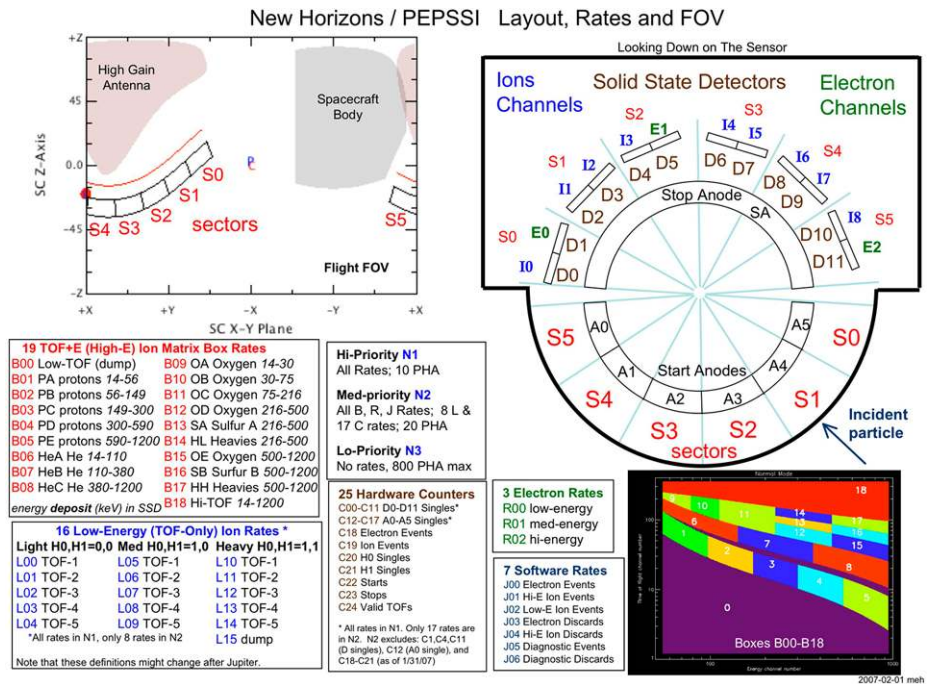


**Fig. 11** Schematic layout of PEPSSI showing the nominal FOV and detectors and rates for the various modes and channels

**Table 5** Electronics boards in the PEPSSI instrument

PEPSSI board	Board function(s)
Energy Board	Amplify SSD event signals (12 channels—signal proportional to particle energy) and digitize (10 bits). The measurement is achieved with low-power, low-noise Energy (CSA + Shaper)—Peak Detector ASICs
TOF Board	Amplify start (six) and stop anode signals, compute TOF (time duration between start and stop anode signals). The measurement is achieved with the low-power, low-jitter, and low-walk TOF chip (CFD + TDC)
HVPS Board	Provide high voltage to entry/exit foils (−2600 V), MCP (−2100 V and −100 V), deflector plates (−2900 V), and SSD bias voltage (−100 V)
Digital (Interface) Board	Event validation logic; energy and TOF event counters; interface functions
Events Processor Board	Command and Telemetry communications to spacecraft; events processing
LVPS Board	Supply ±15 V, ±5 V, 2.5 V to electronic boards

anode for each of the six angular segments, determines the direction of travel, particularly for lower-energy ions that do not yield an SSD signal above threshold. A nominal 500-volt accelerating potential between the foil and the MCP surface controls the electrostatic steering of secondary electrons. The dispersion in transit time is less than 400 picoseconds (ps).

### 3.3.3 Electronics

The six electronics boards in the electronics stack (cf. Fig. 3) each provide a specific function for the instrument (Table 5). The common board size has also been used on other APL spacecraft subsystems, notable the electronics for the (redundant) digital processing units and several of the instruments on the MESSENGER spacecraft (Gold et al. 2001).

### 3.3.4 Operation

**3.3.4.1 Science Mode** In the science mode, three basic classes of measurements are concurrently made. The first class, called TOF-plus-Energy, uses SSD measurements in coincidence with TOF measurements to determine energetic ion particle mass (species) and associated energy spectra. Measurements are collected from six different sectors and particle direction to a particular 25° by 12° sector is determined by the start sector.

The second class of measurement is referred to as TOF-Only. It is a measure of ion particle velocity based on the TOF measurement and is made if no coincident energy event is detected at the SSDs. Particle composition is categorized as light (protons), medium (mass < CNO), or heavy (mass ≥ CNO). These measurements occur if the ion particle energy is below the energy threshold of the SSD detector.

The third class of measurements consists of Energy-Only measurements of particles where the SSD measurement event is not coincident with any TOF measurement event. These measurements include electron energy measurements, where transit time of electrons through the TOF chamber is, for practical purposes, zero, as well as ion energy measurements made when the ion fails to generate any secondary electrons (for TOF measurement).

**3.3.4.2 HVPS Activation** The high voltage (HV) supply of the HVPS can only be turned on in vacuum ( $<3 \times 10^{-6}$  Torr). If the HV supply had been turned on accidentally during ground test in air, the MCP could have been degraded. Therefore, when the PEPSSI instrument was powered up on the ground, the HVPS (consisting of HV and bias power supply)

was disabled and no science data was collected. A sequence of instrument commands is required to enable the HVPS, fine-tune voltages, and tweak HVPS clock frequency for optimum efficiency. Valid science data is output after the HVPS command sequence has been executed and science data enabled.

**3.3.4.3 Cover Door Open** At first power-up on orbit, the PEPSSI covers are in the closed position. A spacecraft command must be sent to fire the actuator and open the front covers. Once open, the covers remain open indefinitely, and no cover release commands are required at any subsequent turn-on of the instrument.

**3.3.4.4 Test Mode** The instrument can implement a test mode that allows for data input and output through a test port instead of the C&DH communication ports. This is strictly for use during instrument software development pre-flight and is not for spacecraft level test or for use in space operations.

**3.3.4.5 Calibration** Ground-based calibration was performed with the instrument in a dedicated calibration mode (“diagnostic mode”). Based on an evaluation of telemetered energy and TOF data, instrument calibration tables were configured and subsequently loaded into the instrument.

### 3.3.5 Electrical Interface

There are five electrical interfaces from PEPSSI back to the spacecraft. Only the power and command and telemetry interfaces are still of use. The others were used for ground testing, safing, and the deployment of the cover that occurred as part of the overall commissioning.

The PEPSSI instrument does not require a survival heater for operation. However, PEPSSI does require a spacecraft-provided and controlled heater that can be powered during cruise phase when observatory power is available. The heater provides thermal margin, if required, and dissipates 1 watt when switched on.

**3.3.5.1 PEPSSI Power Interface** Switched power is provided to PEPSSI at 30 volts nominal and is regulated to within  $\pm 1$  volt of nominal. Primary power is supplied to the PEPSSI support electronics through a separate dedicated connector that has no signal or secondary lines. Total power consumed by PEPSSI was initially specified to be 2 watts or less, but was later increased during the design process.

There are specifications regarding input voltage characteristics (operating and survival) regarding regulation, input voltage ripple, source voltage transients, source impedance, and voltage turn-on/turn-off rates. Inrush current transients at power turn-on and power turn-off imposed on the instrument are also specified. The instrument was designed and tested to operate over and survive respective voltage operating conditions as required.

**3.3.5.2 PEPSSI Command and Telemetry Interface** PEPSSI implements a low-speed command and telemetry interface circuit that conforms to the EIA RS-422 standard for serial data transmission. The low-speed buses for PEPSSI each consist of three circuits: a 1-pulse/second (1PPS) sync signal, a command circuit, and a telemetry circuit.

PEPSSI implements two RS-422 bi-directional universal asynchronous receive and transmit (UART) ports to the spacecraft. The first port connects to the spacecraft C&DH system located in the integrated electronics module (IEM) #1, and the second port connects to the spacecraft C&DH system located in IEM #2. Normally, only one of the two IEMs is active, and PEPSSI responds to and interacts with the active IEM (Fountain et al. 2008).

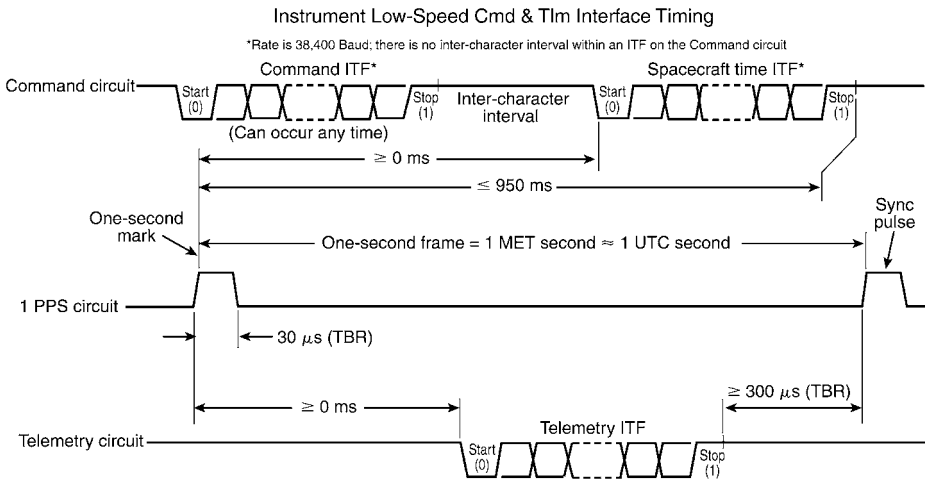


**Fig. 12** PEPSSI command and telemetry timing

The serial ports are bi-directional and PEPSSI is capable of simultaneously sending and receiving at 38.4 k baud rate with 8 data bits, no parity, 1 start bit, and 1 stop bit. The least significant bit of each byte is sent first. For multi-byte values, “big endian” format is used, where the most significant byte is sent first; the least significant bit is referred to as “b0”. PEPSSI receives instrument commands and MET time from the spacecraft over this port, and sends instrument science and housekeeping data to the spacecraft. Data sent to the spacecraft is normally recorded in the SSR of the respective IEM for latter downlink to the ground station.

The active IEM and PEPSSI exchange messages over the UART using the standard UART protocol to govern the lower-level aspects of the transfer. A higher-level construct, an Instrument Transfer Frame (ITF) protocol, is used for higher-level synchronization and error control. The IEM provides PEPSSI with command messages and spacecraft time messages. PEPSSI provides the IEM with TLM messages that contain instrument state data as well as science data. PEPSSI does not exchange messages with any other instrument and every message to or from PEPSSI is contained within an ITF.

In addition to Transmit (to spacecraft) and Receive (from spacecraft) signal lines, each port includes the 1PPS signal input to PEPSSI. This signal provides nominal one-second timing information; command and telemetry transfer is synchronized to 1PPS epochs as illustrated in Fig. 12.

Commands, instrument telemetry, and MET time are packed in the ITF format that is described below. This frame is defined by the time between the rising edges of any two adjacent 1PPS signals. Command and telemetry data frames are transferred as a serial 8-bit byte stream.

MET time is transferred from the spacecraft to PEPSSI over each one-second interval. MET time is transferred to 1-second precision and is valid when the 1PPS signal is asserted. MET time is transferred within 0 to 950 ms following each 1PPS.

PEPSSI telemetry data may be transferred anytime between 1PPS epochs except when the 1PPS rising edge occurs. All telemetry transmissions terminate 300  $\mu$ s prior to the rising edge of the 1PPS. All three signals (Transmit, Receive, 1PPS) are implemented as complementary RS-422 electrical standard interfaces.

PEPSSI sends a number of different science and housekeeping data products to the spacecraft. These products are packed in CCSDS telemetry packet format. A number of CCSDS telemetry packets may be included in each telemetry ITF sent to the spacecraft.

**3.3.5.3 Test Port Interface** For early hardware and software development, PEPSSI implemented an RS-232 protocol test interface to the instrument processor. However this was intended only for early development and test and was not accessed at the spacecraft level of integration and test.

**3.3.5.4 HVPS Safing** The PEPSSI HVPS could be safely turned on to full level only when the instrument is in vacuum. Damage to the MCP may result if high voltage power is applied at atmospheric or partial atmospheric pressures. To prevent accidental turn-on of the HVPS, the PEPSSI instrument was designed to accept a safing plug connection—installation of the safing plug was required to disable HVPS operation. The safing plug was removed before launch to enable on-orbit HVPS operation.

**3.3.5.5 PEPSSI Cover Release** The PEPSSI design includes a cover for the instrument aperture. One purpose of this cover is to protect the instrument foils during ground vibration and acoustic shock tests. Prior to launch, the cover is opened only during T-V, calibration, and special cover tests; the cover remained closed at all other times. The instrument cover is opened by spacecraft command. The spacecraft command system and associated spacecraft ground support equipment (GSE) included implementation of an arming plug. The arming plug was removed during ground system test to prevent accidental opening of the cover and then installed before launch to enable on-orbit cover release operation.

The spacecraft provided a one-time activation signal to open the cover. An electrical non-explosive shape memory alloy (SMA) pin-puller is incorporated in the instrument and was used for the release. The SMA pin-puller employs redundant circuitry. Each circuit requires a current load of between 0.5 to 2.0 amps at 30 VDC. Depending upon the operational load selected, the spacecraft power distribution unit could apply this power for a minimum of 200 ms. The pin-puller employs an auto shut-off switch removing power after it has activated, approximately 100 ms after power is applied. The cover has been successfully opened, and this feature will no longer be used.

## 3.4 Telemetered Data Products

### 3.4.1 Proton and Electron Energy Spectra

In the energy spectra data for detected electron, proton, and heavy ion particles each energy bin corresponds to a particular particle energy range (defined in the software data base look-up Table 6), and the telemetered value represents the number of particles detected in the respective energy bin. The initial look-up table that defines the energy bin coordinates for each particle was determined and loaded during pre-launch instrument calibration.

Ion particle data is output for each of six sectors; electron data is output for each of three sectors. The integration interval, i.e., the time interval over which the data is collected, is nominally 10 seconds, but data integration interval may be changed by command from 1 second to 65,535 seconds.

For those sectors that include an electron detector (sectors 0, 2, 5), the number of ion events counted in each energy bin represents the number of ion particles impinging on the respective single ion detector. For those sectors that include ion detector pairs (sectors 1, 3, 4), the number of ion events counted in each energy bin represents the sum of ion particles impinging on the respective ion detector pair.

**Table 6** Proton/electron/heavy ion energy spectra data products

Species	Number of energy bins	Bits per bin	Scaling	Number of sectors	Number of bits per integration interval
Electrons	3	10	Log compressed, 5-bit mantissa, 5-bit exponent, base 2	3	90
Protons	6	10		6	360
Heavy Ions (>1 AMU)	4	10		6	240
Total bits per integration interval→					690

**Table 7** Heavy ion energy spectra

Species	Number of energy bins	Bits per bin	Scaling	Number of sectors	Number of bits per integration interval
CNO	6	10	Log compressed, 5-bit mantissa, 5-bit exponent, Base 2	6	360
N <sub>2</sub>	3	10		6	180
Total bits per integration interval→					540

### 3.4.2 Heavy Ion Energy Spectra

The energy spectra data for heavy ions, output from each of six sectors, is conditional; it is output only if the particle event rate exceeds a predefined threshold (Table 7). The event rate threshold includes hysteresis, so that once heavy ion spectra data is output, the event rate must drop to a somewhat lower value for output to cease. The particle event rate threshold is programmable by instrument command and is typically set at 100 particle events per second. The data integration interval, nominally 10 seconds, is identical to the integration time interval for all other spectra type data. It may be adjusted by instrument command over a range of 1 to 65,535 seconds.

For those sectors that include an electron detector (sectors 0, 2, 5), the number of heavy ion events counted in each energy bin represents the number of ion particles impinging on the respective single ion detector. For those sectors that include ion detector pairs (sectors 1, 3, 4), the number of heavy ion events counted in each energy bin represents the number of ion particles impinging on the respective pair of SSD ion detectors.

### 3.4.3 TOF-Only Velocity Spectra

Particle velocity spectra data, derived from TOF-only measurements are comprised of three sets of particle velocity data corresponding to particle mass categorized as light, medium, or heavy (Table 8). The two stop-anode discriminators are employed to differentiate between light, medium, and heavy particles. The discriminator threshold settings normally are set so that light particles correspond to protons, medium particles correspond to the CNO group, and heavy particles correspond to particles with mass greater than the CNO group. Similar to heavy ion spectra, particle velocity spectra data is output only if the particle event rate exceeds a predefined threshold. As with the other products just mentioned, the data integration interval, nominally 10 seconds, is identical to the integration time interval for all



**Table 8** TOF-only velocity spectra

Mass category	Number of spectral bins	Bits per bin	Scaling	Range	Number of sectors	Number of bits per integration interval
Light	5	10	Units = km/s	200 km/s	6	300
Medium	5	10	Log compressed, 5-bit mantissa,	to 2000 km/s	6	300
Heavy	5	10	5-bit exponent, base 2	spanning 5 bins	6	300
Total bits per integration interval→						900

**Table 9** Singles event data (event validity check)

Event description	Number of event counters	Bits per counter	Number of count bits	Scaling
SSD Leading Edge Discriminator—Ion Event	9	10	90	Log compressed, 5-bit mantissa, 5-bit exponent, base 2
SSD Leading Edge Discriminator—Electron Event	3	10	30	
SSD Peak Detector—Ion Event	9	10	90	
SSD Peak Detector—Electron Event	3	10	30	Log compressed, 5-bit mantissa, 5-bit exponent, base 2
Start Anode Discriminator Event	6	10	60	
CFD Start Event	1	10	10	
CFD Stop Event	1	10	10	
Valid TOF Events	1	10	10	
Ion Events	1	10	10	
Electron Events	1	10	10	
Software Counters	3	10	30	
Total data bit count per integration interval →			380	

other spectra type data. It may be adjusted by instrument command over a range of 1 to 65,535 seconds.

#### 3.4.4 Singles-Event Data (for Event Validity Check)

To allow validation of instrument science data, PEPSSI counts and telemeters a number of instrument single events (Table 9). Single-event data is collected over the same identical data integration intervals as ion-energy spectra and velocity spectra data. It is nominally 10 seconds, but may be adjusted by instrument command over a range of 1 to 65,535 seconds.

#### 3.4.5 PHA (Pulse Height Analysis) Event Data

Detailed particle event data are retained for a sub-set of the total number of events due to data volume limitations on the SSR (Table 10). A rotating priority scheme is used to save the most important data and done for each of the data types using integration intervals,

**Table 10** PHA event data

Data item	Description	Number of bits
TOF [units = ns]	Particle TOF Measurement. All zero fill for energy-only events. Log Compressed Scaling	8
Energy [units = keV]	Particle energy measurement. All zero fill for TOF-only events. Log Compressed Scaling	8
Ion sector	SSD channel/sector identifier, 9 channels	4
Start sector	Identifies the sector where the TOF start anode signal is detected	3
Heavy Discriminator	TOF Stop Anode Discriminator States (Flags). Identifies event particle as light, medium, or heavy	2
Quality flag	Set if multiple-ion hits detected	1
Reserved	Reserved	6
Bits/PHA event →		32
Bits/40 PHA events →		1280

N1, N2, and N3. A separate buffer is maintained for the PHA data that is output in the high-, medium-, and low-telemetry packets. The maximum number of PHA events saved per integration period is 10 for N1 data, 20 for N2 data, and 800 for the N3 data. PHA events are distributed among the buffers in a round-robin fashion: the first detected event is stored into the high-priority (N1) packet buffer, the next event is stored into the medium-priority (N2) packet buffer, and the next event is stored into the low-priority (N3) packet buffer, etc. Each event allocated to a particular buffer is simply stored into the next slot within the buffer until the buffer fills up. Thereafter, the rotating priority PHA replacement scheme is used in deciding which events may be displaced from the filled buffer.

All PHA events are assigned to a priority group based on the event type 1, 2, or 3 (Energy-only or “electron”, TOF-plus energy or “high-energy ion”, and TOF-only or “low-energy ion,” respectively) and the bin number, determined from the appropriate lookup table, for the event. Eight such priority groups have been defined for the PEPSSI system with an 8-element priority array maintained for each event type. Group numbers are held in the array elements in priority order, i.e., the first element contains the group number of the highest priority group, the second element contains the group number of the next lower priority group, and so on. The priority of a particular group can be determined by finding which array element contains that group number.

As PHA events are stored into their respective buffers, the assigned priority and group numbers are stored along with each event. As long as each buffer contains a vacant slot, the next detected event is simply stored into the vacant slot. Once the buffer becomes full, the assigned PHA group priority for a new event will determine its relative ability to displace events that are already in the buffer. For the data in the N1 and N2 telemetry packets, the lowest priority event already in the buffer is identified and displaced by the new event, if the priority of the new event is higher.

A record is maintained of the frequency of occurrence of each group during each integration interval. The most frequently occurring group number is used at the conclusion of the interval to “rotate” the PHA-priorities by pushing the corresponding most frequently occurring group to the bottom of the priority list. This rotated priority list is then used in determining the priority of PHA events in the next integration interval. For the N3 data with up to 800 PHA events, a modified scheme is used. Operationally, the N3 integration rate is set to a long interval (2 hours) to minimize the N3 data, which we are not relying on for PHA data.

**Table 11** PEPSSI non-packetized housekeeping data

Parameter	Name	No. of bits	Units
HV Input Current Monitor	CDH_PEPSSI_HV_CURR	8	MICROAMPS
HV Output Voltage Monitor	CDH_PEPSSI_HV_VOLT	8	VOLTS
Bias Input Current Monitor	CDH_PEPSSI_BIAS_CURR	8	MICROAMPS
Bias Output Voltage Monitor	CDH_PEPSSI_BIAS_VOLT	8	VOLTS
Energy Board Temperature	CDH_PEPSSI_ENE_BD_TEMP	8	DEGREES C
HVPS Board Temperature	CDH_PEPSSI_HVPS_BD_TEMP	8	DEGREES C
LVPS Board Temperature	CDH_PEPSSI_LVPS_BD_TEMP	8	DEGREES C
Total bits		56	

### 3.4.6 Non-Packetized Housekeeping Data

PEPSSI telemeters non-packetized housekeeping data. These include voltage and current measurements that are monitored during activation of the instrument energy measurement system and TOF measurement system. PEPSSI non-packetized housekeeping data are placed in the instrument-defined status field of Instrument Transfer Frames sent from PEPSSI to the spacecraft C&DH system. Housekeeping data is updated at a regular 1-second rate. The total number of bits in each housekeeping frame is 56 bits, resulting in an average output data rate of 56 bps (Table 11).

### 3.4.7 Quick look Diagnostic Data

For a quick look analysis of instrument status and measurement results, PEPSSI can output a diagnostic set of data at a fixed 300-second rate. It is intended that PEPSSI diagnostic data be downlinked as soon as possible following the near Pluto encounter, i.e., on a first-look basis. This will allow for examination of instrument performance in the quickest and most timely manner. It is estimated, over a 24-hour timeline, roughly the time duration of the near-Pluto encounter, about 480 kbits of PEPSSI quick-look data will be available for downlink.

The diagnostic data is identical to the electron/proton/heavy-ion energy spectra and rate-counter data previously defined, except that it is collected over 300-second integration time intervals. In addition, 600 bits of extended housekeeping data are included. The diagnostic integration time interval is constant at 300 seconds, and the subsequent average output data rate is less than 6 bits per second.

### 3.4.8 Instrument Data Rate Summary

The telemetry system of the PEPSSI instrument may be configured in a number of different ways by instrument command. The data integration interval for a number of products may be adjusted, heavy ion and TOF velocity data products may be enabled or disabled, and the maximum PHA event rate may be changed. The volume of data telemetered from PEPSSI, and the resulting average data rates, will vary accordingly.

Table 12 lists PEPSSI data products and computes telemetry data rates for a number of representative telemetry system configurations. The first four products listed (proton/electron energy spectra, heavy-ion spectra, TOF velocity spectra, and rate-counter data)

**Table 12** Example PEPSSI telemetry data rates as function of telemetry configuration

Telemetry data product	Number of data bits	Data integration interval	Example bit rate (bps)				
			In-space, low-rate configurations		In-space, typical configurations		Ground test only
			300-second data interval	10-second data interval	300-second data interval	10-second data interval	1-second data interval
Proton/Electron Energy Spectra	690	10 seconds typical	2.3	69	2.3	69	690
Heavy Ion (CNO, N2) Energy Spectra <sup>a</sup>	540	Programmable 1 to 7200 seconds	1.8	Disabled	1.8	54	540
TOF-Only Velocity Spectra <sup>a</sup>	900		3.0	Disabled	3.0	90	900
Singles Events (Rate Counters)	380		1.3	38	1.3	38	380
PHA	32 per PHA event	10 second (fixed)					
Event Rate ≤40 events/s					≤1280	≤1280	≤1280
Event Rate ≤10 events/s			≤320	≤320			
“Non-Packetized” Housekeep Data <sup>b</sup>	64	1 second (fixed)	64	64	64	64	64
Quicklook Diagnostic	1670	300 seconds (fixed)	5.6	5.6	5.6	5.6	5.6
Proton/Electron Spectra							
Rate Counters							
Extended Housekeep							
CCSDS Frame Overhead			8.5	16.5	8.5	16.5	88.3
Average total data bit rate, bps →			≤407	≤513	≤1367	≤1617	≤3948

<sup>a</sup>Heavy ion spectra and TOF velocity spectra outputs are conditional. They are output only if the particle event rate exceeds a predefined threshold. The particle event rate threshold is programmable by instrument command. The output may also be disabled by instrument command regardless of particle event rate

<sup>b</sup>Non-Packetized housekeeping data is packed in the Instrument Transfer Frame instrument status field and is intended for inclusion in spacecraft telemetry packets

represent data collected over a data integration time interval that is changeable and may be set by instrument command. The remaining data products (PHA data, non-packetized housekeeping, and quick look diagnostic data) are collected and output at fixed rates.

The data integration interval, for the first four products listed, is nominally set to 10 seconds and is never set any lower during in-space operation. For anticipated in-space operations, where the heavy-ion spectra and TOF velocity spectra are enabled, and the PHA limit is set to 40 PHA events per second, the maximum output data rate is about 1620 bits per second. For certain ground test operations, prior to spacecraft integration, where data is integrated over short, one-second time intervals, the output data rate averages about 3950

**Table 13** Average data rates and volumes

Estimates of nominal PEPSSI telemetry data rates and volumes (prior to compression by Fast algorithm). (The 152 bit ITF overhead is not included)

Packet	Bit length (including CCSDS header)	Nominal output rate (seconds)	Average data rate (bits/second)	24-hour data volume (Megabits)
High priority packet	3640	300	≈12	≈1.0
Medium priority packet	2464	10	≈250	≈21
Low priority packet (first)	30,720 <sup>a</sup>	300	≈100	≈8.8
Low priority packet (second)	30,720 <sup>a</sup>	300	≈100	≈8.8
Common status packet	456	300	≈1.5	≈0.13
Average bit rate			≈720	

<sup>a</sup>Assumes a maximal length CCSDS packet of 4096 data bytes

bits per second. If required by mission operation or spacecraft constraints, as illustrated, the instrument telemetry system may be configured to telemeter less data.

The PEPSSI instrument outputs four types of telemetry packets on regular time intervals:

- High Priority (N1)
- Medium Priority (N2)
- Low Priority (N3), and
- Common Status (“housekeeping”)

The time intervals may be modified by instrument command. Table 13 lists the packet types and provides pre-launch estimates of average data output rates and 24-hour data storage volume for the Pluto encounter. The data rate and volume figures are raw values and do not include reductions due to use of the Fast data compression algorithm. The amount of reduction, in data volume and rate, depends upon the variability of the raw data stream and therefore, is not fixed. It is anticipated the reduction of data volumes and rate will be 50% or more; therefore, the actual output data rates at the PEPSSI command and telemetry interface depend upon mission phase and ongoing planning. The data rates and volumes given in the table should be considered upper bounds.

The table also indicates that the 24-hour volume for High Priority data is on the order of 1 Mbit. However, the Fast compression algorithm can reduce this volume by up to 50% leaving the remaining volume less than 2% of the spacecraft 24-hour ‘first-look’, day one downlink capability following the Pluto encounter.

The instrument is quite flexible; for example, the actual bit rate at Jupiter was ~60 bps.

### 3.4.9 Calibration

For instrument calibration prior to launch, PEPSSI test software included a capability to read out raw instrument measurements. Raw measurement data was evaluated in order to configure the look-up calibration table that was subsequently loaded into the instrument software database.

**Table 14** PEPSSI energy measurement system commands

Command description	LED threshold	
	Granularity	Range
Energy discriminator threshold commands		
Set leading edge discriminator (LED) threshold [Chan 1: Chan 12]	≈1 keV	≈15 to 255 keV

### 3.4.10 Memory Image Dump

PEPSSI implements a capability to load selected portions of processor memory, e.g., look-up tables for instrument calibration. The PEPSSI instrument includes a capability to telemeter an image of the newly loaded segment of memory, to allow load verification in the spacecraft command center.

## 3.5 Commands

PEPSSI uses a variety of commands to provide functionality to the instrument and set various parameters that affect how the data is collected and processed before being sent to the ground.

### 3.5.1 Energy Commands

Commands related to energy measurement are given in Table 14. These include commands to adjust energy detection thresholds of leading edge discriminators. The leading edge discriminator thresholds operate in current mode so that a threshold current essentially corresponds to an energy threshold.

### 3.5.2 HVPS Commands

High-voltage PEPSSI operation requires a vacuum environment. At power turn-on, the HVPS is disabled by default. PEPSSI includes a set of HVPS and bias-voltage-supply commands to enable high-voltage operation, adjust high-voltage power supply clocks for optimum efficiency, and fine-tune the high-voltage outputs. A summary of these commands is given in Table 15.

### 3.5.3 TOF Commands

In concert with energy threshold commands, PEPSSI implements a set of commands to adjust the thresholds of the start and stop constant fraction discriminators (CFD). With the threshold set to zero, about  $5 \times 10^5$  electrons are required to generate a start or stop pulse respectively (and thus initiate a TOF measurement). The threshold can be adjusted upward, requiring more electrons and proportionally higher energy levels to initiate a TOF measurement event. A summary TOF command list is given in Table 16.

### 3.5.4 Process Control Commands

PEPSSI implements a number of commands to manage instrument operations, including energy measurement integration times, enable/disable event pile-up checks, etc. A summary list follows in Table 17.

**Table 15** PEPSSI HVPS commands

Description	Scaling	
	Resolution	Range
High voltage power commands		
Enable/disable HVPS commands (safety feature)	NA	NA
Enable/disable HVPS & bias supply clocks	NA	NA
Adjust high voltage clock rate	$\approx 750$ Hz	$\approx 75$ kHz $\pm 20\%$
Set high voltage command limit	$\approx -15$ V	$\approx -3500$ V
Set high voltage level	$\approx -15$ V	$\approx -3500$ V
Set high voltage alarm level	$\approx -15$ V	$\approx -3500$ V
Enable/disable high voltage alarm	NA	NA
Bias voltage power commands		
Set bias voltage level	$\approx -0.5$ V	$\approx -125$ V
Adjust bias voltage clock rate	$\approx 350$ Hz	$\approx 47.25$ kHz $\pm 20\%$

**Table 16** PEPSSI TOF measurement system commands

TOF measurement system commands		
Description	Units scaling	
	Resolution	Range
Start anode leading edge discriminator thresholds		
Set TOF sector threshold [Sector 1:Sector 6]		
Stop anode leading edge discriminator thresholds		
Set heavy 0 threshold		
Set heavy 1 threshold	$\approx 10$ mV	$\approx 0$ to 2500 mV
TOF constant fractional discriminators		
Set CFD start threshold		
Set CFD stop threshold		
Anode enable/disable		
Enable/disable start anode [anode 1: anode 6]	NA	NA
Enable/disable stop anode [anode 1: anode 6]	NA	NA
Miscellaneous		
Set TOF chip mode	NA	NA
Reset TOF chip	NA	NA

### 3.6 Telemetry and Command Format

The C&DH system receives all telemetry from PEPSSI as non-packetized critical house-keeping data and as CCSDS packets. The CCSDS formatted packets can be common packets with standard formats, common packets with PEPSSI-specific formats, and PEPSSI-specific packets.

**Table 17** PEPSSI process control commands

Description	Scaling Resolution	Range
Measurement process control		
Load look-up tables	NA	NA
Load PHA rotating priority structure	NA	NA
Set integration time for energy, TOF spectra (seconds)	1	65,535
Set maximum telemetered PHA event rate (events per second)	1	1 to 100
Set event rate threshold to enable telemetry of heavy ion & velocity spectra (events per second)	1	0 to 1000 (0 ⇒ enable unconditionally)
Enable/disable telemetry of heavy ion & velocity spectra	NA	NA
Set coincidence window delay	Determined during design phase	
Set coincidence window width		
Mask SSD discriminator firings for selected channel	NA	NA
Enable/disable electron multiple-hit check	NA	NA
Enable/disable ion multiple-hit check	NA	NA
<i>Miscellaneous</i>		
Reset event FIFO	NA	NA
NO-Op command	NA	NA
Memory load command	NA	NA
Memory dump command	NA	NA

### 3.6.1 Data Rate and Volume

As just noted, the raw data rate, with the instrument telemetry system configured in the preferred manner for space operations, is a maximum of about 2500 bps, representing a total raw data volume collected over 24 hours of about 200 Mega-bits. These are raw figures that apply prior to application of the Fast data compression, which may reduce data volume by up to one-half. If necessary, the instrument telemetry system may be configured for lower data rates.

Telemetry data sent from the PEPSSI instrument is compressed using the Fast algorithm. Fast is an APL-developed data-compression algorithm that is imbedded in instrument common code used by a number of MESSENGER and New Horizon instruments. Fast is a lossless compression algorithm; the reduction of data volume is variable, data volume may be reduced by up to one-half.

### 3.6.2 Telemetry Formatting

**3.6.2.1 Instrument Transfer Frame (ITF)** All messages exchanged between the spacecraft C&DH and PEPSSI are transported using the ITF format. The format applies to all telemetry data sent from the instrument and to commands and MET time received from the spacecraft. The 48-bit frame header associated with this format is outlined in Table 18.

Byte 0 is first byte transmitted/received by PEPSSI. The instrument resynchronizes to the incoming sync pattern on each ITF to limit error propagation in case of bit errors. An ITF contains a single message, (S/C time, Command, or Telemetry) and will have variable



**Table 18** Instrument transfer frame format

Major field	Field	Byte #	Description
ITF Header	sync pattern 1	0	$0 \times fe$
	sync pattern 2	1	$0 \times fa$
	sync pattern 3	2	$0 \times 30$
	Message type	3	S/C TIME, COMMAND, or TELEMETRY
	Checksum	4	Byte-wise exclusive-OR of all bytes following the checksum
	Message length	5–6	Number of bytes following the length field
Message	Message data	7 to $N - 1$	<i>New Horizons</i> formatted S/C time, command, or instrument state/telemetry message. $N =$ length of ITF in bytes. max $N = 12$ for S/C time message max $N = 279$ for Command, max $N = 1250$ for Telemetry

length depending on the length of the contained message. The maximum length for command messages is selected to accommodate memory load commands. The maximum length for telemetry messages is selected to provide adequate margin for the one-second timing requirements for telemetry transfer. S/C time messages are fixed length. The time messages contain information in addition to time that vary from instrument to instrument. The ITF header includes a checksum (byte 4) on the data that follows. In the case of Command and S/C Time messages transferred to PEPSSI, the C&DH computes and adds the checksum to the ITF when the telecommand packet from the spacecraft is parsed into PEPSSI commands. PEPSSI computes and adds the checksum to all telemetry messages sent to the C&DH. PEPSSI does not receive or send messages to any other instrument or subsystem other than the C&DH.

**3.6.2.2 Telemetry Interface** Once per second, the PEPSSI instrument formats a telemetry message containing data in an ITF for transfer to the C&DH. This frame is defined by the time between the rising edges of any two adjacent 1PPS signals. The message includes one or more CCSDS-formatted telemetry packets. The format is shown in Table 19.

**3.6.2.3 CCSDS Packetization** The header of the CCSDS-formatted packet is defined in Table 20. The length of the packet is variable and is specified in the CCSDS header. The data field of each CCSDS telemetry packet is compressed using the lossless Fast algorithm.

The application process id (ApID) in the primary header identifies the type of packet. The eleven-bit id is divided into a four-bit source and a seven-bit data. This gives an instrument up to 128 possible packet types that can be produced. The four-bit source for the PEPSSI instrument is shown in the table below. For memory dump packets, an instrument should set the lower seven bits of the ApID to a value of 1 (0000001). All other ApID assignments are at the discretion of the instrument. The mapping of PEPSSI instrument data products to specific application process identification (ApID) packets is specified in the PEPSSI software specifications document.

**3.6.2.4 Memory Dump Packet** *New Horizons* uses a single memory dump telemetry format for all onboard processors. The format of the telemetry packet is specified in Table 21.

**Table 19** Standard telemetry instrument transfer frame format

Name	Length (bits)	Value	Description
Sync pattern 1	8	$0 \times fe$	
Sync pattern 2	8	$0 \times fa$	
Sync pattern 3	8	$0 \times 30$	
Message type	8	$0 \times 04$	Telemetry
Checksum	8	$\rightarrow$	Byte-wise exclusive-OR of all bytes following the checksum
Message length remaining	16	$\rightarrow$	Number of bytes following the message length field
Heartbeat	1	$\rightarrow$	Alternating bit
Boot/application (optional)	1	0 = Running boot code 1 = Running appl. code	Flag describes if boot or application code is running
Turn-off request (optional)	1	0 = No turn-off requested 1 = Turn-off requested	Flags describes if instrument requests spacecraft to turn off power or reset
Reserved standardized instrument status	5	$\rightarrow$	Other bits not yet assigned.
Valid command count	8	$\rightarrow$	Module $2^8$ count of commands accepted
Invalid command count	8	$\rightarrow$	Module $2^8$ count of commands rejected
Instrument defined status	$8 \cdot N$	N/A	Instrument non-packetized status or housekeeping. The C&DH processor will place this data in spacecraft-produced telemetry packets, and will use it in the evaluation of autonomy rules.
Offset to first packet header	16	$0 \times 0000$ = A packet begins in first byte of telemetry packets field $0 \times FFFE$ = There is no telemetry data in this frame $0 \times FFFF$ = There is telemetry data in this ITF, but no packet begins in this frame	Offset within telemetry data field to start of first data packet header in frame. If an instrument never has more telemetry than can fit in a single ITF, this field will always be 0.
Telemetry data	$8 \cdot M$	$\rightarrow$	New Horizons formatted CCSDS telemetry packets

### 3.6.3 Command Formatting

**3.6.3.1 Command Message** The format of a command ITF is defined in Table 22. The command message may be variable in length and length is specified in the header. One command is included in each ITF; however multiple command ITFs may be received from

**Table 20** CCSDS telemetry packet header format

Item	Bit Field	Length (Bits)	Value (Binary)	Description	
Primary header	Version number	3	000	Designates a source packet	
	Type indicator	1	0	Designates a telemetry packet	
	Secondary header flag	1	1	Secondary header flag present	
	Application process identifier	11	1101 xxxxxxx	PEPSSI packet Identification	
	Grouping flags			01	First packet in group
				00	Intermediate packet
				10	Last packet in group
11				Not part of group	
Source count	14		Continuous sequence count (mod 16384) of packets for specific ApID		
Packet length	16		Number of bytes in [packet secondary header + packet data field] – 1		
Secondary header	MET	32		Spacecraft MET at time the source Packet is constructed	
Data		$8 \cdot M$		Additional data bytes, M, can range from 1 to TBD	

the C&DH in any one-second frame. For command verification, command acceptance and command rejection counts are included in the PEPSSI telemetry ITF.

**3.6.3.2 Command Format** The format of the message data within a command ITF is specified in Table 23.

This format is identical to the NH Spacecraft formatted commands and allows for multiple commands to be packed into a single CCSDS packet. However, only a single instrument command will be sent via ITF at a time.

**3.6.3.3 Memory Load Command** New Horizons has adopted a single memory load command format for all onboard processors. The format of the command is specified in Table 24.

**3.6.3.4 Memory Dump Command** The format for the New Horizons memory dump command is specified in Table 25.

### 3.6.4 MET Time Message

An MET time message is sent from the C&DH to the instrument once per second. The MET time is the predicted time of the next 1PPS. The MET ITF is defined in Table 26. The MET ITF is transferred within 950 ms following each 1PPS epoch.

**Table 21** Memory dump telemetry packet format

Item	Length (bits)	Value	Description
Packet primary header	48		For memory dump packets, the lower seven bits of the 11-bit ApID should be binary '000 0001'.
Packet secondary header	32		MET
Address	32		Start Address
Byte count	16	1–256	Number of bytes in this dump packet (not including pad) New Horizons has chosen a maximum dump size of 256 bytes.
Memory type	8	TBD	This field is available for memory architectures that cannot determine the memory type from the address. This field is spare (0 × 00) for architectures that can.
Spare	8	0	Unused (0 × 00)
Data	$N \cdot 8$		$1 \leq N \leq 256$ (From 1 to 256 8-bit bytes)
Pad	$M \cdot 8$	0	$0 \leq M \leq 3$ Pad up to 32-Bit boundary.

**Table 22** Command message in instrument transfer frame

Name	Byte #	Value	Description
sync pattern 1	0	0 × fe	0 × fe
sync pattern 2	1	0 × fa	0 × fa
sync pattern 3	2	0 × 30	0 × 30
Message type	3	0 × 02	<i>COMMAND</i>
Checksum	4		<i>byte-wise exclusive-OR of all bytes following the checksum</i>
Message length	5–6		<i>number of bytes following the length field (field sized for length ≤ TBD bytes; messages do NOT span this data structure)</i>
Message data	7 to $N$		<i>New Horizons formatted instrument command max <math>N</math> is TBD</i>

**Table 23** Message data

Name	Length (bits)	Value	Description
Opcode	16		Instrument splits this into 2 8-bit fields (dest, opcode).
Macro field	2	00 = Execute real-time 01 = Invalid	Instrument use only.
Command word count	14	10 = Add to Inst. Macro 11 = Add to DPU Macro $N + 2$	Unused or spare ( $0 \times 00$ ) for non-instrument commands. Number of 32-bit command words ( $N$ ) + 2
Command words	$32 \cdot N$		
Checksum	32		32-bit XOR of the fields defined above

**Table 24** Memory load command message

Item	Length (bits)	Value	Description
Opcode	16		
Macro Field	2	→	00 = Execute real-time 01 = Invalid 10 = Add to Inst. Macro 11 = Add to DPU Macro Unused (00) for non-APL instruments
Length	14	5–68	Command length in 32-bit words ( $4 + (N + M)/4$ ).
Address	32	→	Start address
Byte Count	16	1–256	Number of bytes to be loaded (not including pad). <i>New Horizons</i> has chosen a maximum load size of 256 bytes.
Memory Type	8	TBD	This field is available for memory architectures that cannot determine the memory type from the address. This field is spare ( $0 \times 00$ ) for architectures that can.
Spare	8	0	Unused ( $0 \times 00$ )
Data	$N \cdot 8$		$1 \leq N \leq 256$ (From 1 to 256 8-bit bytes)
Pad	$M \cdot 8$	0	$0 \leq M \leq 3$ Pad up to 32-bit boundary. This data will not be loaded but will be included in XOR calculation.
Checksum	32	→	32-bit XOR

**Table 25** Memory dump command message

Item	Length (bits)	Value	Description
Opcode	16	→	
Macro Field	2	→	00 = Execute real-time 01 = Invalid 10 = Add to Inst. Macro 11 = Add to DPU Macro Unused (00) for non-APL instruments
Length	14	5	Command length in 32-bit words
Address	32	→	Start Address
Byte Count	32	→	Number of bytes to be dumped.
Memory Type	8	TBD	This field is available for memory architectures that cannot determine the memory type from the address. This field is spare (0 × 00) for architectures that can.
Spare	24	0	Unused (0 × 00)
Checksum	32	→	32-bit XOR

**Table 26** C & DH-to-instrument spacecraft time message in instrument transfer frame

Name	Length (Bits)	Value	Description
sync pattern 1	8	0 × fe	
sync pattern 2	8	0 × fa	
sync pattern 3	8	0 × 30	
Message type	8	0 × 01	S/C-Time
Checksum	8		Byte-wise exclusive-OR of all bytes following the checksum
Message length	16	$0 \times 0004 + N$	Expressed in number of bytes of time information plus any additional information sent to that instrument.
S/C-Time	32	MET	Mission elapsed time corresponding to the predicted S/C time at the next SYNC pulse
Additional information sent to the instrument	$8 \cdot N$	N/A	Additional information sent to an instrument can include a closest approach countdown, whether that instrument is allowed to produce a memory dump packet in the next second, scan rate, etc. This field will be customized for PEPSSI, and will be fixed from one second to the next.

## 3.7 Instrument Environmental Design Requirements

### 3.7.1 *Thermal Interface*

The PEPSSI-to-spacecraft thermal interface includes a conduction component via the spacecraft-mounting surface and a radiation component derived by a ratio between blanketed and painted surfaces. Two spacecraft-monitored temperature sensors are continuously monitored via the spacecraft Command and Data Handling (C&DH) system. These sensors are used to ascertain the temperature of the instrument. The spacecraft thermal control system maintains the temperature on the spacecraft side of the PEPSSI mounting plate and the support electronics box mounting points. The spacecraft has no specific requirement for control of the temperature gradient across the mounting interface from any one point to another. The spacecraft also has no specific requirement for control of the interface temperature rate of change. Internal temperature measurements for PEPSSI (two in the instrument and one on the mounting bracket) are included in PEPSSI's housekeeping telemetry data.

### 3.7.2 *PEPSSI Thermal Design Requirements*

Design and test limits give the temperature ranges over which PEPSSI was cycled during thermal vacuum testing. The spacecraft interface temperatures include: Operating/Test temperatures 0°C to +40°C, Non-Operating Survival -20°C to +40°C, and Internal Operating Limits with baseplate control for the instrument itself with -45°C to +45°C for the electronics boards and -35°C to +35°C for the solid state detectors. The non-operating survival limits assume the PEPSSI cruise heater is not on. The heater may be turned on during the cruise phase when PEPSSI is off and when observatory power is available to provide margin with respect to the non-operating -20°C limit.

### 3.7.3 *Radiation Shielding Requirements*

The New Horizons radiation environment includes exposure to solar protons, Jovian electrons, galactic cosmic rays, and neutrons and gamma rays emitted from the radioisotope thermoelectric generator (RTG) power source. PEPSSI is designed to survive a total ionizing dose of 15 kilorads without failure and to be immune to latch-up. Additional spot shielding to parts was added as required to bring the instrument to this overall shielding level.

### 3.7.4 *Electrostatic Requirements*

The electrostatic requirement for PEPSSI is that the observatory's total potential be less than 1000 volts. Analysis by the New Horizons project for the Jupiter flyby showed a worst case ( $35R_J$  closest approach) potential of  $\sim +5$  to  $+10$  volts on isolated solar-illuminated surfaces, and  $\sim -200$  volts on isolated surfaces in darkness. There is no hard information of the plasma environment of Pluto, but it is not expected to possess a strong intrinsic magnetic field and, therefore, is not expected to have a mechanism to produce a population of particles sufficiently energetic to charge the observatory to a level of concern. The worst Jupiter case is less than the maximum allowable for PEPSSI by a margin of five; and the electrostatic charge at Pluto is expected to be substantially less.

**Table 27** PEPSSI thermal test limits

Condition	Limits
Typical	+30°C to +40°C
Operating	0°C to +40°C
Operating test	−10°C to +50°C
Non-operating survival	−30°C to +50°C (Includes 10°C margin)

### 3.8 Test Requirements

#### 3.8.1 Vibration

Instrument test vibration levels are specified in project documentation for levels appropriate to the launch vehicle stack used for New Horizons. Testing philosophy was based on a protoflight approach, where flight hardware is tested to qualification levels for flight acceptance durations. Tests included sine vibrations test at levels applicable at the spacecraft-mounting interface, with vibration test of three orthogonal axes, including the thrust axis, performed, as well as random vibration tests with the same geometry.

#### 3.8.2 Thermal

The PEPSSI instrument is mounted on a bracket on a side deck of the spacecraft and is thermally conductive through the mounting interface. The instrument temperature is controlled by a tailored thermal coupling at the mounting interface and use of instrument radiating surfaces. No heaters are required. The ranges of mounting interface temperatures, at the bracket-to-spacecraft deck interface, are given in Table 27.

#### 3.8.3 Acoustics and Shock

All instruments, including PEPSSI, were mounted on the spacecraft during separation shock and acoustic test. In addition, acoustic tests were performed on the PEPSSI engineering model instrument, using protoflight acoustic levels, to verify the integrity of the design with respect to acoustic noise. No instrument level acoustic test was carried out for the flight PEPSSI hardware.

#### 3.8.4 EMI/EMC

PEPSSI electromagnetic interference (EMI) and electromagnetic contamination (EMC) level requirements are set forth in the New Horizons project documents. Full conducted emissions and conducted susceptibility as well as radiated emissions, radiated susceptibility, and transients measure tests were run prior to integration with the spacecraft.

## 4 Performance

### 4.1 Data Conversion to Physical Units

PEPSSI measurements are intended to generate the information needed to derive the charged ion and electron differential intensities (**I** [ $\text{cm}^{-2} \text{sr}^{-1} \text{s}^{-1} \text{keV}^{-1}$ ]) and phase space densities (**PSD** [ $\text{s}^3 \text{cm}^{-6}$ ]). The significance of **I** and **PSD** are that, for many particle transport



processes within planetary magnetospheres and interplanetary space, they satisfy the collisionless Boltzmann equation, derived from Liouville’s Theorem for collision-less transport, for energy preserving, and for non-energy preserving processes, respectively. Our purpose here is to develop the quantitative procedures for converting the count rates ( $\mathbf{R}$  [counts  $s^{-1}$ ]) reported by PEPSSI in the many predefined channels described in preceding sections, or in channels defined on the ground using the pulse-height-analysis (PHA) data, into estimates of  $\mathbf{I}$  and  $\mathbf{PSD}$  for the various defined ranges of energies, particle species, and arrival angles. The approach follows classical procedures.

4.1.1 Flux, Differential Intensity and Phase Space Density

The rate  $\mathbf{R}$  [particles/s] that traverse an area  $A$  can be given by the Flux  $\mathbf{F}$  [ $cm^{-2} s^{-1}$ ] with:

$$\mathbf{R} = A\mathbf{F} \tag{1}$$

or by the intensity  $\mathbf{i}$  [ $cm^2 s^{-1} sr^{-1}$ ]

$$\mathbf{R} = A \int \mathbf{i} \cos(\hat{u}) d\Omega \tag{2}$$

where  $\Omega$  is solid angle and  $\hat{u}$  is the angle to the area normal.

Often used is the quantity differential intensity  $\mathbf{I}$  [ $cm^2 s^{-1} sr^{-1} keV^{-1}$ ], defined as the number of particles of a given species  $S$  with energy between  $E$  and  $E + \Delta E$  that traverse the area  $A$  during the time  $t$ , where

$$\mathbf{R}(S, E) = \mathbf{I}(S, E)A\Delta\Omega\Delta E \tag{3}$$

In three dimensions, with  $\theta$  being the polar angle and  $\phi$  the azimuthal angle of a polar reference system:

$$d^3\mathbf{R} = \mathbf{I}(S, E, \theta, \phi)A(\theta, \phi) \cos(\hat{u})dE \cos\theta d\theta d\phi \tag{4}$$

where we note that the area  $A$  and the unit vector  $\hat{u}$  pointing normal to  $A$  are both functions of  $\theta$  and  $\phi$ .

Note that for non-relativistic energies,  $\mathbf{I}(S, E, \theta, \phi)$  is related to the phase space density  $\mathbf{PSD}$  (number of particles in the configuration space element  $d^3R$  and with velocity between  $v$  and  $v + d^3v$ ) by the simple relationship

$$\mathbf{PSD} [s^3 cm^{-6}] = \mathbf{I} [cm^2 s^{-1} sr^{-1} keV^{-1}]m/v^2 \tag{5}$$

For relativistic energies, the phase space density (identified with lower case letters here:  $\mathbf{psd}$ ) is defined in terms of particle momentum  $\mathbf{p}$  ( $\mathbf{psd}$  [ $s^3 cm^{-6} kg m^{-3}$ ]), and the relationship to differential intensity  $\mathbf{I}$  is:

$$\mathbf{psd} [s^3 cm^{-6} kg m^{-3}] = \mathbf{I} [cm^2 s^{-1} sr^{-1} keV^{-1}]/\mathbf{p}^2 \tag{6}$$

4.1.2 Definition of Sensor Transfer Function and Geometric Factor

Using (4), the rate  $\mathbf{R}$  [particles/s] of particles of species  $S$ , in the energy band  $\Delta E$  around mean energy  $E$ , angular band  $\Delta\theta$  around mean polar direction  $\theta$ , and angular band  $\Delta\phi$  around the mean azimuthal direction  $\phi$ , measured by the instrument can be expressed as:

$$\mathbf{R}(S, E) = \int_{\Delta E} \int_{d\theta} \int_{d\phi} \mathbf{I}(S, E, \theta, \phi)A(\theta, \phi) \cos(\hat{u})dE \cos(\theta)d\theta d\phi \tag{7}$$

One may take the kernel approach to relating  $\mathbf{R}$  to  $\mathbf{I}$  by allowing  $\mathbf{I}(S, E, \theta, \phi)$  to be a Dirac  $\delta$ -function (mono-energetic, infinitely narrow beam). Then:

$$d\mathbf{R}(S, E, \theta, \phi) = d\mathbf{I}(S, E, \theta, \phi)\mathbf{T}(S, E, \theta, \phi) \tag{8}$$

where  $\mathbf{T}(S, E, \theta, \phi)$  [ $\text{cm}^2 \text{ sr keV}$ ] is the kernel, also known as the ‘‘transfer function’’ of the instrument. Then:

$$\mathbf{R}(S, E) = \int_{\Delta E} \int_{d\theta} \int_{d\phi} \mathbf{I}(S, E, \theta, \phi)\mathbf{T}(S, E, \theta, \phi) \cos(\theta)d\theta d\phi \tag{9}$$

It is typical for the first estimate to assume that the particle intensities are constant over the energy-species-angle bandwidths of any one channel. The estimated intensity  $\mathbf{I}_{kj}$  associated with a specific detector  $\mathbf{k}$ , which at a specific time views a range of angles centered in a specific direction  $(\theta_k, \phi_k)$ , and which is associated with a specific energy channel  $\mathbf{j}$ , which measures particle species  $S_j$  over an energy range that stretches from  $E_j$  to  $E_j + \Delta E_j$ , is given by (9) as:

$$\mathbf{R}_{kj} = \int_{\Delta E_j} R_k(S_j, E_j)dE = \int_{\Delta E_j} \mathbf{I}_k(S_j, E)\mathbf{T}(S_j, E)dE \sim \langle \mathbf{T}_{kj} \rangle \mathbf{I}_k(S_j, E_j)\Delta E_{kj} \tag{10}$$

where  $\mathbf{R}_{kj}$  is the channel count rate and where  $\langle \mathbf{T}_{jk} \rangle$  is called here the Transfer Factor  $\mathbf{H}_{kj}$ . It is convenient to separate  $\mathbf{H}_{kj}$  into a counting efficiency ‘‘ $\epsilon_{kj}$ ’’ and a factor that relates strictly to geometry, the so-called geometric factor  $\mathbf{G}_{kj}$ . That is:

$$\mathbf{I}_k(S_j, E_j) \sim \mathbf{R}_{kj} / (\epsilon_{kj}\mathbf{G}_{kj}\Delta E_{kj}) \tag{11}$$

Therefore, the first goal of calibration is to obtain detector-channel-averaged transfer factors  $\mathbf{H}_{kj}$  (or the equivalent efficiency factor  $\epsilon_{kj}$  since  $\mathbf{G}_{kj}$  is easy to calculate), the detector-channel energies  $E_{kj}$  and the detector-channel energy band pass  $\Delta E_{kj}$ .

More quantitative work may require a full inversion of the kernel equation given in (9). Here we are usually aided by the fact that to some level of approximation the Transfer Function  $\mathbf{T}$  is separable in the form:

$$\mathbf{T}(S, E, \theta, \phi) = K(S, E)\mathbf{P}(\theta, \phi) \tag{12a}$$

and hopefully even

$$\mathbf{T}(S, E, \theta, \phi) = \mathbf{K}(S, E)\mathbf{C}(\theta)\mathbf{D}(\phi) \tag{12b}$$

Note that even with these separations, an exact inversion of the integral is rarely possible, and we can compute only the coefficients of some tailored expansion of  $\mathbf{K}$ ,  $\mathbf{C}$ , and  $\mathbf{D}$ , as for example in spherical harmonics (using Legendre polynomials). The accuracy of these coefficients depends on both the raster coverage of the measurements and on the calibration.

#### 4.1.3 Goals of the PEPSSI Characterization and Calibration Efforts

The goal of PEPSSI characterization and calibration efforts, then, is to relate the rates,  $\mathbf{R}_{kj}$ , of the on-board or ground-defined channels to the *in situ* particle intensities  $\mathbf{I}(S, E, \theta, \phi)$  by developing a hierarchy of information about the transfer function  $\mathbf{T}(S, E, \theta, \phi)$ . Specifically, we wish to derive for each channel:

$$E_{kj}, \Delta E_{kj}, \epsilon_{kj}\mathbf{G}_{kj}, \mathbf{C}_{kj}(\theta), \mathbf{D}_{kj}(\phi), \mathbf{K}_{kj}(S, E), \mathbf{P}_{kj}(\theta, \phi), \quad \text{and finally,} \quad \mathbf{T}_{kj}(S, E, \theta, \phi)$$

Clearly, the further to the right we move into this list, the higher the fidelity the characterization and calibration efforts must be.

Typical calibration procedure consists of stimulating the instrument with energetic particles, first from radiation sources, and then from accelerator beams (fair approximation of a delta function) and recording the response of the different channels. The ideal calibration for PEPSSI meant a scan of the following variables:

- Species and Mass: e, H, He, O, Ar (proxy for heavier species, e.g., Fe)
- Energy: 1 keV–1 MeV ( $\sim 30$  energies for 10 points/decade)
- Polar angle:  $\pm 10$  deg (12 degrees nominal FOV)
- Azimuthal angle:  $\pm 90$  deg (160 degrees nominal FOV)

Note that even given this level of discreteness, complete characterization to the level of establishing  $\mathbf{T}_{kj}(S, E, \theta, \phi)$  for all channels would have required: 5 masses  $\times$  30 energies  $\times$  21 polar angles  $\times$  180 azimuthal angles = 567,000 calibration points! Clearly it was (and is) not possible to run this many beam values without significant infrastructure and automation. Therefore, we are dependent to a substantial degree on the separability of the transfer function as described in (12). An important goal of the characterization and calibration efforts was, in fact, to establish that degree of separability. Simulations play an important role in establishing expectations for the instrument, as well.

## 4.2 Simulations

Numerical simulation provides an efficient and effective means of verifying and quantifying the flight instrument response. Hence, a range of simulation tools are developed in order to characterize PEPSSI. The results from these simulation tools allow us to calculate the end-to-end expected performance of the instrument which one can use to compare with in-flight and calibration data. Different sections of PEPSSI are simulated using different tools to gain better understanding of each part of the instrument.

### 4.2.1 Geometric Factor

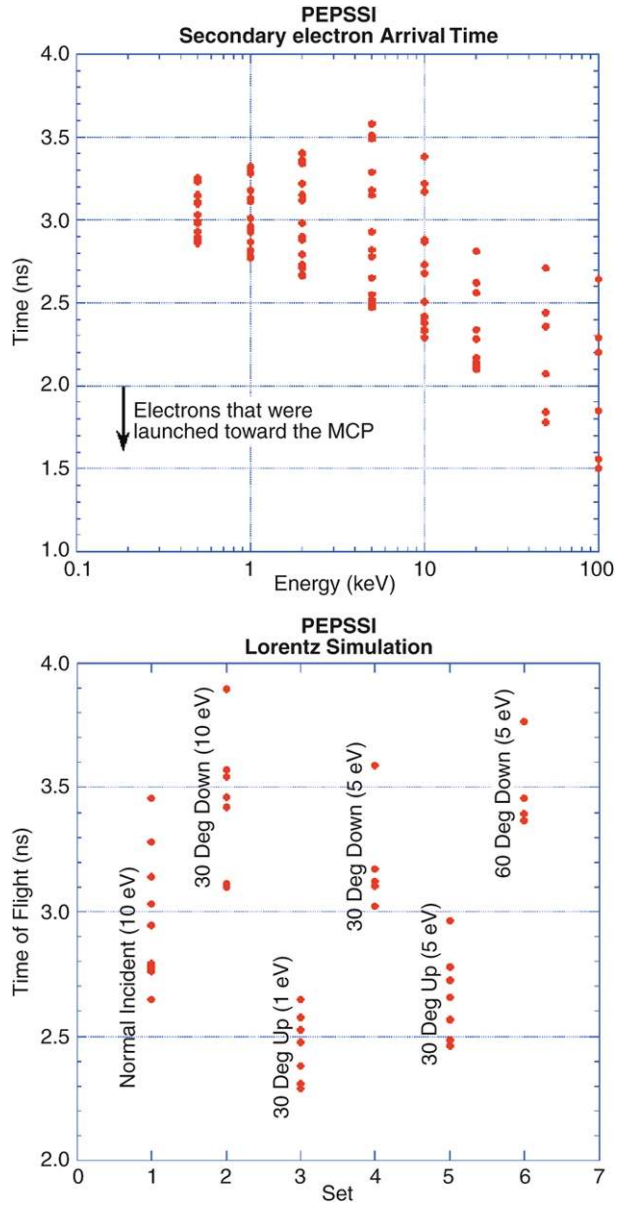
The number of data points needed to measure the geometric factor is very large, and the time needed to perform these measurements was well beyond the available time. Instead, estimates of the geometric factor rely on computer modeling and analysis. The very same analysis formed the base for the selection of the best collimator configuration: 23 blades, each 25 mm long. This geometry for the collimator defines the maximum acceptance angles through the collimator and the geometric factor  $GF = 0.15 \text{ cm}^2 \text{ sr}$ , which is the total geometric factor for the start system.

### 4.2.2 Ion Measurements

**4.2.2.1 Electron Optics** As discussed previously, secondary electrons generated by primary ions in a start and a stop foil are used to generate timing signals to measure the ion's time-of-flight (TOF) within PEPSSI. They are also used to determine the directionality of the low energy ions that do not stimulate the SSDs.

Here, a pie-shaped cutout of the cylindrical PEPSSI sensor was analyzed (cylindrical symmetry is assumed for the electrostatic fields). The electron optics for both the start foil/MCP and stop foil/MCP are identical, hence the analysis yields a good representation for both start and stop electron trajectories. Electrons are generated at the foil when ions

**Fig. 13** Time dispersion associated with varying angles for electrons emitted from the center of the foil



transverse through the foil. These low energy electrons (typically <10 eV) are immediately affected by the accelerating voltages within PEPSSI (the high energy ions are not significantly affected by the accelerating voltages) and are steered towards the MCP. An important issue is the dispersion in the arrival times of the secondary electrons as a function of foil position and the angle of emittance of the secondary electrons from the foil. Such dispersion adds to the error in the measurement of time-of-flight. Figure 13 (top) shows the time dispersion associated with varying angles for electrons emitted from the center of the foil. In Fig. 13 (bottom) the dispersion shown for any one column is associated with varying

the emission position over the  $\sim 6$  mm vertical extent of the foil. The combination of position and angle yields a time dispersion of roughly 1.5–2 ns. Combining the dispersions associated with the start and stop detections in a root-mean-square sense yields a total time dispersion error of roughly 2.1–2.8 ns. Combining that value in a root-mean-square sense with the  $\sim 1.5$  ns electronic dispersion yields a total time dispersion that resides between 2.5 and 3.2 ns.

**4.2.2.2 Ion Energy Losses** As ions transverse the TOF section of PEPSSI through the front foil ( $\sim 10 \mu\text{g}/\text{cm}^2$ ), back foil ( $\sim 19 \mu\text{g}/\text{cm}^2$ ), dead layer of the solid state detector ( $\sim 550 \text{ \AA}$ ), and eventually stop and deposit their total energy in the SSD, they lose energy and scatter depending upon the ion's initial energy, mass, and the medium through which they pass. We have incorporated data from the SRIM particle-interaction-with-matter code (Biersack and Haggmark 1980) in our simulation to simulate realistically the energy loss and scattering as ions transverse through different materials in the PEPSSI sensor.

**4.2.2.3 TOF Measurements** When ions penetrate through the front foil, a distribution of ion velocities is created, as calculated using SRIM. This distribution of ions is then used to calculate the distributions of ion TOFs. The uncertainty due to secondary electron dispersion and electron noise together with SRIM data are all incorporated in our simulation. Figure 14 shows the simulated response of PEPSSI TOF spectra as a function of particle initial energy for four species (H,  $^4\text{He}$ ,  $^{16}\text{O}$ , and  $^{56}\text{Fe}$ ). At low energy ( $\sim 10$  s of keV), ions lose significant amounts of energy and scatter significantly when going through the front foil. These effects explain the spread in TOF measurement at low energy. However, at higher energy ( $\sim 100$  s of keV), the TOF spreads are mostly consequences of the uncertainties in the TOF measurement from both the electronics jitter ( $\sim 1.5$  ns), and secondary-electron dispersion in the TOF optics as discussed in previous section (except for very heavy ions, e.g., Fe).

**4.2.2.4 Total Energy Measurement** If an ion has sufficient energy left once it transits the front and back foil, it ends up in the SSD. Depending on the ion's final energy and mass when it reaches the SSD, it can penetrate through the dead layer of the SSD and produce an electronic signal to be measured. Figure 15 shows the simulated measured energy by PEPSSI as a function of the ion's initial energy before entry into PEPSSI. The measured energy shows the cumulative effect of the energy spread due to energy lost throughout the PEPSSI detector (start foil, stop foil, dead layer, and electron hole pair production). The energy loss is greatest for ions with the greatest nuclear charge, here Fe.

**4.2.2.5 TOF Versus Energy** Finally, the energy measurement is combined with the TOF measurement on a particle-by-particle basis. Even with a  $\sim 3$  ns time dispersion, the major elemental species of interest (H, He, CNO, Fe) are discriminated except at the lowest energies for CNO and Fe, where the error in the energy measurements dominates.

**4.2.2.6 Efficiencies** The efficiency for detection of an ion within the SSDs is roughly  $\sim 100\%$  (except at the very lowest energies where energy straggling can position the energy below the low energy threshold). The efficiency for obtaining a TOF measurement is estimated using the efficiency of generating secondary electrons in both the front and the rear foil. To emit a secondary electron, such electrons must be generated close enough (distance " $\rho$ ") to the surface of the foil so that the electron can escape before it is re-assimilated. Thus, very roughly, it is expected that the efficiency for the generation of a secondary electron is proportional to the amount of energy per unit distance ( $dE/dx$  [keV/micron]) that

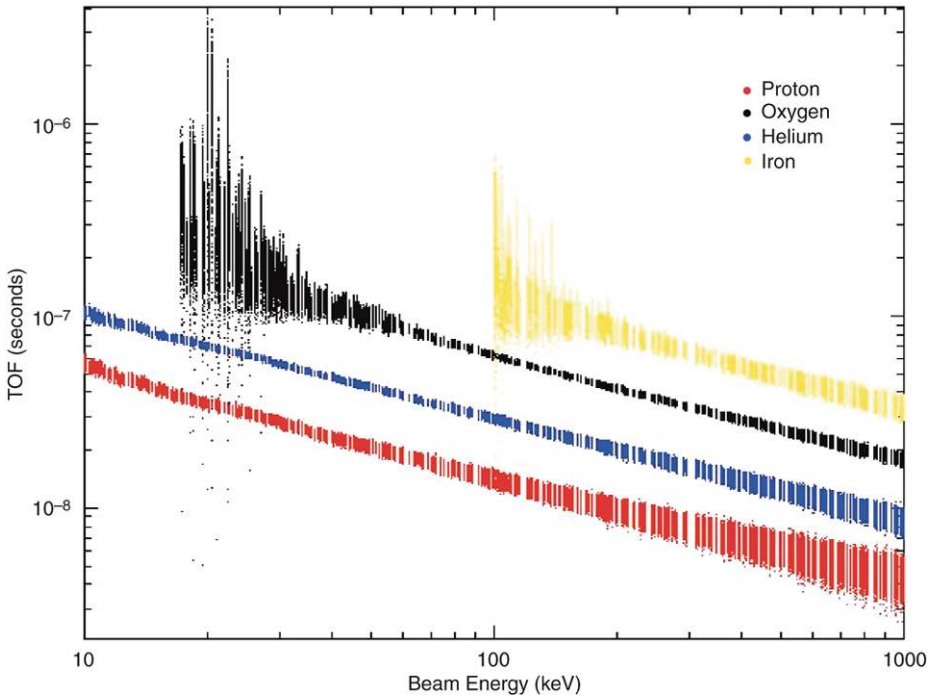


**Fig. 14** Simulated TOF spectra as a function of accelerator beam energy for protons and oxygen, helium and iron nuclei

an ion deposits as it goes through this outer thin layer of the foil. The canonical number of secondary electrons generated out of each surface as a proton with 10's of keV energy encounters the foil is between 0.5 and 1 on average (Frischkorn et al. 1983; R.W. McEntire, private communication, 2004; estimated here as 0.75). Since we require a simultaneous start and stop electron, the efficiency of proton detection at 10's of keV is  $(1 - e^{-0.75})^2$ , where  $(1 - e^{-0.75})$  is the Poisson probability of having at least 1 or more electrons emitted when the mean emission number is 0.75. Thus, the efficiency is roughly 28%. Other energies and species may be roughly scaled with this number using tabulated  $dE/dx$  values. For example, at 50 keV total energy the  $dE/dx$  values for protons and oxygen ions are 120 and 250 keV/micron, respectively (we ignore for now the energy losses suffered by the ion in getting to the position in either foil where the secondary electron is generated). Thus, since the average number of secondary electrons for oxygen will be  $\sim 0.75 \times (250/120)$ , or 1.56. Poisson statistics tells us that the probability of detecting an oxygen ion with 50 keV energy is  $(1 - e^{-1.56})^2$  or 62%.

#### 4.2.3 Electron Measurements

The PEPSSI electron measurement strategy depends on the use of the aluminum flashing on the electron SSD. We therefore need to understand the effect of that flashing on both the ion and electron measurements within the electron SSDs. Based on simulations with GEANT-4 (Agostinelli et al. 2003), Fig. 16 shows the effect of Al flashing on proton measurements, and Fig. 17 shows the effect on electron measurements, for a varying thickness of Al flashing. The baseline spectrum assumed for both protons and electrons is a power-law spectrum with

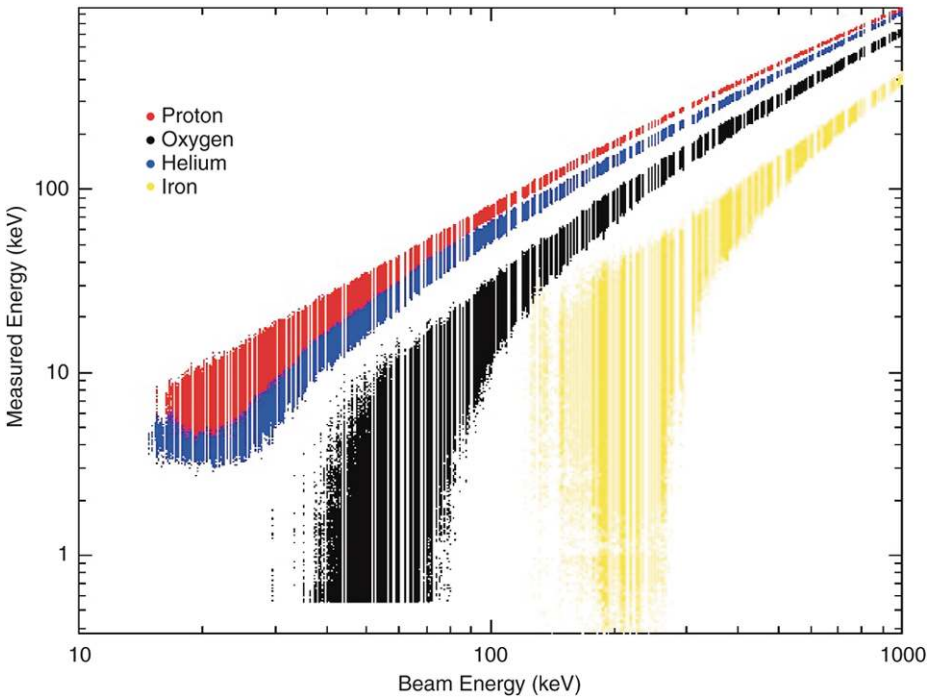


**Fig. 15** Simulated measured energy versus incident energy for the same ions as in the previous figure

a spectral index of 3; that is,  $\text{Intensity} = A \times E^{-3}$ , where “ $A$ ” is a constant. With the flashing thickness utilized with PEPSSI, 1 micron Al, the proton intensities are severely depleted for energies  $<250$  keV. With that flashing thickness, the electron intensities are maintained to energies down to about 20 keV. The drop off of electron intensities at the highest energies occurs because of the electron penetration of the 500-micron detectors. That drop-off is rounded because of electron scattering within the SSD, as demonstrated with an examination of the detailed trajectories of individual electrons with the GEANT-4 simulations. There may be periods of time when the ion counts overwhelm the electron measurements. The most important issue is not that the electrons may be occasionally contaminated, but whether or not the electrons are contaminated in a way that the ion counts are confused with what are really electron counts. This problem is intrinsic to the technique used here to measure the electrons. Extensive experience with similar measurement made by the EPIC instrument on Geotail (Williams et al. 1994) demonstrates that, because of the clean proton measurements (below and above 250 keV) made in roughly the same direction, it is unlikely that ions and electrons will be confused.

### 4.3 PEPSSI Flight Unit Calibration

#### 4.3.1 The JHU/APL Calibration Facility

Calibration of the PEPSSI instrument was conducted at the JHU/APL instrument testing facility through a combination of long-duration, radiation-source exposures (Am-241 degraded alpha source) and discrete exposures from the 170-kV particle accelerator beam. The

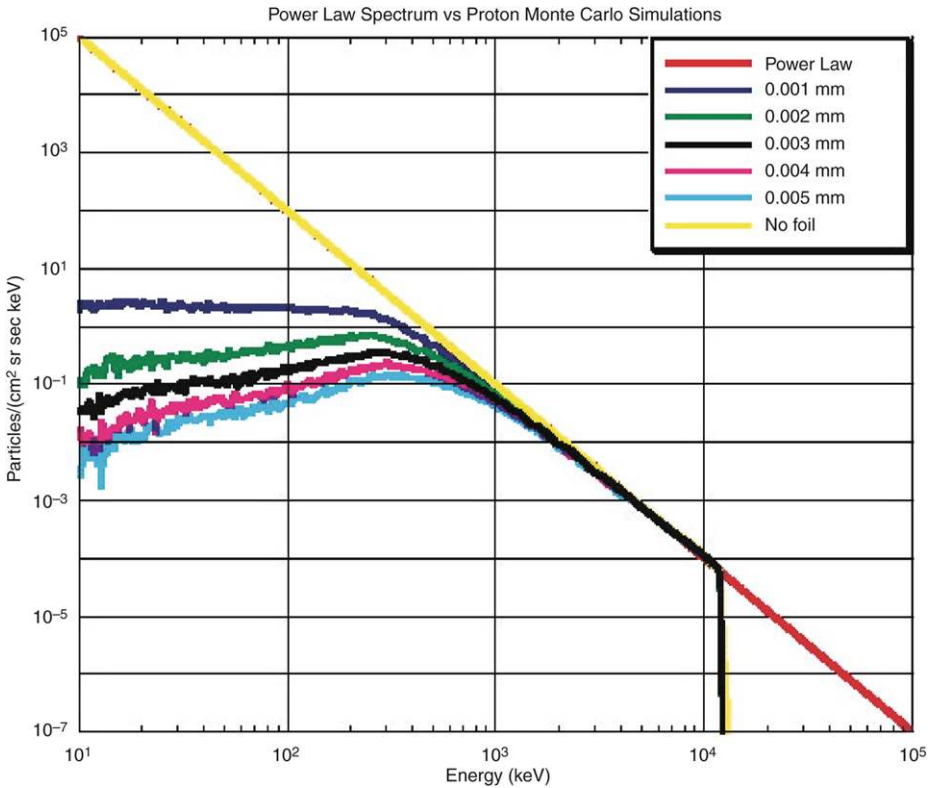


**Fig. 16** Simulated measured proton spectra for different Al flashing thicknesses from a known incident spectrum (*red*) on a 500  $\mu\text{m}$  thick silicon detector

Air Insulated Accelerator, obtained from Peabody Scientific, is a versatile system capable of producing a broad range of ion species to energies of 170 keV. The system produces beams of H, O, and noble gas ions with intensities over the range of  $\sim 10^2$  to  $10^6$  particles/ $\text{cm}^2/\text{s}$  at the target position in an energy range of 3 to 170 keV. Figure 18 shows the picture of the accelerator HV terminal.

A one-meter diameter and one meter tall cylindrical vacuum chamber is attached to the end of the accelerator beam line with a small gate valve to serve as the shutter (shown in Fig. 19). The chamber has two rotation stages ( $\pm 0.1^\circ$ ) and two translation stages ( $\pm 2 \mu\text{m}$ ) that are controlled by stepper motors with digital read-out capability. Within the beam line and in the chamber itself there are various mechanical shutters that are used to control the ion beam size from  $1 \text{ mm}^2$  to  $1 \text{ cm}^2$ . Three different beam monitors are used in the accelerator and chamber for diagnostics. A Faraday cup in the beam line before the beam enters the chamber wall is used for initial diagnostics of the beam intensity. In addition, within the chamber itself there is a stepper-motor-controlled moveable fixture that is mounted with both a channeltron and an SSD to serve as the primary beam monitor. The moveable fixture allows measurement of the species, energy and intensity of the beam inside the chamber itself.



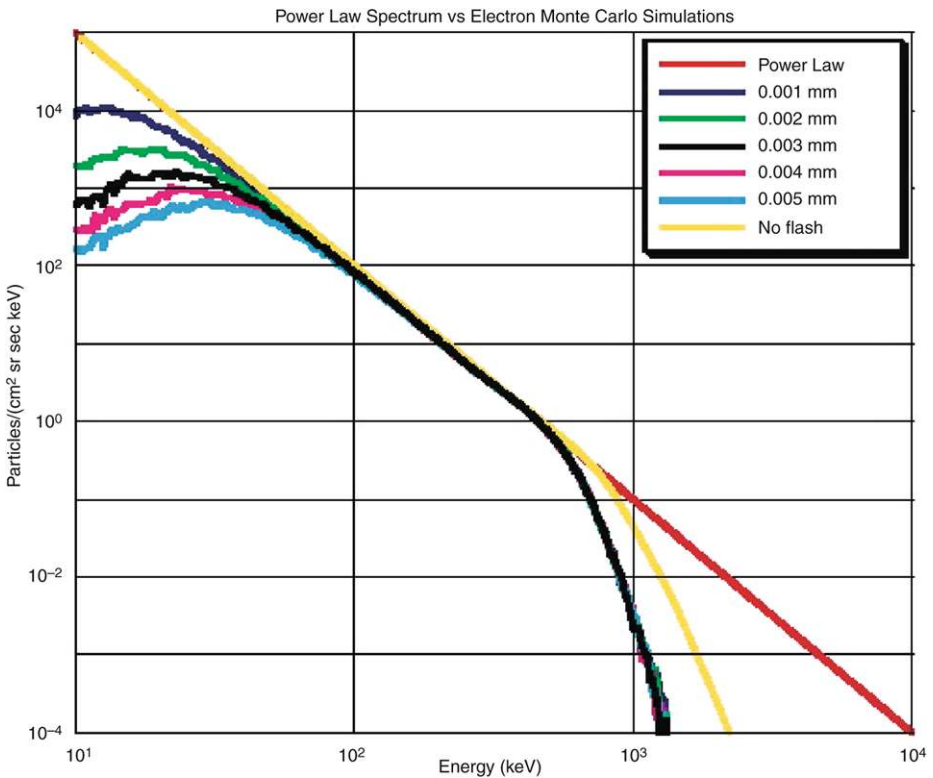


**Fig. 17** Simulated measured electron spectra for different Al flashing thicknesses from a known incident spectrum (red) on a 500  $\mu\text{m}$  thick silicon detector

### 4.3.2 Test Set Up

For both the alpha particle and beam calibration test, the PEPSSI unit was mounted inside the vacuum chamber. An emulator box was connected to PEPSSI to act as the New Horizons spacecraft in providing commands and power to the instrument. The emulator box was controlled by a Window-PC running GSEOS to operate and collect data from PEPSSI. All the calibration data were recorded under GSEOS as a recorded file in binary format.

PEPSSI was in full flight configuration during calibration, including the collimator, flight SSDs and foils. The PEPSSI instrument was mounted to a rotating turntable that allowed the beam to be scanned in full  $160^\circ$  in the azimuth direction. The response of the instrument to the vertical angle was not investigated with the accelerator beam.

### 4.3.3 Ground Calibration

Numerous proton, helium, and oxygen beams, along with radioactive sources, were used to calibrate and characterize PEPSSI performance over the course of two weeks during the ground calibration period. Protons at energies from 30 to 170 keV and oxygen ions at energies from 50 to 170 keV were used to stimulate PEPSSI.

**4.3.3.1 Directionality** Calibration runs like those depicted in Fig. 20 document the ability of the PEPSSI sensor to determine the directionality of the incoming charged particles. Fig-

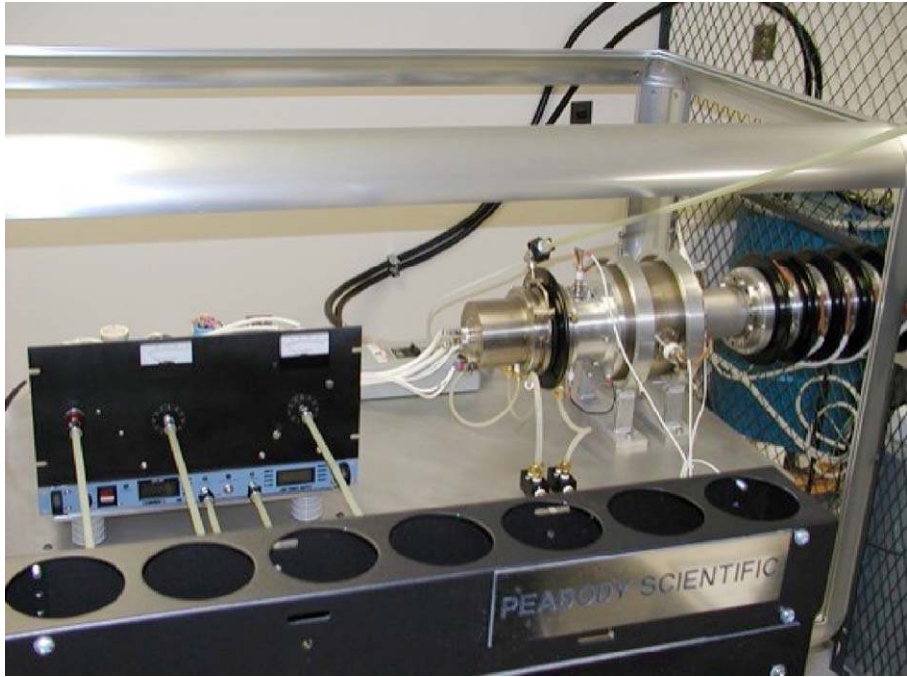


**Fig. 18** The JHU/APL particle accelerator showing the high-voltage terminal

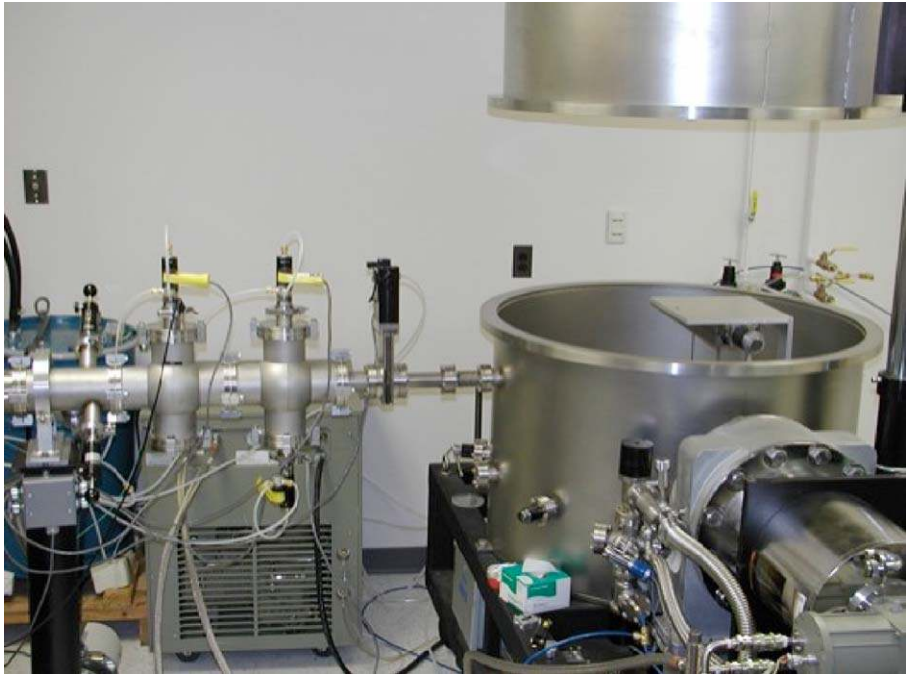


**Fig. 19** The vacuum chamber used in calibrating the PEPSSI unit. The beam line enters the chamber horizontally from *left to right* in the picture

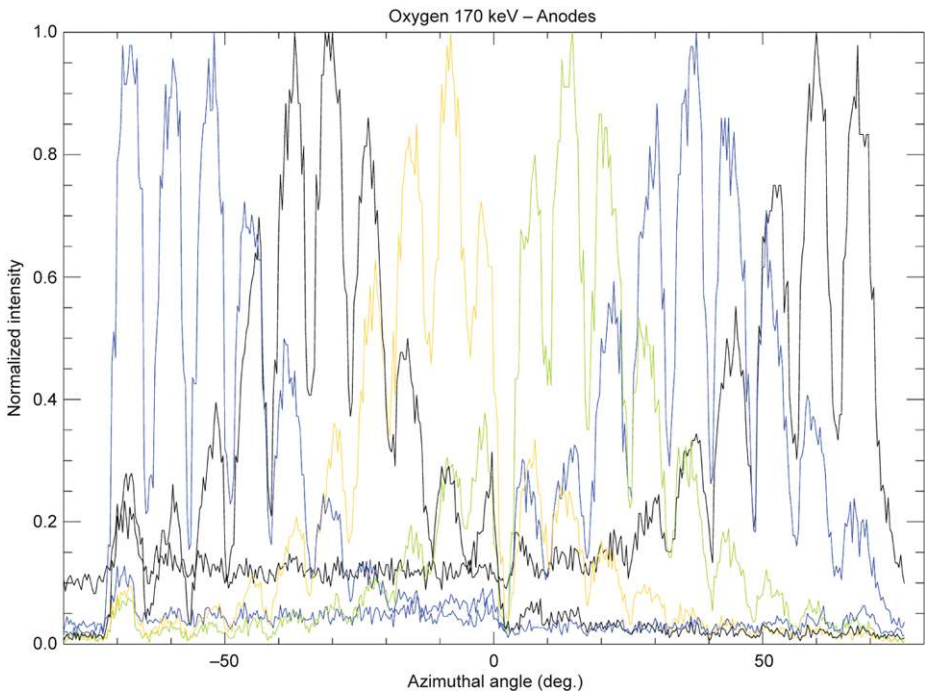


**Fig. 20** Angular scan in the azimuth angle direction showing response of discrete start anode (colors) and the internal fins of the collimator to a narrowly collimated oxygen-ion beam (170 keV). All 20 internal fins are seen in the scan. The oxygen beams used have angular spreads on the order of  $\sim 1$  degree. For these anode scans, from the left (see identification and locations in Fig. 11): A5—blue, A4—black, A3—yellow, A2—green, A1—blue, A0—black; note the collimator features (see next figure as well), secondary electrons spread and/or electronic cross-talk, i.e., response into two channels at the same incidence angle

ure 20 shows the ability of the discrete “start” anodes to determine the directionality of the incoming particles for the low-energy ion events (no SSD signals). During this test, a constant, collimated oxygen beam is used, and PEPSSI rotated in the full  $160^\circ$  in the azimuth direction. All twelve internal collimator fins can be seen clearly in the figure overlaying the discrete anodes count rate. The discrete anodes perform the imaging function for low-energy ions. The proton beams used have angular spreads on the order of  $\sim 1^\circ$ . The angular resolution achieved is adequate for the science to be performed. Figure 21 shows the normalized response of the SSDs to the same angular scan. All six pairs of SSD are accounted for except sector 0, 2, and 5 where the electron SSDs are located.

**4.3.3.2 Time-of-Flight Resolution** The TOF spectrum of an 80 keV proton beam is shown in Fig. 22 with a 2.0 ns FWHM of the TOF peak. Intrinsicly the TOF spread ranges between  $\sim 2$  and 4 ns for the PEPSSI instrument. There are two causes that contribute to the TOF spread: (1) the dispersive spread in the secondary electrons ( $\sim 2$  ns), and (2) the performance of the TOF electronics (most notably the CFDs which is  $< 1$  ns). The measured TOF spread agrees with the expected PEPSSI performance (2.5–3.5 ns). Figure 23 shows the conversion coefficients taken from simulation to relate the measured TOF bin number into actually TOF in nanoseconds. Figure 24 summarizes the TOF performance of PEPSSI during beam calibration; the lowest energy that has a resolvable TOF spectrum for protons (oxygen ions) is 30 keV (50 keV).

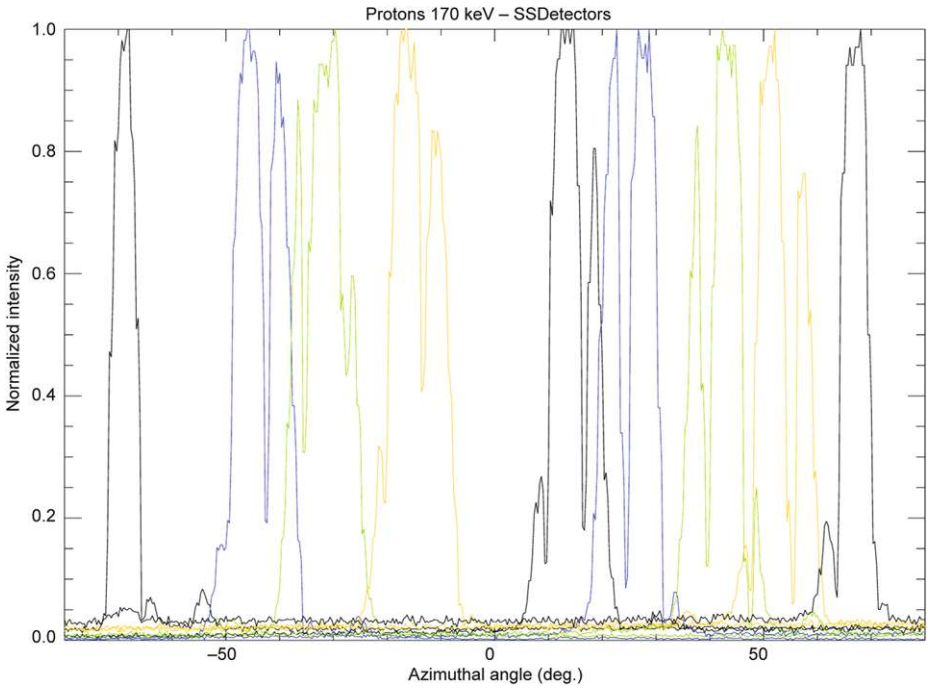


**Fig. 21** Normalized responses of all SSDs to the same angular scan using 170 keV protons. All detectors showed response from the beam, except sector 1, 5, and 11 where the electrons SSDs are located. The color code is (cf. identification of detectors and positions in Fig. 11): I0—black, I1—blue, I2—green, I3—yellow, I4—black, I5—blue, I6—green, I7—yellow, I8—black; note the coverage void between I0 and I1 (E0), as well as I3 and I4 (E1) and the collimator blades absorption features in every detector. A  $\sim 1^\circ$  beam of protons was used due to lower noise; stimulation of the anodes (shown previously) used oxygen beams to provide larger pulses for the measurements

**Fig. 22** The TOF spread of an 80 keV proton beam is shown in this figure. The fitted TOF FWHM is  $\sim 2$  ns, better than the expected 2.5 ns TOF resolution

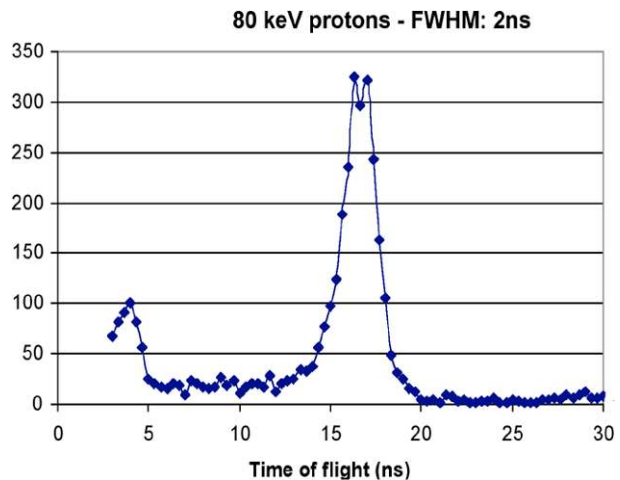


**Fig. 23** The conversion coefficients relating the measured bin number and the actual TOF in nanoseconds. Conversion coefficients are calculated from the sensor simulation, taking into account pre-acceleration as well as losses through start foil

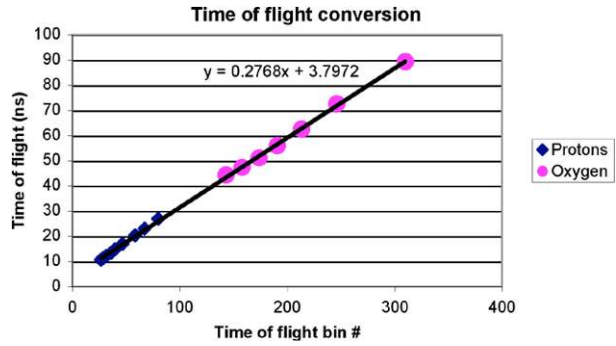
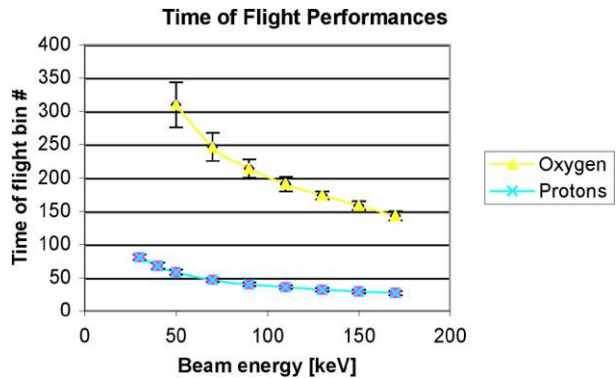


**Fig. 24** TOF performance of all beam runs that were performed during the PEPSSI flight unit ground calibration. The lowest energy TOF spectrum that was observed for proton (oxygen) is 30 keV (50 keV)



**4.3.3.3 Energy Resolution** Figure 25 shows the energy spectrum of a 130 keV proton beam measured by PEPSSI. The upper panel shows the entire spectra from 0 to 200 keV, and the lower panel is a close-up of the spectrum. The measured energy peak is at 120 keV and the fitted FWHM is 8.9 keV in excellent agreement with the simulation. The conversion coefficients for relating energy bin number into actual energy in keV are shown in Fig. 26 and Fig. 27 summarizes the energy performance of PEPSSI during beam calibration; the lowest energy that has a resolvable energy spectrum for protons (oxygen ions) is 40 keV (150 keV).

**4.3.3.4 Time-of-Flight versus Energy** Events that have both TOF and energy measurement are called triple events. Depending on the ion mass, each species will have a distinct track in a TOF vs.  $E$  plot. Figure 28 shows a 100-keV proton and 170-keV oxygen beam and the expected location of the tracks through simulation. Both energies fall exactly where we expected them to be. Multiple energies and species were calibrated, and their combined results are shown in Fig. 29. Typical TOF (Energy) FWHMs are 2, 3.5, and 4.7 ns (10, 15, and 25 keV) for H, He, and O respectively.

A degraded radioactive source provides a broad energy spectrum that is difficult to reproduce using a mono-energetic accelerator beam. A Mylar-degraded  $^{241}\text{Am}$  radioactive source was employed to extend the  $\sim 5$  MeV alpha line into a broad energy spectrum all the way down to  $\sim 100$  keV. Figure 30 shows the color spectrogram of the source spectrum as measured by PEPSSI during ground calibration. The y-axis shows the TOF in nanoseconds, while the x-axis shows the measured energy in keV. The spectrum falls exactly on top of the red curve, which is the expected TOF by  $E$  curve for helium calculated from the simulation.

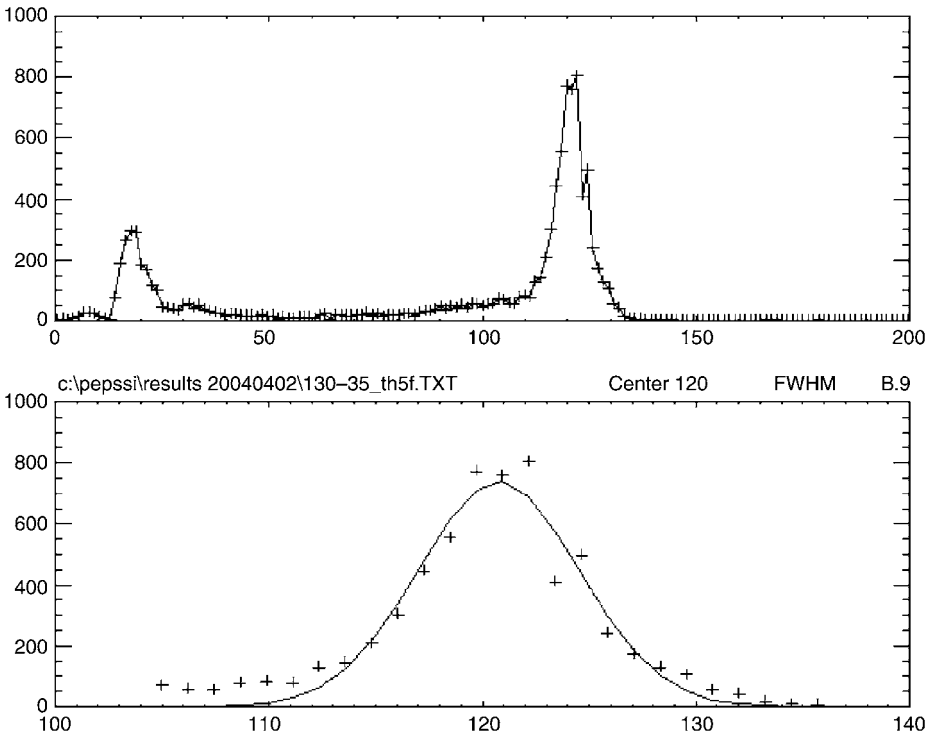
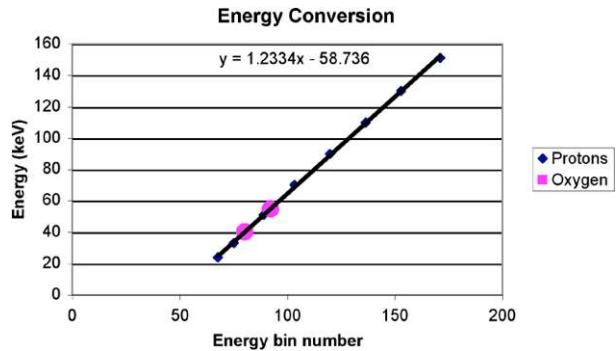


**Fig. 25** The figure shows the energy spectrum of a 130 keV-proton beam measured by PEPSSI. The *upper panel* shows the energy spectra from 0 to 200 keV, and the *lower panel* is a close-up of the spectrum (100 to 140 keV). The measured energy peak is at 120 keV and the fitted FWHM is 8.9 keV in excellent agreement with the simulation developed and used for all preflight work

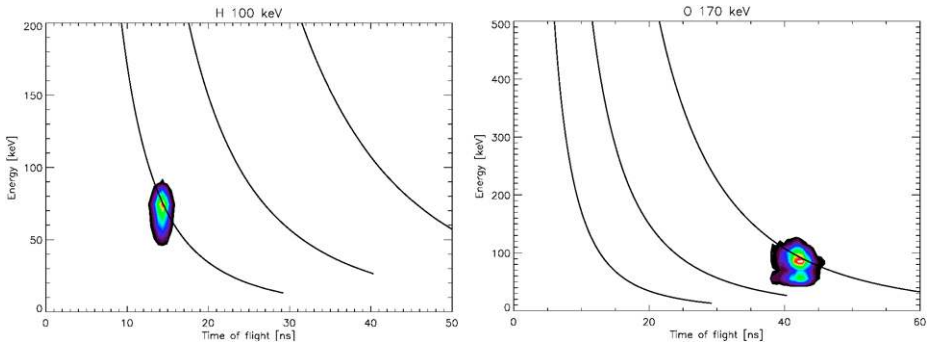
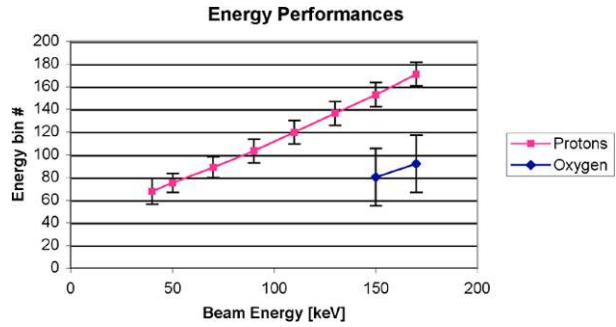
**Fig. 26** Conversion coefficients for relating energy bin number into actual energy in keV. The coefficients are slightly detector chain dependent, however, the variation is  $\sim \pm 2\%$



Additional testing with degraded alpha sources was performed during the instrument thermal vacuum tests. The goal was to characterize PEPSSI performance over a wide range of temperatures, confirming stability over the operational temperature range.

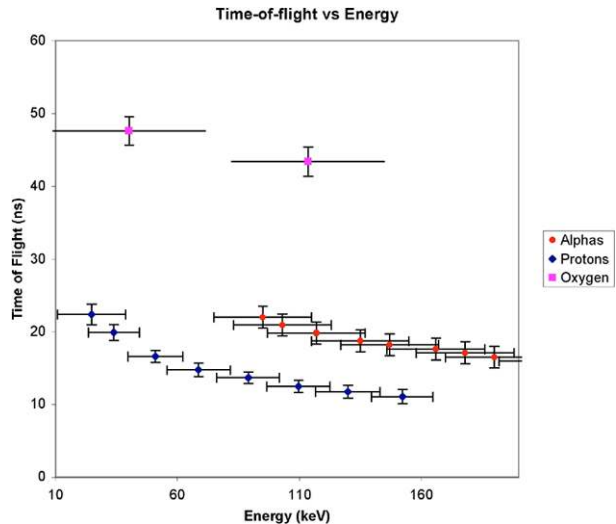
**4.3.3.5 Pulse Height Analysis** Due to the limited time available for calibration on the ground, the dependency of pulse height on the particle mass was not calibrated. Character-

**Fig. 27** Energy performance of all beam runs that were performed during the PEPSSI flight unit ground calibration. The lowest energy spectrum that was observed for protons (oxygen ions) is 40 keV (150 keV)



**Fig. 28** Proton-beam and oxygen-beam results are shown in these TOF versus energy plots. The simulated proton, helium, and oxygen tracks are shown as a *thick line* in the figures. The measured TOFs and energies of both beams fall very close to the expected values (the simulation used a thinner stop foil than actually implemented in these calibration runs; the expected lack of sensitivity to foil thickness at these beam energies is confirmed by the good agreement)

**Fig. 29** Combined results from all the beam runs that were performed to characterize PEPSSI performance



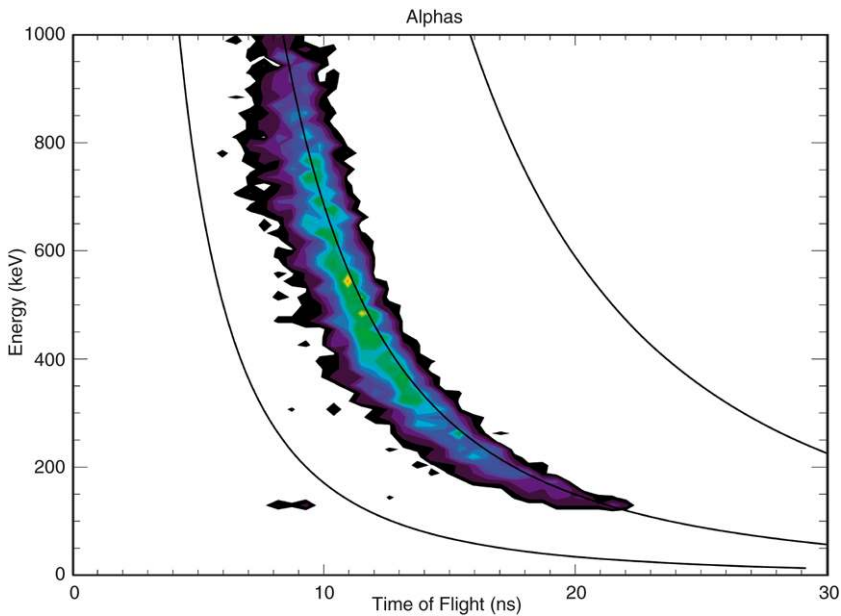


**Fig. 30** Alpha-particle energy versus time-of-flight plot from the stimulation of the PEPSSI flight unit by a degraded  $^{241}\text{Am}$  source. This produces a flat energy spectrum in the range of  $\sim 100$  keV to  $\sim 5$  MeV. The *central line* on the plot is from the simulated instrument response to He nuclei

ization of the heavy ion discriminators is being done during the commissioning phase in flight.

**4.3.3.6 Efficiencies** Figures 31 and 32 show the counting efficiency for both proton and oxygen beams as a function of the voltage across the MCP plates. The expected efficiency for 170 keV protons is 30–40% for the singles rate, and the measured stop foil efficiency is in agreement with that value. However, the start foil efficiency is clearly lower than expected, and it dominates the overall measured efficiency. The expected single efficiency for oxygen is in the 80–90% range. Here the efficiency is dominated by the start foil and does not reach a plateau even for relatively high values of the MCP voltage.

#### 4.3.4 Summary of PEPSSI Flight Model Calibrations

Tables 3 and 4 summarize the results of the PEPSSI flight model ground calibration. Ion-beam calibrations of the flight PEPSSI instrument demonstrate it met most of the flight requirements. Most notably, the measured energy resolutions are in agreement with the expected simulated performance. The measured 2.5 to 3.5 ns TOF (FWHM) resolution is better than anticipated (probably through better than expected electronics performance).

The major outstanding issues following calibration of the PEPSSI flight model include: (1) lower than expected ion counting efficiencies, and (2) higher energy threshold of heavy ions. Major progress has been made in addressing both issues with the engineering model.

#### 4.4 PEPSSI Engineering Model Calibrations

After the ground calibration and completion of all environmental and acoustic tests, PEPSSI was mounted on the spacecraft in December 2004. As noted previously, PEPSSI uses thin



**Fig. 31** The 170 keV proton efficiency plot as a function of the MCP bias voltage (across the plate). Expected efficiency for protons is 30–40%. Start foil efficiency is clearly lower than expected, and dominates the overall efficiency. These measurements are for the flight foils

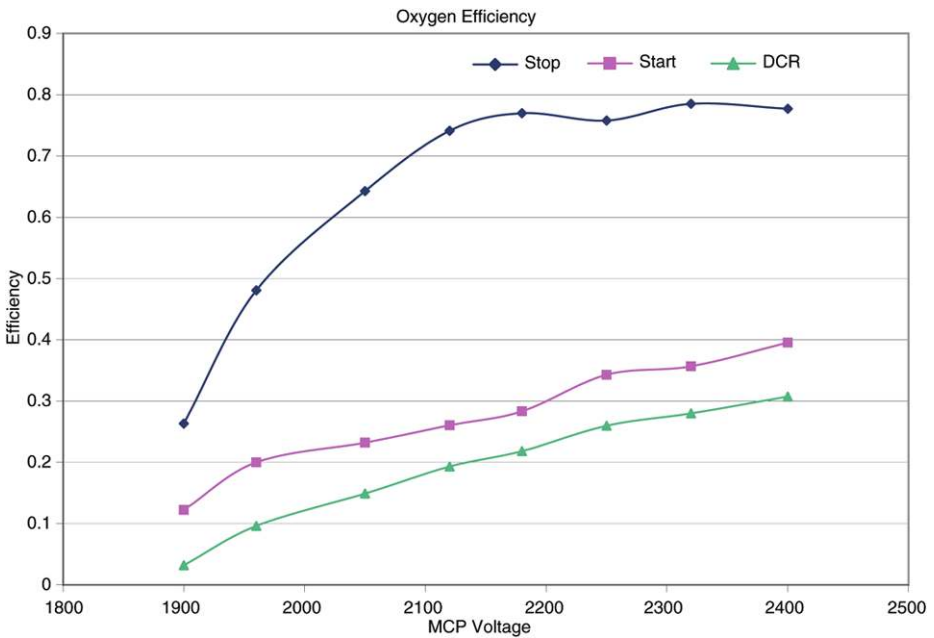
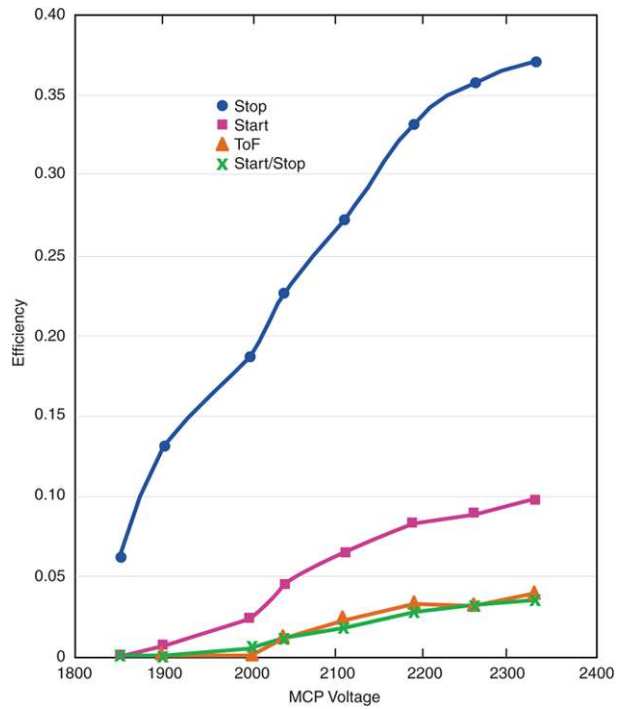


**Fig. 32** The 170 keV oxygen efficiency as a function of the MCP bias voltage (across the plate). Expected efficiency for oxygen is 80–90%. Here the efficiency is dominated by the start foil efficiency, and does not reach a plateau even for relatively high values of the MCP voltage. These measurements are for the flight foils

foils to generate timing signals to gate the time needed for an ion to transverse a known path. The flight unit has a thicker back foil than the original design. The change was due to the fact that during the initial ground calibration on the PEPSSI engineering unit, we observed a lower than expected efficiency on the instrument TOF system. Subsequently, the problem was traced to both front and back foils being used on PEPSSI. Replacement of both front and back foils before instrument delivery to the spacecraft was not possible; hence, a stopgap measured was taken. A flight-qualified MESSENGER Energetic Particle Spectrometer (EPS) back foil (Andrews et al. 2007) was located and installed in the PEPSSI flight unit as the new back foil. It is this combination of PEPSSI original front foil and EPS back foil that has gone through ground calibration and is in the PEPSSI flight unit.

#### 4.4.1 Original PEPSSI Foils

The original PEPSSI design uses aluminum-coated polyimide as the material for both the front and back foils. Both foils are made with 300-Å polyimide as support structure and then coated with 50 Å of aluminum on both sides to make it conductive. The total foil thickness is equivalent to 7  $\mu\text{g}/\text{cm}^2$ . With both aluminum front and back foils, the expected TOF efficiency of a 170 keV proton beam was expected to be  $\sim 10\%$ . However, less than 1% was measured on the engineering unit.

The discrepancy between the measured and expected efficiency is hypothesized to be produced by an oxidation layer on the thin aluminum coating on the foil. When aluminum is exposed to air, an oxide layer immediately forms. This oxide layer can be up to tens of Å in thickness, the same order of thickness as the aluminum coating. With such a relative thick oxide layer, the foil becomes an insulator, which affects both (1) the secondary electron production at the surface, and (2) the electrostatic optics within PEPSSI. These effects will be more pronounced for backward scattered (those secondary electron that travel opposite from the ion beam) electrons. We believe this is the reason why the measured stop efficiency is much lower than the expected value.

#### 4.4.2 PEPSSI Start and EPS Stop Foil

The decision was made to replace the PEPSSI flight unit back foil with a spare MESSENGER EPS back foil, which is constructed with 500 Å of polyamide and 100 Å of palladium, while retaining the aluminum-coated front foil. This combination of foils has been calibrated fully in the flight unit that was then mounted on the New Horizons spacecraft in December 2004. The measured TOF efficiency of this combination for 170 keV protons is  $\sim 4\%$ , which is dominated by the lower-than-expected start-foil efficiency since we still retain the original PEPSSI aluminum start foil.

#### 4.4.3 Engineering Model Plans

Calibration and characterization of the PEPSSI instrument is an ongoing activity that has two major thrusts: (1) continued characterization and testing of the flight-like engineering model, and (2) extensive in-flight calibrations.

The engineering model is essentially complete with a full complement of SSDs. Preliminary testing has already begun with one SSD pair to verify the carbon foil performance. After the full complement of SSDs are installed on the unit, it will then be extensively exercised in both the ball jar vacuum chamber with radiation sources and with accelerator beams to help determine the right set of parameters for optimum efficiency, TOF and energy measurement

performance (MCP voltage, CFD bias, CFD discriminators, Anode discriminators, etc). In addition, to characterize better the relative efficiencies of different mass species, work will investigate possible cross-talk in the valid-event identification circuitry that may occur when multiple energies and species are measured at the same time.

#### 4.5 In-flight Calibration

Energetic particles in interplanetary space will be used to test the mass classification algorithm and verify the content of the various look-up tables. Because the interplanetary environment is variable, it is highly desirable to have the PEPSSI instrument operating substantially longer than that planned for the checkout period. Interplanetary energetic particles tend to vary on the time scale of a solar rotation:  $\sim 27$  days. It is highly desirable to operate the PEPSSI sensor for at least 27 days during each yearly checkout prior to the Pluto flyby in order to optimize the Pluto encounter measurements. The Jupiter flyby provided a key opportunity for checking out multiple instrument features as noted below.

##### 4.5.1 Flight Performance

Following the launch of New Horizons on 19 Jan 2006, PEPSSI commissioning began with initial checkout on 20 Feb, a month later. Activities of spacecraft instruments are keyed to a Science Activity Plan (SAP) number. A total of 23 SAPs were executed in 2006. These included tests, the one-time door opening (3 May 2006), determination of thresholds, detector configuration, efficiency tests, and mapping of the orientation of the sensor head by monitoring when the Sun was in the sensor field of view. These tests are listed in Table 28.

PEPSSI was powered on again at 00:00 UTC 6 Jan 2007 and run through 19:20 UTC on 8 Jan; the instrument was powered on again at 00:09 UTC 9 Jan and run for seven and a half hours. On Jan 10 at 08:00 UTC PEPSSI was again turned on and run through 14 Jan 16:30 UTC. Each exercise was used to change instrument configuration for checkouts as Jupiter was approached. From 16 Jan 01:00 UTC through 20 Jan 23:00, 22 Jan 07:00 through 24 Jan 03:30, 24 Jan 06:00 through 31 Jan 05:00, and 31 Jan 07:00 through 10 Feb 12:30 further testing was conducted, including the uploading of new table parameters for the Jupiter flyby.

##### 4.5.2 Jupiter Flyby

Coincident with the Jupiter flyby various setting changes were made to check the instrument response. Early on, PEPSSI high voltage was turned down to protect the microchannel plates from direct sunlight. The flyby provided significant science at Jupiter, especially on the Jovian magnetotail (McNutt et al. 2007), while also providing additional data on instrument performance and sensitivity. The scope of both efforts is shown in Fig. 33 that shows both energy spectra and tests that were conducted between days 40 and 140 (9 Feb–20 May 2007); scientific analysis of these data are provided in the referenced article. The instrument was finally fully powered down for the first New Horizons hibernation period on 21 Jun (day 172) at 19:40 UTC. Analysis of both science and instrument calibration data from this period is ongoing.

## 5 Operations and Science

### 5.1 Instrument Operations

After power-up and software boot, PEPSSI operates in either one of two operational modes—Standby and Science. Power requirements for each mode differ and depend upon

**Table 28** PEPSSI commissioning activities

SAP No.	Stol/Seq	Date Performed	Title	Description	Test Successful?
014	Stol	20-Feb-06	Initial checkout/functional	Run same test as pre launch ground CPT to verify the instrument is fully operational and has survived launch	Yes
004	Stol	22-Feb-06	Table load	Load new science classification tables	Yes
005	Stol	22-Feb-06	Heater test	Test flight cruise heater	Yes
006	Stol	1-Mar-06	SSD checkout	Power on bias voltage and monitor SSDs for 24 hours to characterize background with doors closed	Yes
012	Stol	2-Mar-06	Power off	Standard power off procedure, used for all commissioning activities.	Yes
016	Stol	27-Apr-06	Table load	Load new science classification tables	Yes
001	Stol	2-May-06	Power on for door opening	Power on and establish SSD background counts to observe difference when door is opened.	Yes
007	Stol	3-May-06	Open door	Open door, and verify with SSD counts, S/C primary current circuit (fire twice), S/C inertial data, and SDC sensor	Yes
008	Stol	16-May-06	Initial HV ramp	Ramp up HV to 2000 V, and manually verify current and voltage after each step	Test aborted due to Sun in FOV, only ramped to Sun safe levels. This was expected before running the test
008c	Stol	6-Jun-06	Load HV macros	New macros step HV in controlled sequence so a S/C reset can not occur between sending a HV command and re-enabling HV safing	Yes
008a	Stol	6-Jun-06	Initial HV ramp	Repeat 008 with new macro and S/C pointing so Sun is not in FOV	Yes
017	Stol	21-Jun-06	2000 V threshold scan	Determine optimal thresholds for most channels at 2000 V, also stayed on for 24 hours	Yes

**Table 28** (Continued)

SAP No.	Stol/Seq	Date Performed	Title	Description	Test Successful?
016	Stol	13-Jul-06	Table load	Load new science classification tables	Yes
018	Stol	14-Jul-06	Sun scan test	Scan when the Sun is in FOV by monitoring count rates and current when S/C is in spin mode	Yes
019	Stol	14-Jul-06	MCP plate scrub	Power MCPs to low voltage with Sun in FOV for 2 weeks to scrub plates	Yes
018	Stol	27-Jul-06	Sun scan test	Scan when the Sun is in FOV by monitoring count rates and current when S/C is in spin mode	Yes
015	Stol	11-Aug-06	Load macro 11	Load macro 11 to fully initialize PEPSSI at 2000 V, use data from 017 to set all thresholds	Yes
018	Stol	11-Aug-06	Sun scan test	Scan when the Sun is in FOV by monitoring count rates and current when S/C is in spin mode	Yes
018	Seq	26-Aug-06	Sun scan test	Scan when the Sun is in FOV by monitoring count rates and current when S/C is in spin mode	Yes
020	Seq	8-Sep-06	2150 V Threshold Scan	Found optimal thresholds for all channels at 2150 V	Yes
022	Seq	9-Sep-06	Enhanced Threshold Scan	Additional scans at 2000 V to determine thresholds for some detectors that were not determined during 017	Yes
021	Stol	25-Sep-06	Load and test macro 12	Load macro 12, verify it loaded correctly, then run and stay on for 24 hours	Yes
027		23-Nov-06	Efficiency test		Yes

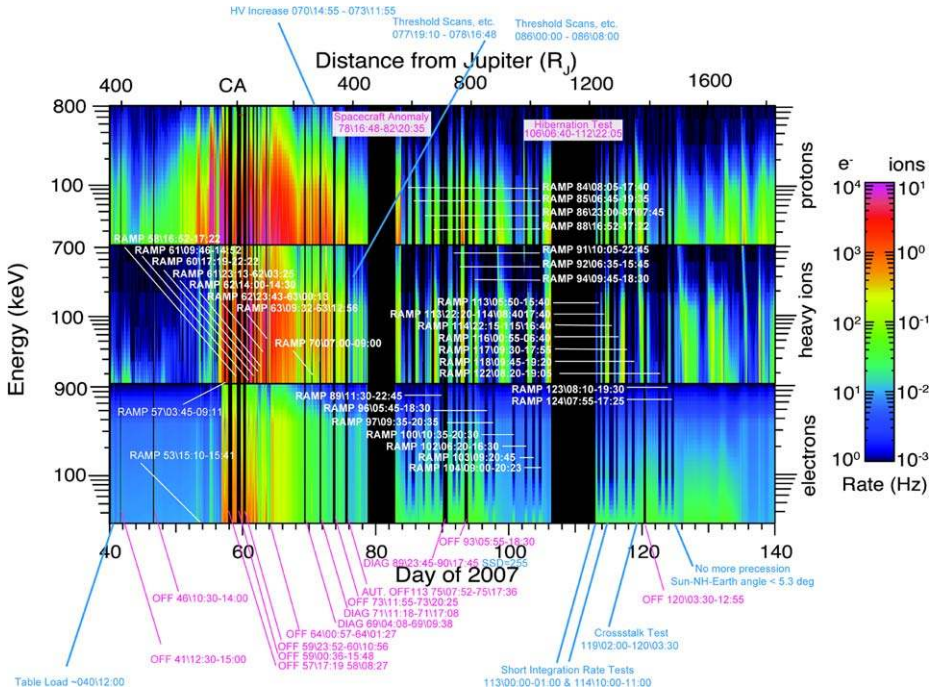


**Fig. 33** Energy spectrograms from the electron, heavy ion, and proton channels during the Jupiter encounter showing variations from before the last inbound magnetopause crossing until after the first outbound crossing. Labels indicate instrument activity and show the scope of this effort, both for diagnostics and for instrument health (the high voltage on the MCPs was ramped down when sunlight could enter the instrument aperture. This is not an issue at Pluto)

the state of the HVPS as well as the rate at which data is collected. The not to exceed power allocation for PEPSSI is 2.55 watts.

The modes and the current best estimate (CBE) of power for each mode are:

- Boot/Standby: Power on, HVPS disabled (no science data).
  - Housekeeping status and instrument checkout—1.84 watts
- Science: Power on, HVPS enabled, science data sent to the C&DH.
  - Nominal Event Rate, measured (Pluto flyby)—2.43 watts
  - High Event Rate (measured at Jupiter flyby)—2.46 watts

### 5.1.1 Cover Release In Space

The NH spacecraft was launched into heliocentric orbit with the PEPSSI instrument aperture covers closed. To prevent thermal damage to entry foils in the sensor module, the covers were not to be opened until the distance from the Sun to the NH spacecraft was least 2 AU. With no specific housekeeping flag to indicate the instrument covers are open the bias supply of the HVPS was activated and science data enabled. Open covers are evidenced by detection of background particle energy events. This operation showed that the covers were indeed open, but it also led to the discovery of the misalignment of the instrument on the spacecraft deck.

### 5.1.2 *Idle State (HVPS Disabled)*

At instrument power-up, the HVPS is always in the disabled state. The instrument idles indefinitely, waiting for command input from the spacecraft. In this state housekeeping data is output at a preset rate, and output science data packets contain only filler data. Prior to science data collection, the HVPS must be enabled and brought on-line.

### 5.1.3 *HVPS Activation*

To activate the HVPS, a preconfigured sequence of commands must be executed to enable HVPS operation, adjust the power supply clock rates, ramp up the output voltages, and set HVPS alarm limits. Once the HVPS is operating and functioning at the appropriate voltage levels, flowed science data is valid.

Following launch into space, prior to first activation of the HVPS, at least 14 days must be allowed to elapse to allow sufficient time for outgassing. In practice, the HVPS was not turned on until after the doors were open, much more than 14 days after launch.

Following HVPS activation, a number of HVPS parameters may be adjusted by command. These include commands to adjust the levels of the SSD bias voltage and the high voltage (HV) outputs. The HV voltages are adjusted during the cruise phase to compensate for known aging of the MCP electron gain characteristics. By adjusting to a slightly higher voltage, constant MCP gain (and hence TOF system characteristics) may be maintained. Similarly, the SSD bias voltage may be periodically adjusted to compensate for SSD aging characteristics.

HV and SSD bias supply clock frequencies may also be adjusted by command. As the HVPS components age, HVPS efficiency will be monitored. Slight adjustments to the HVPS clock frequencies may be made to retain power efficiency.

### 5.1.4 *Science Mode Operation*

In Science mode, particle TOF-plus-Energy, electron energy, and TOF-only measurements are made and output on a regular basis. Specific science mode data products are defined above. The rates at which science data products are collected are programmable (by adjusting the data integration time interval) and the range of data rates possible is outlined in prior sections that specify PEPSSI telemetry. Regardless of science data rates, the data collection intervals are synchronized to the MET 1PPS input from the spacecraft.

During PEPSSI science mode operation, the PEPSSI instrument requires few if any commands. However, there are a number of instrument operating adjustments, in addition to the data integration interval, that can be made by command. These adjustments are described below. These adjustments, if required, are typically made during early in-space operations. During cruise mode operations, and prior to any major instrument data collection campaign, instrument operation is monitored to determine if any further adjustments are required.

**5.1.4.1 *Energy Leading Edge Discriminator (LED) Threshold*** PEPSSI implements a Leading Edge Discriminator (LED) for each of the 12 SSD energy channels. Only particle energy events that exceed the LED threshold are counted and included in the telemetry science data output. The threshold for each LED is adjustable by instrument command over a range up to  $\sim 250$  keV and to a quantization of  $\sim 1$  keV.

The purpose of the LED is to provide a means to detect particles of minimum energy while minimizing false counts due to system noise. During ground calibration, the LED

threshold of each channel is adjusted so that the false count rate is low, much less than one event per second, while maintaining the capability to detect particles at or below the energy thresholds required.

During initial in-space PEPSSI operations, the energy LED thresholds may be tweaked slightly to achieve optimum performance. After the initial tweaking, the threshold of any particular LED will be adjusted only if increased noise is detected in that channel.

**5.1.4.2 Stop Anode Light and Heavy Discriminator Thresholds** PEPSSI applies two discriminators to the TOF stop-anode signal. The discriminator thresholds are adjustable over a range of signal input levels by instrument command.

For TOF-only measurements, the magnitude of the respective anode signal is a coarse indicator of particle mass. The threshold levels are adjusted so that, for TOF-only measurements, the particles may be differentiated on the basis of light or heavy mass. The threshold level of one discriminator is set to a low value, low enough to detect  $H^+$  ions, the other is set to a higher threshold, to detect CNO and higher mass particles. One is referred to as the light discriminator, the other the heavy discriminator.

Due to time constraints, the light and heavy discriminator thresholds were not calibrated and adjusted prior to launch. The thresholds will be adjusted for optimum performance as part of ongoing flight operations. It is anticipated that the final light and heavy thresholds will rarely, if ever, be changed; thresholds will be readjusted only in response to detected changes in TOF system noise or front-end sensitivity.

**5.1.4.3 Constant Fraction Discriminator (CFD) Thresholds** The composite TOF-start and TOF-stop signals are each passed through a CFD to generate digital level signals. Digital level TOF-start and TOF-stop pulses are required for input to the TOF chip. The CFD thresholds are adjustable over a range of values by instrument command; only TOF anode signals that exceed the CFD thresholds will result in a TOF measurement.

The CFD thresholds determine the lower signal threshold for TOF measurements. It is set during ground calibration to as low a threshold possible consistent with acceptable false TOF detection rates due to TOF system noise. During ground calibration, the threshold of each CFD was adjusted so that the false TOF event rate is low, much less than one event per second, while maintaining the capability to detect particles at or below the energy thresholds set previously. During initial in-space operations and checkout of PEPSSI, the CFD thresholds were tweaked to achieve optimum performance. After the initial tweaking, the CFD thresholds will be adjusted only if increased noise is detected in the TOF system.

**5.1.4.4 Start Anode Discriminator Thresholds** The PEPSSI design includes leading edge discriminators for each of the six start anode signals. The discriminator thresholds are adjustable over a range of values by instrument command. The discriminator outputs are used to determine the direction (i.e., sector) of the respective TOF measurement.

Only TOF anode signals that exceed the discriminator threshold will provide a signal output indicative of particle direction. During ground calibration, the threshold of each discriminator is adjusted to be consistent with CFD thresholds. During in-space operations, adjustments may be required if the CFD thresholds are changed.

**5.1.4.5 Multiple Hit Check Enable/Disable** As heritage from the MESSENGER EPS design, PEPSSI includes a multiple-energy-event detect/reject feature. This feature, enabled by command, causes the instrument to reject (not count) multiple energy events that occur closely in time. Multiple events occurring in close proximity may cause degradation in the



accuracy of energy measurements, and the intent is to provide a means to prevent these types of events from being counted. If this feature is disabled, and multiple energy events occur closely in time, the multiple events are counted as a single event, and, if an event crosstalks to an adjacent detector, the wrong detector could be read out, misclassifying the energy.

### 5.1.5 Power Down Operation

PEPSSI is designed so that power to the instrument may be switched off while the HVPS is operating. No damage to the instrument can occur. However, for normal operations, the instrument HVPS is ramped down in voltage and turned off in a controlled sequence prior to switching off power to the instrument.

## 5.2 Data and Data Archiving

The New Horizons Science Operations Center (SOC) is part of the ground system that processes data returned from the New Horizons planetary spacecraft. Data down-linked from the spacecraft in raw packetized form are retrieved by the SOC from the Mission Operations Center (MOC) along with navigation and related ancillary data. The SOC generates the higher-level data products used by the instrument teams and science teams. In addition, the SOC performs archiving of data to the Planetary Data System (PDS). The science data processing component of the SOC is called the SOC pipeline.

The SOC pipeline is divided into three main parts: the Level 1 pipeline segment, the Pre-Level 2 pipeline segment, and the Level 2/3 segment. Pipeline processing is carried out sequentially. Results of the Level 1 pipeline are provided as inputs to the instrument Pre-Level 2 pipeline segment. The Level 2/3 segment combines the pre-Level 2 temporary data files into easily used (Level 2) and science/calibrated (Level 3) formats. The instrument pipeline generates Level 2 and Level 3 results that the SOC forwards to the PDS archiving process. All levels of science data files (Level 1, Pre-Level 2, Level 2, and Level 3) are stored in FITS format.

### 5.2.1 Level 1

The Level 1 data product is a FITS format data file and all data is contained in FITS extension Header Data Units (HDUs). Each HDU contains a PEPSSI science data telemetry block. The non-status HDUs are stored as 1-D FITS images containing the binary data of a de-commutated science data telemetry block. Status extensions have been “unrolled” into a normal 2-D FITS binary table with columns for each uncalibrated status quantity and a separate row for each measurement time. Level 1 files are not present in the PDS archive. Data from different telemetry classifications are placed in different files (Table 29).

### 5.2.2 Level 2

The Level 2/3 pipeline is run on the SOC processing station to transform Level 1 de-commutated data into Level 2 and Level 3 calibrated science data. The instrument pipeline creates PDS standard, Level 2 and Level 3 provisional products in FITS format.

The Level 2 files “unroll” the data in the Level 1 files into flat, single datum per cell, tables that are easily human readable using standard FITS tools like *fv* (<http://fv.gsfc.nasa.gov>).

In the Level 2 files, all of the data for a single UTC day of observation are present in a single file. Each type of PEPSSI data: High Priority Rate Data (N1), Low Priority Rate Data (N2), Status Data, and the various forms of PHA data, in both normal and diagnostic modes is placed in a different FITS binary table with associated header keywords to create a separate FITS extension or header data unit (HDU).

**Table 29** Data file layout

File Type	HDU Type
N1	Primary HDU: High Priority Telemetry Block Extension 1: PHA Telemetry Block Extension 2: Status Telemetry Block
N2	Primary HDU: Medium Priority Telemetry Block Extension 1: PHA Telemetry Block Extension 2: Status Telemetry Block
N3	Primary HDU: Low Priority PHA Telemetry Block

**5.2.2.1 Summary of the Level 2 Header Data Units (HDUs)** In PEPSSI Level 2 files, each HDU represents a different type of data; there is only one HDU of each type (EXTNAME). An HDU will only be present if there is data of that type taken during the time period covered by that file. Each file contains exactly one UTC observing day worth of data. The Primary HDU contains no data; it contains only informational header keywords identifying mission information, observational start time, and information about the file creation (date, software version, etc.).

The available HDUs are:

D\_N1, D\_N1\_STATUS, D\_N2, D\_N2\_STATUS, N1, N1\_STATUS, N2, N2\_STATUS, PHA\_DIAG, PHA\_ELECTRON, PHA\_LOW\_ION, PHA\_HIGH\_ION

The different extensions are described below.

When a charged particle enters the PEPSSI detector, we measure its energy and/or TOF. Because there is insufficient bandwidth to telemeter all of our events, we use a round-robin priority scheme to decide which PHA events to discard and which to telemeter. All events are counted in various histograms in the Rate data.

**5.2.2.2 PHA HDUs** The four PHA HDUs: PHA\_DIAG, PHA\_ELECTRON, PHA\_LOW\_ION, and PHA\_HIGH\_ION contain columns for the end time of the accumulating interval, the uncalibrated Energy and Time of Flight values and the detectors involved in measuring a given event (e.g. which solid state energy detector fired and which start anode fired).

Each row represents a separate charged particle event.

**5.2.2.3 Rate HDUs** The N1 and N2 (and D\_N1 and D\_N2) extensions contain several types of “Rate” data. The Rate data is accumulated in histograms that are then dumped at set intervals. For N1 data, usually the histograms are accumulated for 600 seconds. For N2 data, the accumulation time is usually 60 seconds except for the first hour of the day when it is 15 seconds. This can be changed, but during normal observing it is almost always true:

- B Rates: The number of high-energy ion events in the various “Rate Boxes”. For example: a Rate labeled B01S03 represents Protons which deposited between 60 and 94 analog to digital units (ADUs) of energy in the solid state detector.
- C Rates: The contents of various hardware counters
- HK Rates: Various housekeeping quantities such as power levels and discriminator thresholds
- J Rates: Software counters that represent overall quantities like total number of Electron Events.
- L Rates: The number of low energy (TOF-only) ion events sorted into Boxes.
- R Rates: The number of electron events.

All of the rate column contents are specified in detail in the comment field of their respective TFORM keywords in the FITS Header.

The N1 and D\_N1 data are identical in format; the D\_N1 data are merely taken when the instrument is in diagnostic mode. The definitions of some of the Rate Boxes are different in diagnostic mode and normal mode. N2 (and D\_N2) are identical to their N1 counterparts except that they are typically sampled much more frequently (every 15 or 60 seconds) and only a subset of the L and C rates are present.

**5.2.2.4 Status HDUs** All the STATUS HDUs contain the same quantities for their respective coverage periods and are the same values as in the Level 1 files calibrated to physically meaningful values.

The Level 2 data files represent all of the scientifically useable data from the PEPSSI instrument and are meant to be the starting point for science analysis of that data.

### 5.2.3 Level 3

The Level 3 data is a calibrated, scientifically useful subset of the Level 2 data. As with the Level 2 data, each Level 3 file covers all of a single day of observation. There are three basic types of data in the L3 files: Quick-Look, flux-calibrated Rate Data, and calibrated PHA data. No Diagnostic mode data is present in the L3 files.

The Level 3 files are meant to be, as much as possible, self-documenting. All calibration constants, calibration formulas, and physical units are present in the FITS header in an easily readable format.

The image in the primary array of the L3 file is a rate-weighted 2-D histogram of the PHA data for that day binned in calibrated deposited energy. The priority scheme distorts ion abundances, so we correct for that by using a “rate-weighted” rather than a single count histogram.

The next five HDUs: SPEC\_Protons, SPEC\_Helium, SPEC\_Heavies, SPEC\_Electrons, SPEC\_LowIon, contain quick-look spectrograms of their respective species. These spectrograms present counts/second N2 data, averaged over 60 second intervals and summed over all incidence directions.

The FLUX HDU contains calibrated fluxes, uncertainties, and raw counts/sec rates for all of the High Energy Ion and Electron N2 Rate data. There is also an accumulation time column (**DT**) and three timing columns. Separate calibrations are given for different ion species for some of the rate boxes if the composition in that rate box is complicated (e.g. both oxygen and sulfur in a single box).

The three PHA extensions: PHA\_ELECTRON, PHA\_LOW\_ION, and PHA\_HIGH\_ION contain the PHA event data telemetered in the N2 data. Each row represents a single PHA event. Cross-talk events are excluded. Quantities of limited usefulness (such as Heavy Ion Discriminator triggers) are excluded. Calibrated Deposited Energy and/or Time of Flight values are given. The linear calibration constants and formulas are in the FITS headers. A **Speed** column is calculated from the Time of Flight. The Rate Box classification for each event is given in the **Rate\_Box** column.

The PHA\_HIGH\_ION HDU contains additional columns: **H\_Incident\_Energy**, **He\_Incident\_Energy**, **O\_Incident\_Energy**, and **S\_Incident\_Energy** columns contain the calculated Incident energy assuming that the event is of that (H, He, O, or S) species. The Rate\_Normalized\_Weight column has removed Priority Group artifacts from the PHA data. This column is usually used in making histograms of the High Energy Ion PHA data.

#### 5.2.4 MIDL

PEPSSI data can be viewed using a software suite known as the Mission Independent Data Layer (MIDL). A full complement of analysis tools is available: line plots of individual particle rate channels, energy spectra and spectrograms, and histograms (one-dimensional and two-dimensional) of the PHA event data. MIDL also incorporates and makes available spacecraft ephemeris and pointing information vital to interpreting the *in situ* PEPSSI data. Each of the plotting tools also serves as a data access mechanism, because the data values used to make any plot can be extracted and saved separately. All discovery, downloading, and local caching of science and ancillary data are handled automatically, providing a seamless view of the entire PEPSSI dataset.

MIDL reads the Level 2 (or Pre-Level 2) data in FITS format as produced by the SOC, and applies the appropriate calibrations, allowing the user to select from a variety of units in which to view the data—everything from raw counts to fully calibrated intensity. Detailed calibration options are available for members of the instrument team, with reasonable defaults provided for non-expert users.

Created prior to PEPSSI, MIDL uses a modular approach in which plotting tools are isolated from dataset-specific read routines. New datasets can take advantage of the existing plotting tools by simply providing the appropriate set of read routines. Most plotting tools used by PEPSSI existed in MIDL prior to their use with PEPSSI. The exception is the PHA histogram tools, which were specifically developed for PEPSSI (but could also be used by other missions with PHA data). The original version of MIDL was funded as a research effort by NASA's Applied Information Science Research (AISR) program but has now been used as a primary analysis suite for three energetic particle instruments (others are Geotail/EPIC and Cassini/MIMI).

Written in Java, MIDL can be launched (via Java Web Start) as a client program on any modern operating system from any web browser.

## 6 Conclusion

The PEPSSI instrument on the New Horizons spacecraft will measure the outermost reach of Pluto's escaping atmosphere at the time of the flyby in 2015. Recent observations (Elliot et al. 2007) suggest that the atmospheric escape rate may not be significantly diminished from its value near Pluto's perihelion in 1988. Observations at comets and at Jupiter with PEPSSI indicate that the interaction region and pickup ions from Pluto's atmosphere should be easily discernable and diagnostic of the magnitude and extent of the interaction of Pluto with the solar wind.

The PEPSSI instrument is another step in an evolving suite of combined energy/time-of-flight instruments for probing the properties of multispecies energetic particles across the solar system, and, potentially, beyond. The origins of these capabilities in a compact, low-mass, low-power design trace back to early planning for the inclusion of particle instruments on a Pluto flyby mission. The development and inclusion of PEPSSI on this mission to Pluto and the Kuiper Belt objects beyond can also be seen as a significant achievement of NASA's PIDDP efforts. With the successful measurements made near Jupiter and down the Jovian magnetotail, the instrument is fully checked out and calibrated for use during the encounter with Pluto in 2015.

With a trajectory near the same ecliptic longitude of Voyager 2, New Horizons has the capability to provide a platform for monitoring the solar wind flow and energetic particle propagation toward the heliopause during the regular annual checkouts and comparing

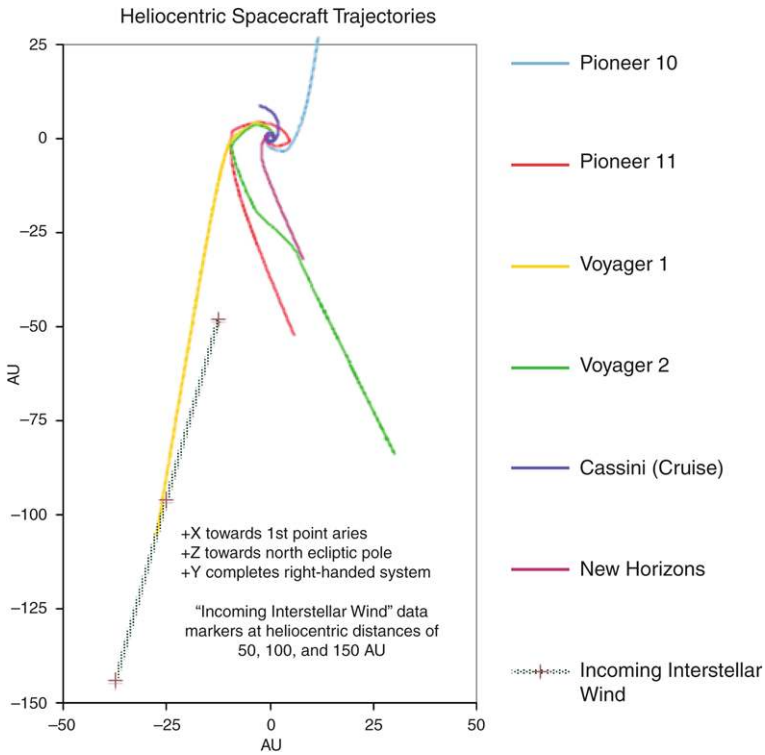


**Fig. 34** Trajectories of all solar-system escaping spacecraft as projected into the plane of the ecliptic along with that for Cassini during its cruise to Saturn (for scale). Voyager 2 and New Horizons are escaping the solar system at roughly the same longitude and close to the flow direction of the very local interstellar medium

conditions with those at Voyager 2 (Fig. 34). In addition to probing the puzzle of Pluto's escaping atmosphere and its interaction with the solar wind in 2015, as well as potentially looking near a Kuiper Belt Object for cometary activity, PEPSSI will thus continue our research into how the solar system interacts with its environment of the very local interstellar medium.

**Acknowledgements** We would like to thank the support of the engineering support and technical services and support staffs at APL that made the design, fabrications, and the delivery of the PEPSSI instrument to the New Horizons spacecraft possible. We thank the two referees for their detailed, helpful comments. This work has been supported as part of the New Horizons effort under NASA Contract NAS5-97271.

## References

- S. Agostinelli et al., GEANT4—a simulation toolkit. *NIM(A)* **506**, 250–303 (2003)
- G.B. Andrews, R.E. Gold et al., *Compact Particle Detector for Space Measurements: Prototype Performance* (SPIE, San Diego, 1998)
- G.B. Andrews, T.H. Zurbuchen et al., The energetic particle and plasma spectrometer instrument on the MESSENGER spacecraft. *Space Sci. Rev.* **131**, 523–556 (2007)
- F. Bagenal, T.E. Cravens et al., Pluto's interaction with the solar wind, in *Pluto and Charon*, ed. by S.A. Stern, D.J. Tholen (University of Arizona Press, Tucson, 1997), pp. 523–555
- F. Bagenal, R.L. McNutt, Jr., Pluto's interaction with the solar wind. *Geophys. Res. Lett.* **16**, 1229–1232 (1989)

- J.P. Biersack, L. Hagmark, Stopping and range of ions in matter. *NIM* **174**, 257 (1980)
- N. Brosch, The 1985 stellar occultation by Pluto. *Mon. Not. R. Astron. Soc.* **276**, 571–578 (1995)
- A.J. Coates, A.D. Johnstone et al., Pick-up water group ions at Comet Grigg-Skjellerup. *Geophys. Res. Lett.* **20**, 483–486 (1993a)
- A.J. Coates, A.D. Johnstone et al., Velocity space diffusion and non-gyrotropy of pickup water group ions at comet Grigg Skjellerup. *J. Geophys. Res.* **98**, 20985–20994 (1993b)
- S.J. De Amicis, Instrumentation developed by the Johns Hopkins University Applied Physics Laboratory for Non-APL Spacecraft, Laurel, MD, JHU/APL, 1988
- P.A. Delamere, F. Bagenal, Pluto's kinetic interaction with the solar wind. *Geophys. Res. Lett.* **31**, L04807 (2004). doi:[10.1029/2003GL018122](https://doi.org/10.1029/2003GL018122)
- M. Dryer, A.W. Rizzi et al., Interaction of the solar wind with the outer planets. *Astrophys. Space Sci.* **22**, 329–351 (1973)
- J.L. Elliot, E.W. Dunham et al., Pluto's atmosphere. *Icarus* **77**, 148–170 (1989)
- J.L. Elliot, A. Ates et al., The recent expansion of Pluto's atmosphere. *Nature* **424**, 165–168 (2003)
- J.L. Elliot, M.J. Person et al., Changes in Pluto's atmosphere: 1988–2006. *Astrophys. J.* **134**, 1–13 (2007)
- U. Fink, B.A. Smith et al., Detection of a CH<sub>4</sub> atmosphere on Pluto. *Icarus* **44**, 62–71 (1980)
- G.H. Fountain, D.Y. Kusnierkiewicz et al., The New Horizons spacecraft. *Space Sci. Rev.* (2008), this issue. doi:[10.1007/s11214-008-9374-8](https://doi.org/10.1007/s11214-008-9374-8)
- H.J. Frischkorn et al., Total yield and escape depth of electrons from heavy ion solid interactions. *IEEE Trans. Nucl. Sci.* NS-30 (1983)
- A.A. Galeev, Encounters with comets: discoveries and puzzles in cometary plasma physics. *Astron. Astrophys.* **187**, 12–20 (1987)
- A.A. Galeev, T.E. Cravens et al., Solar wind stagnation near comets. *Astrophys. J.* **289**, 807–819 (1985)
- G. Gloeckler, F.M. Ipavich et al., The charge-energy-mass spectrometer for 0.3–300 keV/e ions on the AMPTE CCE. *IEEE Trans. Geosci. Remote Sens.* **GE-23**, 234–240 (1985)
- G. Gloeckler, D. Hovestadt et al., Cometary pick-up ions observed near Giacobini-Zinner. *Geophys. Res. Lett.* **13**(3), 251–254 (1986)
- R.E. Gold, S.C. Solomon et al., The MESSENGER mission to Mercury: scientific payload. *Planet. Space Sci.* **49**, 1467–1479 (2001)
- E.M. Harnett, R.M. Winglee et al., Three-dimensional multifluid simulations of Pluto's magnetosphere: A comparison to 3D hybrid simulations. *Geophys. Res. Lett.* **32**, L19104 (2005). doi:[10.1029/2005GL023178](https://doi.org/10.1029/2005GL023178)
- D.E. Huddleston, A.J. Coates et al., Mass loading and velocity diffusion models for heavy pickup ions at comet Grigg-Skjellerup. *J. Geophys. Res.* **98**, 20995–21002 (1993)
- K. Kecskemeti, T.E. Cravens, Pick-up ions at Pluto. *Geophys. Res. Lett.* **20**, 543 (1993)
- V.A. Krasnopolsky, Hydrodynamic flow of N<sub>2</sub> from Pluto. *J. Geophys. Res.* **104**(E3), 5955–5962 (1999)
- S.M. Krimigis, D.G. Mitchell et al., Magnetospheric imaging instrument (MIMI) on the Cassini mission to Saturn/Titan. *Space Sci. Rev.* **114**, 233–329 (2004)
- L.J. Lanzerotti, R.E. Gold et al., Heliosphere instrument for spectra, composition, and anisotropy at low energies. *Astron. Astrophys. Suppl. Ser.* **92**, 349–363 (1992)
- J.L. Lunine, D. Cruikshank et al., Pluto Express. Report of the Science Definition Team: 65, 1995
- D.J. McComas, F. Allegrini et al., The solar wind around Pluto (SWAP) instrument aboard New Horizons. *Space Sci. Rev.* (2008), this issue. doi:[10.1007/s11214-007-9205-3](https://doi.org/10.1007/s11214-007-9205-3)
- R.W. McEntire, E.P. Keath et al., The medium-energy particle analyzer (MEPA) on the AMPTE CCE spacecraft. *IEEE Trans. Geosci. Remote Sens.* **GE-23**, 230–233 (1985)
- S. McKenna-Lawlor, E. Kirsch et al., Energetic ions in the environment of comet Halley. *Nature* **321**, 347–349 (1986)
- R.L. McNutt Jr., *Physics of Space Plasmas. SPI Conf. Proceedings* (Scientific Publishers, Cambridge, 1982)
- R.L. McNutt Jr., Models of Pluto's upper atmosphere. *Geophys. Res. Lett.* **16**, 1225–1228 (1989)
- R.L. McNutt, Jr., D.G. Mitchell et al., A compact particle detector. *SPIE* **2804**, 217–226 (1996)
- R.L. McNutt, Jr., S.C. Solomon et al., The MESSENGER mission to Mercury: Development history and early mission status. *Adv. Space Res.* **38**, 564–571 (2006)
- R.L. McNutt, Jr., D.K. Haggerty et al., Energetic particles in the Jovian magnetotail. *Science* **318**(5848), 220–222 (2007)
- D.A. Mendis, E.J. Smith et al., Comet-solar wind interaction: Dynamical length scales and models. *Geophys. Res. Lett.* **13**, 239 (1986)
- D. Morrison, D. Cruikshank et al., *Nature* **300**, 425 (1982)
- U. Motschmann, K.-H. Glassmeier, Nongyrotropic distribution of pickup ions at comet P/Grigg-Skjellerup: A possible source of wave activity. *J. Geophys. Res.* **98**, 20977–20983 (1993)
- M. Neugebauer, Spacecraft observations of the interaction of active comets with the solar wind. *Rev. Geophys.* **28**, 231–252 (1990)

- M. Neugebauer, A.F. Cheng et al., Space physics objectives for the Pluto Fast Flyby mission. Report to NASA Space Physics Division, 1993
- I.G. Richardson, S.W.H. Cowley et al., Three dimensional ion bulk flows at comet P/Giacobini-Zinner. *Geophys. Res. Lett.* **13**(4), 415–418 (1986)
- T.R. Sanderson, K.-P. Wentzel et al., The interaction of heavy ions from comet P/Giacobini-Zinner with the solar wind. *Geophys. Res. Lett.* **13**(4), 411–414 (1986)
- R. Sicardy, T. Widemann et al., Large changes in Pluto's atmosphere as revealed by recent stellar occultations. *Nature* **424**, 168–170 (2003)
- A.J. Somogyi, K.I. Gringauz et al., First observations of energetic particles near comet Halley. *Nature* **321**, 285–288 (1986)
- S.A. Stern, The New Horizons Pluto Kuiper Belt mission: An overview with historical context. *Space Sci. Rev.* (2008), this issue. doi:[10.1007/s11214-007-9295-y](https://doi.org/10.1007/s11214-007-9295-y)
- S.A. Stern, D.C. Slater et al., ALICE: The ultraviolet imaging spectrograph aboard the New Horizons Pluto-Kuiper Belt Mission. *Space Sci. Rev.* (2008), this issue. doi:[10.1007/s11214-008-9407-3](https://doi.org/10.1007/s11214-008-9407-3)
- F. Tian, O.B. Toon, Hydrodynamic escape of nitrogen from Pluto. *Geophys. Res. Lett.* (2005). doi:[10.1029/2005GL023510](https://doi.org/10.1029/2005GL023510)
- L.M. Trafton, D.M. Hunten et al., Escape processes at Pluto and Charon, in *Pluto and Charon*, ed. by S.A. Stern, D.J. Tholen (University of Arizona Press, Tucson, 1997), pp. 475–521
- L. Tyler, I.R. Linscott et al., The New Horizons radio science experiment. *Space Sci. Rev.* (2008), this issue. doi:[10.1007/s11214-007-9302-3](https://doi.org/10.1007/s11214-007-9302-3)
- H.A. Weaver, W.C. Gibson et al., Overview of the New Horizons science payload. *Space Sci. Rev.* (2008), this issue. doi:[10.1007/s11214-008-9376-6](https://doi.org/10.1007/s11214-008-9376-6)
- D.J. Williams, R.W. McEntire et al., Energetic particles at Venus: Galileo results. *Science* **253**, 1525–1528 (1991)
- D.J. Williams, R.W. McEntire et al., The Galileo energetic particles detector. *Space Sci. Rev.* **60**, 385–412 (1992)
- D.J. Williams et al., GEOTAIL energetic particles and ion composition experiment. *J. Geomagn. Geoelectr.* **46**, 39–57 (1994)